

2010

## Proteolysis-resistant Type I Collagen and Vascular Smooth Muscle Cell Senescence

Faran Vafaie  
*Western University*

Follow this and additional works at: <https://ir.lib.uwo.ca/digitizedtheses>

---

### Recommended Citation

Vafaie, Faran, "Proteolysis-resistant Type I Collagen and Vascular Smooth Muscle Cell Senescence" (2010). *Digitized Theses*. 4609.  
<https://ir.lib.uwo.ca/digitizedtheses/4609>

This Thesis is brought to you for free and open access by the Digitized Special Collections at Scholarship@Western. It has been accepted for inclusion in Digitized Theses by an authorized administrator of Scholarship@Western. For more information, please contact [wlsadmin@uwo.ca](mailto:wlsadmin@uwo.ca).

**Proteolysis-resistant Type I Collagen and Vascular Smooth Muscle Cell Senescence**

(Spine title: Proteolysis-resistant Type I Collagen and SMC Senescence)

(Thesis Format: Monograph)

Faran Vafaie

Graduate Program in Biochemistry

A thesis submitted in partial fulfilment  
of the requirements for the degree of  
Master of Science

The School of Graduate and Postdoctoral Studies  
The University of Western Ontario  
London, Ontario, Canada

© Faran Vafaie 2010

THE UNIVERSITY OF WESTERN ONTARIO  
SCHOOL OF GRADUATE AND POSTDOCTORAL STUDIES

**CERTIFICATE OF EXAMINATION**

Supervisor

\_\_\_\_\_  
Dr. J. Geoffrey Pickering

Supervisory Committee

\_\_\_\_\_  
Dr. Murray W. Huff

\_\_\_\_\_  
Dr. Caroline Schild-Poulter

Examiners

\_\_\_\_\_  
Dr. David B. O’Gorman

\_\_\_\_\_  
Dr. Martin Sandig

\_\_\_\_\_  
Dr. Walter L. Siqueira

The thesis by

**Faran E. Vafaie**

entitled:

**Proteolysis resistant collagen and  
vascular smooth muscle cell senescence**

is accepted in partial fulfillment of the  
requirements for the degree of  
Master of Science

Date \_\_\_\_\_

\_\_\_\_\_  
Chair of the Thesis Examination Board

## Abstract

Senescence of vascular smooth muscle cells (SMCs) has been identified as a feature of atherosclerosis. However, the factors that lead to premature SMC senescence are not well understood. Plaque SMCs reside within a milieu of type I collagen fibrils that, over time, undergo progressive intermolecular cross-linking. This renders the protein resistant to proteolysis. I hypothesized that SMC lifespan is determined by the extent to which the surrounding type I collagen can be proteolytically modified. To test this, I studied mice harbouring a targeted mutation rendering type I collagen resistant to collagenase cleavage ( $Coll1a1^{r/r}$ ).

**I conclude:** 1)  $Coll1a1^{r/r}$  collagen promotes a premature aging-like syndrome in mice; 2) premature senescence of vascular SMCs and mouse embryonic fibroblasts is accelerated in the presence of  $Coll1a1^{r/r}$  collagen. These findings suggest a novel cross-talk between cells and the insoluble ECM that lead to age-related deterioration in vascular function, and possibly of other tissues as well.

**Keywords:** vascular smooth muscle cell, collagen, senescence, proteolysis

### **Co-Authorship**

All experiments and analysis outlined in this thesis were performed by me, with the following exceptions. Animal breeding and genotyping was performed by Caroline O'Neil and Alanna Watson of Dr. Geoffrey Pickering's laboratory. As well, *in vivo* phenotype data of the first objective (mouse survival and serology) was also acquired by Caroline O'Neil and Alanna Watson. My role in this was data analysis, interpretation and presentation. Micro-CT imaging was performed by Dr. David Holdsworth and his laboratory staff. Harvesting of mouse tail collagen was performed by Caroline O'Neil. Sectioning and staining of mouse aortic wall segments was performed by Dr. Zengxuan Nong of Dr. Geoffrey Pickering's laboratory. Harvesting of mouse embryonic fibroblasts was performed by Alanna Watson.

## Acknowledgements

I would like to express my gratitude to my supervisor, Dr. J. Geoffrey Pickering, for providing me with the opportunity to pursue my studies in his laboratory and acting as a mentor in the world of vascular biology. I would also like to thank my advisory committee, Dr. Caroline Schild-Poulter and Dr. Murray Huff, for their helpful suggestions and encouragement along the way. My project would not have been possible without the assistance and companionship of the past and present members of the Pickering laboratory. My deepest thanks go out to Matt, Theo, Caroline, Alanna, Nong, Nica, Paul, Mellonie, Oula and Eric. Also, the love, support, and guidance from my family has been a blessing. I would like to thank both sets of my parents (Nasrin and Shahab Vafaie, and Pat and Peter Smith) and my two brothers (Erfan Vafaie the budding scientist, and Andrew Smith the budding filmmaker). Finally, I think the person who was affected most by my studies was my lovely wife Melanie Vafaie. Thank you for all your patience, kindness, nurturing, and affection. I love you from the bottom of my heart. The following words of ‘Abdu’l-Bahá have been inspirational in my pursuit of this degree:

*“Exert every effort to acquire the various branches of knowledge and true understanding. Strain every nerve to achieve both material and spiritual accomplishments...penetrating the innermost reality of all things.*

*“The most noble and praiseworthy accomplishment of man therefore is scientific knowledge and attainment.”*

## Table of Contents

Certificate of Examination	ii
Abstract	iii
Co-authorship	iv
Acknowledgements	v
Table of Contents	vi
List of Tables	ix
List of Figures	x
List of Abbreviations	xii
Chapter 1 - Introduction	1
1.1. Atherosclerosis	2
1.2. The Role of Vascular Smooth Muscle Cells	2
1.3. The Fate of Vascular Smooth Muscle Cells in Atherosclerosis	5
1.4. Cellular Senescence	5
1.4.1. Replicative Senescence	6
1.4.2. Stress-induced Premature Senescence	10
1.4.3. Markers of Senescence	11
1.4.3.1. Cumulative Population Doublings	12
1.4.3.2. Morphology	12
1.4.3.3. Senescence-associated $\beta$ -galactosidase Activity	12
1.4.3.4. Senescence-associated Gene Markers	15
1.4.3.5. Telomere Length	20
1.4.3.6. Senescence-associated Heterochromatic Foci	20
1.4.4. Relevance of Senescent SMCs <i>in vivo</i>	21
1.5. Role of the Extracellular Matrix in Atherosclerosis	22
1.5.1. The Interplay Between the ECM and Vascular SMCs	23
1.5.2. Structure of Type I Collagen	24
1.5.3. The Effect of Alterations in Type I Collagen on Vascular SMCs	24
1.5.4. Aging of Type I Collagen	27
1.5.5. The <i>Coll1a1<sup>tr</sup></i> Mouse as a Model of Collagen Aging	28
1.6. Hypothesis and Thesis Objectives	30
Chapter 2 – Materials and Methods	32
2.1. Animals	33
2.2. Data Acquired From Micro-CT Scans	33

2.3.	Histological Assessment of Mouse Aorta	35
2.4.	Harvesting of Mouse Type I Collagen	36
2.5.	Isolation of Primary Human Vascular SMCs	36
2.6.	Isolation of Primary Mouse Embryonic Fibroblasts	37
2.7.	Cell Culture	38
2.8.	Determination of Matrix Production by MEFs	39
2.9.	Assessment of Senescence-associated $\beta$ -galactosidase Activity in Cultured Cells	39
2.10.	Quantitative Real-time Reverse Transcription – Polymerase Chain Reaction	40
2.11.	Western Blot Analysis	41
2.12.	Microscope and Image Analysis	43
2.13.	Data Analysis	43
 Chapter 3 – Results		 45
3.1.	Coll1a1 <sup>r/r</sup> Mice Display Impaired Weight Gain	46
3.2.	Coll1a1 <sup>r/r</sup> Mice Exhibit Decreased Lifespan	46
3.3.	Coll1a1 <sup>r/r</sup> Mice Exhibit Increased Kyphosis of the Spine	51
3.4.	Coll1a1 <sup>r/r</sup> Mice Exhibit Decreased Body Fat	56
3.5.	Coll1a1 <sup>r/r</sup> Mice Exhibit Decreased Bone Mineral Density	56
3.6.	Disrupted Elastin is a Vascular Consequence of Collagenase-resistance in Coll1a1 <sup>r/r</sup> mice	59
3.7.	SMCs in Collagenase-resistant Coll1a1 <sup>r/r</sup> Mice are Predisposed to Expressing Senescence-associated $\beta$ -galactosidase Activity in the Artery Wall	59
3.8.	Human SMCs Replicating on Collagen Derived From Coll1a1 <sup>r/r</sup> Mice Reach Growth Arrest Sooner Than SMCs Replicating on Wild-type Collagen	65
3.9.	Human SMCs Replicating on Collagen Derived From Coll1a1 <sup>r/r</sup> Mice Show Senescent-like Morphology Earlier Than SMCs Replicating on Wild-type Collagen	68
3.10.	Human SMCs Replicating on Collagen Derived From Coll1a1 <sup>r/r</sup> Mice Display Greater Levels of Senescence-associated $\beta$ -galactosidase Activity Than SMCs Replicating on Wild-type Collagen	68
3.11.	Human SMCs Replicating on Coll1a1 <sup>r/r</sup> Collagen Display Increased Transcript Levels of the Cell-cycle and Senescence-associated Genes p21 <sup>CIP1</sup> and p16 <sup>INK4A</sup>	71
3.12.	Coll1a1 <sup>r/r</sup> Collagen Promotes Stress-induced Premature Senescence	74
3.13.	Serum-deprived Human SMCs on Coll1a1 <sup>r/r</sup> Collagen Display Increased Expression of the Cell-cycle and Senescence-associated Genes p21 <sup>CIP1</sup> , p16 <sup>INK4A</sup> and p14 <sup>ARF</sup>	77
3.14.	Embryonic Fibroblasts Derived From Coll1a1 <sup>r/r</sup> Mice are Capable of Collagen Production in Culture	77

3.15.	Coll1a1 <sup>r/r</sup> MEFs Display Morphological Features of Senescence Earlier Than Embryonic Fibroblasts Derived From Wild-type Mice	80
3.16.	Coll1a1 <sup>r/r</sup> MEFs Display Elevated Senescence-associated $\beta$ -galactosidase	85
3.17.	Coll1a1 <sup>r/r</sup> MEFs Exhibit Increased Expression of the Cell-cycle and Senescence-associated Genes p21 <sup>CIP1</sup> , p19 <sup>ARF</sup> and p16 <sup>INK4A</sup>	85
Chapter 4 – Discussion		91
4.1.	Coll1a1 <sup>r/r</sup> Type I Collagen Expression Promotes Accelerated Aging in Mice	92
4.2.	Collagenase-resistant Type I Collagen Promotes Cellular Senescence <i>in vitro</i>	96
4.3.	Limitations of the Study	98
4.4.	Potential Future Implications	100
Bibliography		105
CV		119

## List of Tables

Table 3.1	$Col1a1^{+/+}$ mice display normal serology	53
-----------	---	----

## List of Figures

Figure 1.1	Structure of the arterial wall harbouring a stable fibrous atherosclerotic plaque	4
Figure 1.2	Schematic depicting the triggers of cellular senescence	8
Figure 1.3	Comparison of young, proliferating vascular SMCs and old, senescent vascular SMCs	14
Figure 1.4	Mechanistic interactions between cell-cycle proteins in response to senescence stimulus	17
Figure 1.5	Structure of type I collagen	26
Figure 3.1	Colla1 <sup>r/r</sup> mice display impaired weight gain and decreased lifespan	48
Figure 3.2	Colla1 <sup>r/r</sup> mice exhibit decreased lifespan	50
Figure 3.3	Colla1 <sup>r/r</sup> mice display increased kyphosis of the spine	55
Figure 3.4	Colla1 <sup>r/r</sup> mice display decreased body fat and reduced bone mineral density	58
Figure 3.5	Colla1 <sup>r/r</sup> mice exhibit disrupted elastin in the aortic wall	61
Figure 3.6	SMCs in the ascending aorta display more senescence-associated β-gal activity in Colla1 <sup>r/r</sup> mice than wild-type mice	64
Figure 3.7	Human SMCs replicating on Colla1 <sup>r/r</sup> collagen reach growth arrest more rapidly than those replicating on wild-type collagen	67
Figure 3.8	Human SMCs replicating on Colla1 <sup>r/r</sup> collagen show premature senescent-like morphological changes and increased senescence-associated β-gal activity	70
Figure 3.9	Human SMCs replicating on Colla1 <sup>r/r</sup> collagen display increased transcript levels of p16 <sup>INK4A</sup> and p21 <sup>CIP1</sup>	73
Figure 3.10	Human SMCs exposed to serum-deprivation are more susceptible to premature senescence in the presence of Colla1 <sup>r/r</sup> collagen	76
Figure 3.11	Serum-deprived human SMCs grown on Colla1 <sup>r/r</sup> collagen display increased protein expression p21 <sup>CIP1</sup> , p14 <sup>ARF</sup> and p16 <sup>INK4A</sup>	79

Figure 3.12	MEFs grown in culture for two weeks elaborate an extensive collagen fibril network as detected by circular polarization microscopy	82
Figure 3.13	Colla1 <sup>tr</sup> MEFs display spread morphology and multinucleation earlier than wild-type MEFs	84
Figure 3.14	Serum-starved Colla1 <sup>tr</sup> MEFs are more susceptible to premature senescence as indicated by increased SA-β-gal activity	87
Figure 3.15	Colla1 <sup>tr</sup> MEFs display increased protein expression of the senescence-associated genes p21 <sup>CIP1</sup> , p19 <sup>ARF</sup> and p16 <sup>INK4A</sup>	89
Figure 4.1	Schematic depicting the ECM as a novel determinant of cellular lifespan and senescence	104

## List of Abbreviations

AGE	advanced glycation end product
ApoE	apolipoprotein E
ARF	alternative reading frame
ATM	ataxia telangiectasia mutated
CDK	cyclin-dependent kinase
CDKI	cyclin-dependent kinase inhibitor
CIP/KIP	CDK/kinase interacting protein
CPD	cumulative population doubling
CT	critical threshold
DMEM	Dulbecco's modified Eagle's medium
ECM	extracellular matrix
FBS	fetal bovine serum
GAPDH	glyceraldehyde 3-phosphate dehydrogenase
ICAM-1	intercellular adhesion molecule-1
IGF-1R	insulin-like growth factor-1 receptor
IgG	immunoglobulin G
IL-1	interleukin-1
ITA	internal thoracic artery
M199	Medium 199
MEF	mouse embryonic fibroblasts
micro-CT	micro computed tomography
MMP	matrix metalloproteinase
NS	non-significant
PBS	phosphate-buffered saline
pRb	retinoblastoma protein
PVDF	polyvinylidene fluoride
RGD	arginine-glycine-aspartic acid
ROS	reactive oxygen species
RT-PCR	reverse transcription polymerase chain reaction
SA- $\beta$ -gal	senescence-associated beta-galactosidase
SAHF	senescence-associated heterochromatic foci
SE	standard error
SIPS	stress-induced premature senescence
SMC	smooth muscle cell
TIMP	tissue inhibitor of metalloproteinases
TNF- $\alpha$	tumor necrosis factor-alpha
tTG	tissue transglutaminase

# **Chapter 1**

## **Introduction**

## **1.1 Atherosclerosis**

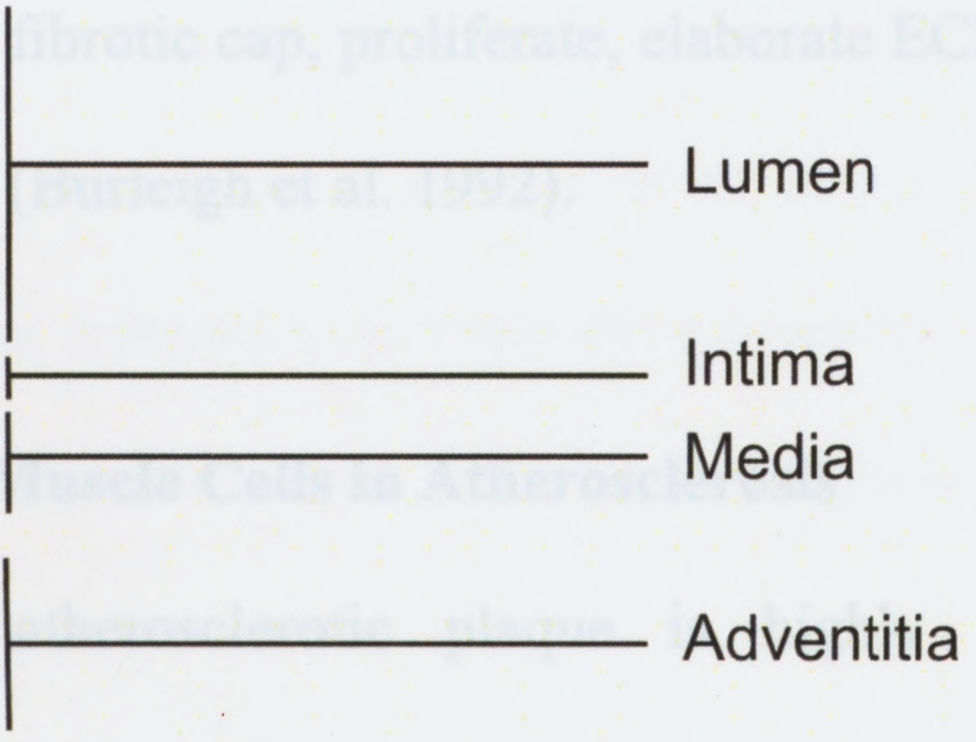
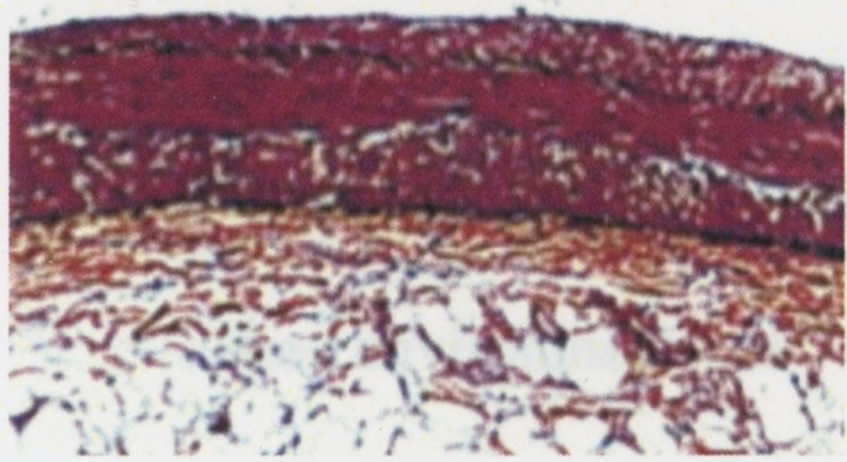
Atherosclerosis is an inflammatory disease of the arterial vessel wall. It is the result of intimal endothelial dysfunction caused by elevated low-density lipoprotein cholesterol plasma levels, free radicals, infection or a combination of other factors (Ross 1993). This is followed by oxidation of low-density lipoprotein particles and their internalization by recruited macrophages, leading to the formation of foam cells. The accumulation of foam cells and T cells results in the formation of a 'fatty streak' – a common characteristic of early stage atherosclerosis found in the arteries of adults, infants and fetuses (Stary 1989; Napoli et al. 1997). If the inflammatory response continues unabated and the injury is not relieved, the sustained protective response eventually become injurious and is referred to as an atherosclerotic plaque (Ross 1999). This stimulates the formation of a fibrous cap that initially serves to isolate the damage, but upon further progression can contribute to serious vascular complications (Figure 1.1).

## **1.2. The Role of Vascular Smooth Muscle Cells**

Although vascular smooth muscle cells (SMCs) play a vital role in normal vascular physiology, they are also critical to atherosclerosis. Atherosclerotic plaque rupture is the cause of 60% of patient death as a result of coronary disease (Virmani et al. 2000). Plaque erosion, thinning and rupture lead to thrombosis and artery occlusion. These deteriorating events in the plaque become more prevalent over time. The predominant structural component of the fibrotic cap is SMC-derived collagen, elastin, proteoglycans and other components of the extracellular matrix (ECM). The stability of

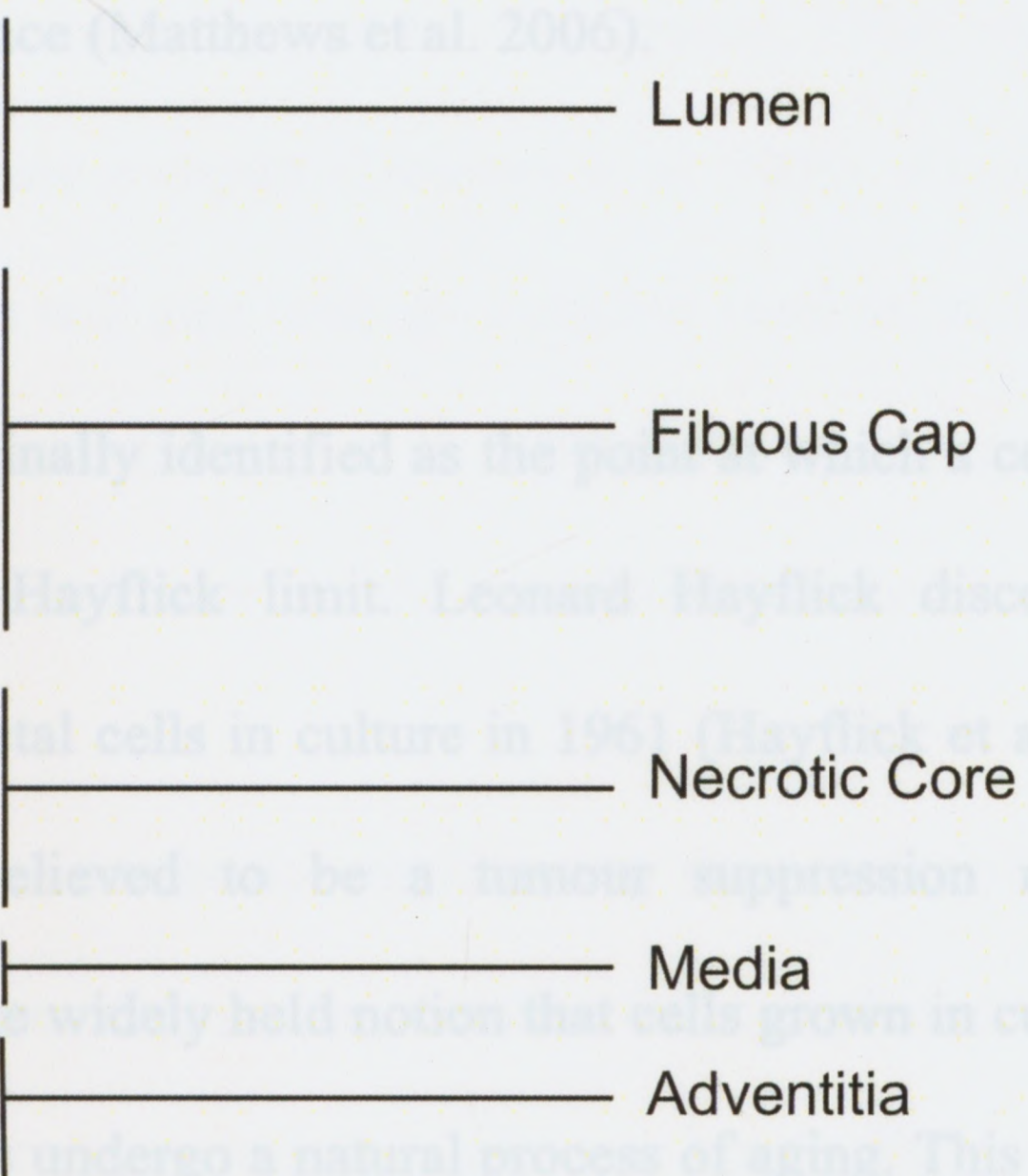
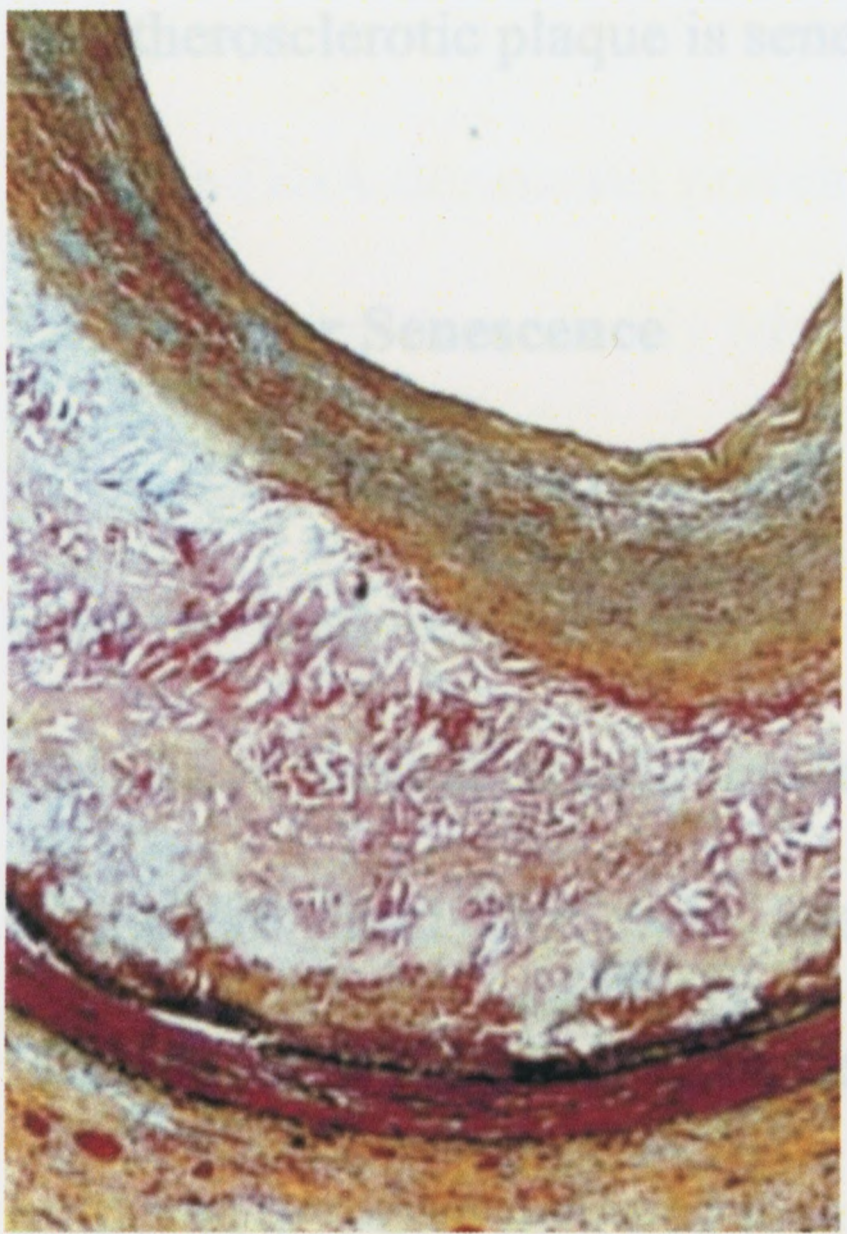
**Figure 1.1.** Movat's pentachrome-stained brightfield images of the arterial wall. *Top*, A normal coronary artery displaying a thin intimal layer is shown. *Bottom*, A coronary artery harbouring a stable fibrous atherosclerotic plaque is shown. The intimal layer has protruded into the lumen, as it now includes a necrotic core and a protective fibrous cap.

the atherosclerotic plaque is thus largely dependent on the ability of vascular SMCs to migrate from the medial layer to the fibrotic cap, proliferate, elaborate ECM, and survive in the otherwise hostile environment. (Burleigh et al. 1992)



Normal Artery Wall

environment can be quite harsh on the SMCs involved in the repair process. This environment can compromise the viability of vascular SMCs in advanced fibrotic caps. It is known that SMCs in advanced plaques are more susceptible to apoptosis (Geng et al. 1995; Clarke et al. 2008) and autophagy (Schrijvers et al. 2007), resulting in further plaque destabilization and increased potential for plaque rupture. In addition to apoptosis and autophagy, another recently identified fate of vascular SMCs in atherosclerotic plaque is senescence (Mathews et al. 2006).



Atherosclerotic Artery Wall

cellular senescence, was later described as G<sub>1</sub>-S transition arrest, despite ample

the atherosclerotic plaque is thus largely dependent on the ability of vascular SMCs to migrate from the medial layer to the fibrotic cap, proliferate, elaborate ECM, and survive in the otherwise hostile environment (Burleigh et al. 1992).

### **1.3. The Fate of Vascular Smooth Muscle Cells in Atherosclerosis**

The environment of the atherosclerotic plaque is highly oxidative and inflammatory and therefore can be quite harsh on the SMCs involved in the reparation process. This environment can compromise the viability of vascular SMCs in advanced fibrotic caps. It is known that SMCs in advanced plaques are more susceptible to apoptosis (Geng et al. 1995; Clarke et al. 2008) and autophagy (Schrijvers et al. 2007), resulting in further plaque destabilization and increased potential for plaque rupture. In addition to apoptosis and autophagy, another recently identified fate of vascular SMCs in the atherosclerotic plaque is senescence (Matthews et al. 2006).

### **1.4. Cellular Senescence**

Cellular senescence was originally identified as the point at which a cell reaches, what is now referred to as, the Hayflick limit. Leonard Hayflick discovered the replicative limit of normal human fetal cells in culture in 1961 (Hayflick et al. 1961), a replicative limit that was later believed to be a tumour suppression mechanism (Dykhuizen 1974). This discarded the widely held notion that cells grown in culture were immortal and demonstrated that cells undergo a natural process of aging. This replicative limit, or cellular senescence, was later described as G<sub>1</sub>-S transition arrest, despite ample

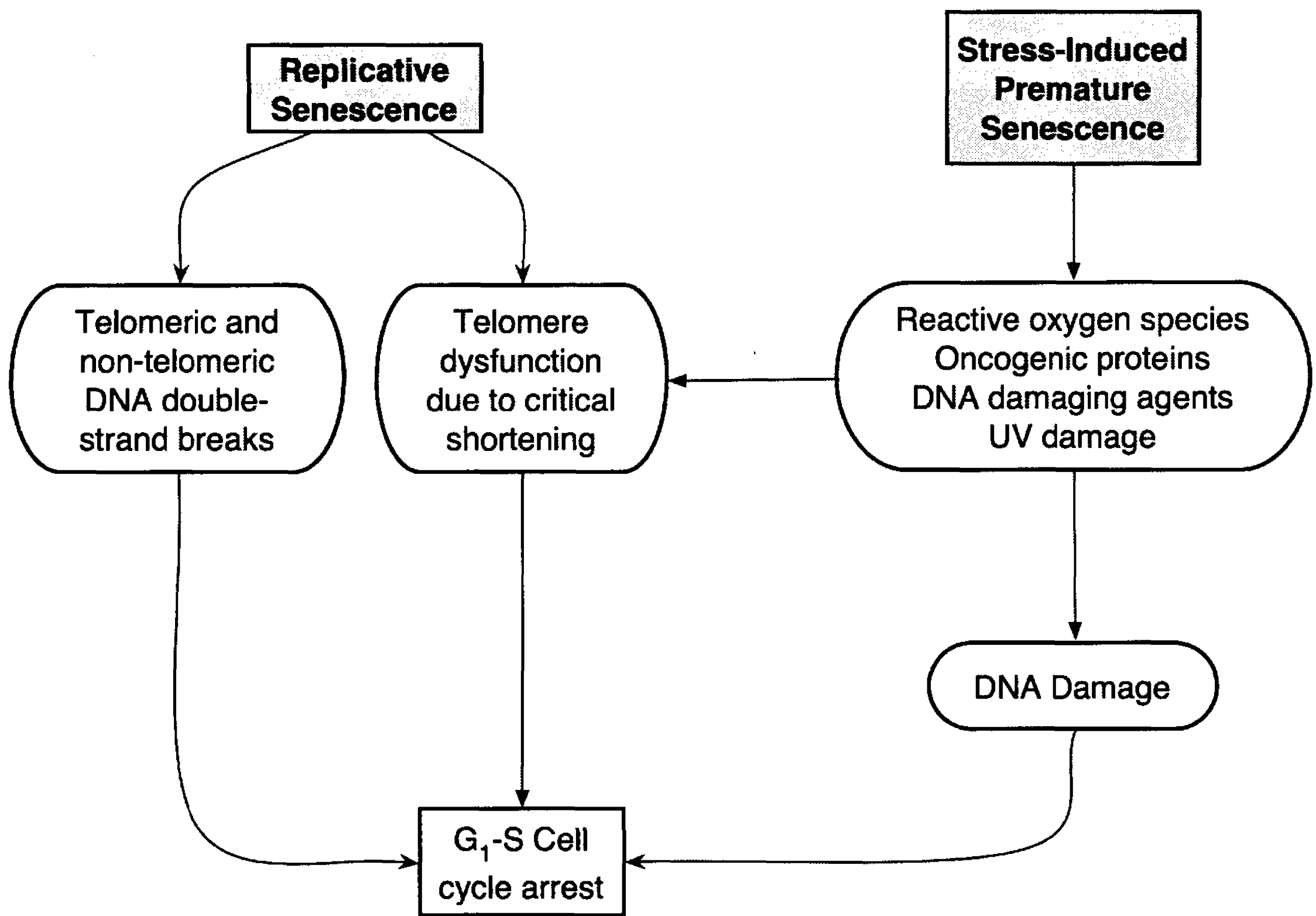
nutrients, space and growth factors (Campisi et al. 2007). Senescent cells remain metabolically active but differ from replicating cells in several respects, including functionality, morphology and gene expression (Toussaint et al. 2000). Another way of categorizing senescence is by what is referred to as replicative senescence (Bodnar et al. 1998), and stress-induced premature senescence (SIPS) (von Zglinicki et al. 1995; Toussaint et al. 2000) (Figure 1.2).

#### **1.4.1. Replicative Senescence**

Senescence triggered by telomere shortening is termed replicative senescence. Telomeres are DNA-protein complexes that serve to protect the ends of eukaryotic DNA from degradation or chromosomal fusion (Blackburn 2001). Telomeres consist of a 3'-single strand DNA overhang that folds back into a loop and is capped by telomere-associated proteins which include, telomere-repeat binding factors, DNA repair factors, and the DNA-dependent protein kinase complex (Gorenne et al. 2006). As cells undergo mitotic replication, ideally telomeres will also undergo complete replication. However, in most circumstances, this is not the case (Harley et al. 1990). DNA polymerases require primer binding to initiate replication and therefore the bound telomeric ends are not fully replicated (Greenberg et al. 1999).

Prevention of telomere erosion can be accomplished by the activity of telomerase. The template region of the enzyme telomerase contains the complementary peptide sequence to human telomeres and serves to maintain telomere length (Feng et al. 1995). Telomerase is mainly expressed in the germline and is either absent or expressed in very

**Figure 1.2.** Schematic depicting the triggers of cellular senescence. The two broad triggers of cellular senescence are excessive replications and stress-induction. The lack or inefficiency of telomerase activity results in a continual shortening of the telomeric ends of replicating somatic cells. Thus, even in ideal conditions, cells will reach a replicative limit due to critical shortening of telomeres resulting in G<sub>1</sub>-S cell cycle arrest or replicative senescence. Excessive replication can also periodically result in telomeric or non-telomeric DNA double-strand breaks. In sub-optimal conditions such as elevated reactive oxygen species levels, increased abundance of oncogenic proteins such as Raf-1 and ras, DNA damaging agents such as H<sub>2</sub>O<sub>2</sub>, or excessive UV exposure, cells can be subjected to DNA damage such as double-strand breaks, or suffer from damage to telomeric regions. Irrespective of the pathway, the result is an irreversible G<sub>1</sub>-S cell cycle arrest.



low levels in human vascular SMCs. Therefore telomere shortening is an unavoidable problem of replicating vascular SMCs (Wright et al. 2002).

At the point at which a cell has undergone enough replications that the telomeric ends cannot be conserved, there is an uncapping of the protein complex associated with the telomeres and a DNA damage response is triggered. Experiments that examined the effect of telomere-repeat binding factor mutations, which affect telomere capping regardless of telomere length and telomerase activity, led to the notion that there is a threshold at which shortened telomere length can promote cellular senescence (Smogorzewska et al. 2002; Bakkenist et al. 2004).

Recent evidence has shown that vascular SMCs in human atherosclerotic plaques display increased levels of senescence. This could, at least in part, be a result of replicative-induced telomere dysfunction (Matthews et al. 2006) due to the increased cellular replications required by vascular SMCs for development and maintenance of the fibrotic plaque.

Telomere dysfunction garners a DNA damage response involving the recruitment and phosphorylation of ataxia telangiectasia mutated kinase (ATM) (Karlseder et al. 1999), DNA protein kinase (von Zglinicki et al. 2005), and other histones and DNA repair enzymes. This DNA damage response eventually leads to the downstream activation of senescence-associated protein complexes such as p53, p16<sup>INK4A</sup>, p21<sup>CIP1</sup> and p14<sup>ARF</sup>. Subsequent hypophosphorylation of retinoblastoma protein (pRb) occurs resulting in G<sub>1</sub> cell-cycle arrest.

In addition to telomere dysfunction, replicative senescence can also be induced by DNA double-strand breaks at any location of the chromosome. A well-known marker for

strand breaks is phosphorylated H2A-X ( $\gamma$ -H2A-X) that is generally found to be associated with DNA damage foci. Previous studies have shown that senescent human fibroblasts in culture exhibit DNA double-strand breaks, as detected by  $\gamma$ -H2A-X association with both telomeric and non-telomeric regions (Sedelnikova et al. 2004). Thus replicative senescence can be either telomere-dependent or telomere-independent.

#### **1.4.2. Stress-Induced Premature Senescence**

Senescence that is independent of replication is generally caused either by endogenous expression of oncogenes or by environmental stress. Previous studies *in vitro* have examined the ability of conditionally active forms of Raf-1 and ras to induce premature senescence via accumulation of p16<sup>INK4A</sup> and p53 (Serrano et al. 1997; Zhu et al. 1998). Forms of environmental stress that can induce premature senescence predominantly result in DNA damage or oxidation and include UV/ionizing radiation or other stresses that lead to oxidizing products.

Skin exposure to UVB and UVA can lead to severe oxidative damage. Premature senescence induced by subcytotoxic levels of UVB radiation has been demonstrated in human fibroblasts (Chainiaux et al. 2002). The aging of skin is associated with an accumulation of senescent keratinocytes and fibroblasts (Campisi 1998) triggered by excessive replications or external insult in the form of UV radiation (Bertrand-Vallery et al. 2010).

Extensive studies concerned with the formation of oxidizing agents and accumulation of sources of oxidative stress have been undertaken. The prolonged imposition of hyperoxic conditions resulted in increased intracellular peroxide levels

(Gille et al. 1992) in numerous human cell types including fibroblasts (von Zglinicki et al. 1995) and umbilical vascular endothelial cells (Michiels et al. 1990). This resulted in increased susceptibility to SIPS that was partly dependent on the anti-oxidative competence of the cells. For example, an increase of ambient oxygen to 40% (considered to be hyperoxic) resulted in negligible increases in intracellular peroxide levels in foreskin fibroblasts versus at least a 100% increase in WI-38 fibroblasts (Toussaint et al. 2000).

Other experiments have focused on the exposure of fibroblasts to acute, sub-lethal doses of agents known to cause oxidative stress such as tumor necrosis factor- $\alpha$ , IL-1 (Toussaint et al. 2000), *tert*-butylhydroperoxide and H<sub>2</sub>O<sub>2</sub> (Dumont et al. 2000). Regardless of the initial trigger or stressor, SIPS can be the result of several different cell-cycle arrest mechanisms. These include telomere single strand breaks leading to telomere shortening (von Zglinicki et al. 2000), or reactive oxygen species (ROS)-induced accumulation of single-stranded regions of DNA also leading to telomere shortening (Petersen et al. 1998). It can even be independent of telomere shortening, but marked by an increase in p21<sup>CIP1</sup> transcript as a result of DNA damage (Chen et al. 2001).

### **1.4.3. Markers of Senescence**

The assessment of cellular senescence *in vitro* requires observation from a wide diversity of vantage points. This includes the assessment of growth rates, morphology,  $\beta$ -galactosidase activity, mRNA transcript and protein levels of senescence-associated genes, telomere length and heterochromatic foci. No one single endpoint can provide

definitive evidence for senescence, and the evidence is thus stronger when multiple endpoints are evaluated.

#### **1.4.3.1. Cumulative Population Doublings**

As senescence is defined by cellular growth arrest, this is manifested as a cessation of cumulative population doublings. Serially subcultured cells, plated at a known density, can be counted prior to each passage and this will give an indication as to whether the cells are dividing as rapidly or not. However, this must be differentiated from other causes of decreased population doublings such as apoptosis and quiescence.

#### **1.4.3.2. Morphology**

Senescent cells in culture can be characterized by increased cell volume, a flattened shape, enlarged nuclei (Goldstein 1990), the formation of prominent actin stress fibres (Cho et al. 2004), prominent cytoplasmic vacuoles and endoplasmic reticulum (Lipetz et al. 1972), an increase in the number of lysosomes in the cytoplasm (Cristofalo et al. 1975) and the presence of multiple nuclei (Matsumura 1980). These senescent-like morphological changes can be observed by light microscopy, and can provide further evidence for senescence (Figure 1.3).

#### **1.4.3.3. Senescence-associated $\beta$ -galactosidase Activity**

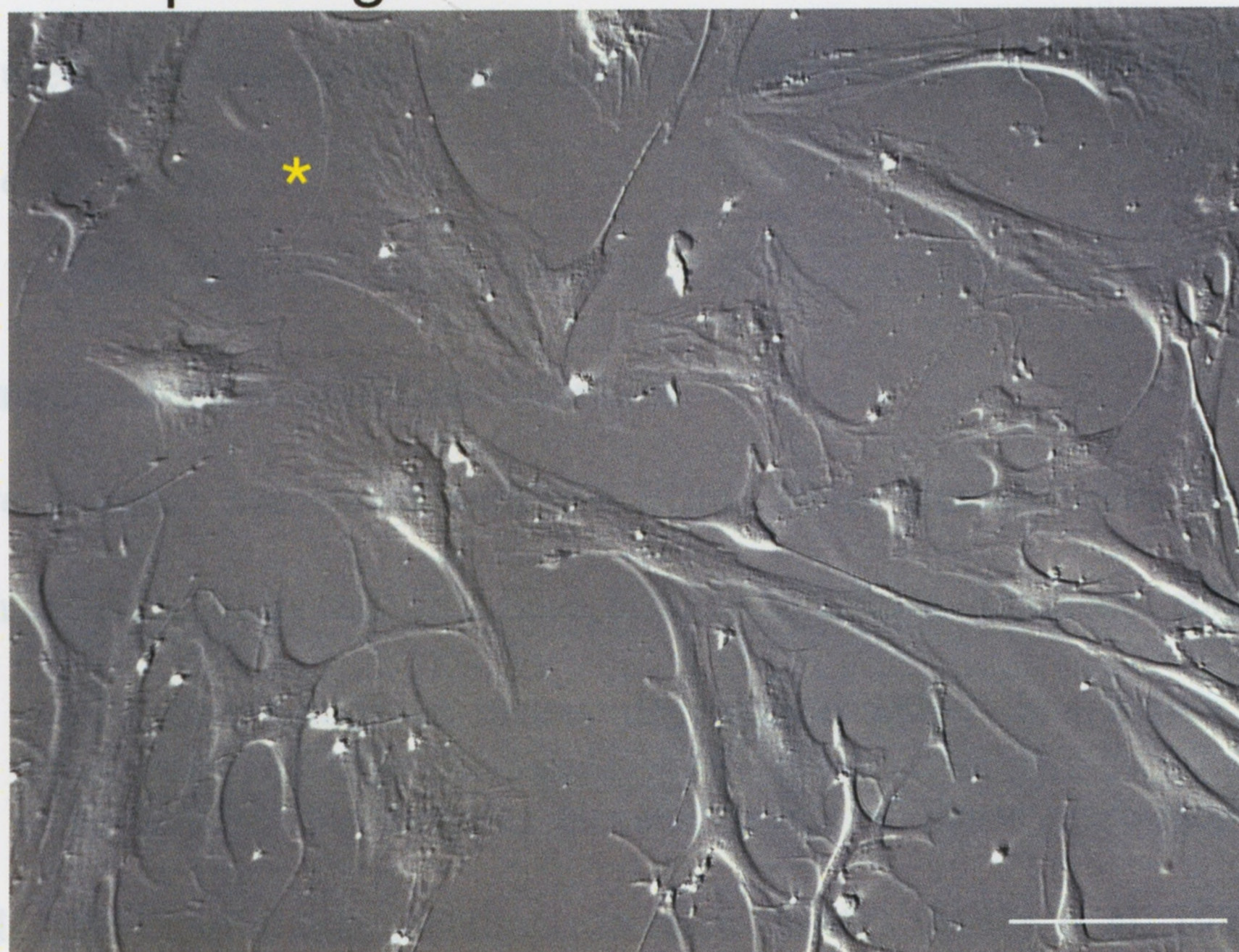
$\beta$ -galactosidase is a ubiquitous enzyme detectable at pH 4.0 and is localized to lysosomes, the rough endoplasmic reticulum, and parts of the smooth endoplasmic

**Figure 1.3.** Hoffman-modulated contrast images of human vascular SMCs. As cells in culture reach their replicative limit, a panel of endpoints can be examined in order to assess for senescence. One endpoint is the morphological changes that take place in senescent cells. In the top image, human vascular SMCs grown in culture at cell passage three are shown. The cells are proliferating and look healthy, as evidenced by their elongated spindle-like shape. In the bottom image, human vascular SMCs grown in culture at cell passage 9 are shown. Some of the cells appear to be reaching senescence, as evidenced by their large, round shape. Asterisk denotes a cell displaying morphological features consistent with senescence. Bar denotes 200 microns.

Cell passage 3



Cell passage 9

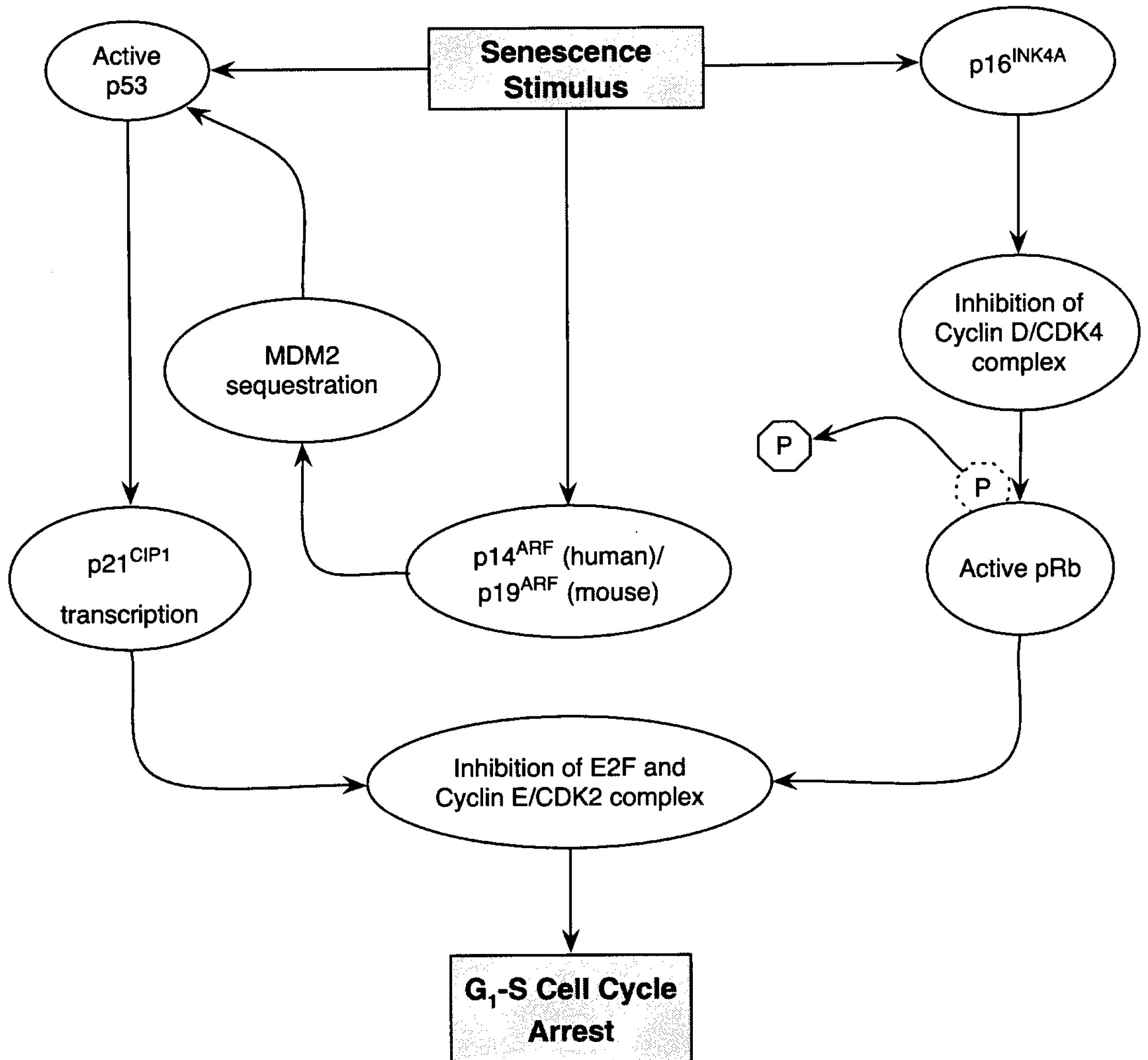


reticulum, (Novikoff et al. 1983). The  $\beta$ -galactosidase enzyme catalyzes the hydrolysis of gangliosides such as monosialotetrahexosylganglioside into monosaccharides (Yoshida et al. 1991). In 1995, it was reported that senescent cells expressed  $\beta$ -galactosidase activity that was also detectable at pH 6.0 (Dimri et al. 1995). They referred to this as senescence-associated  $\beta$ -galactosidase (SA- $\beta$ -gal), and it was detected in senescent cultured human fibroblasts and human keratinocytes, as well as elderly human skin samples *in vivo*. Subsequent studies challenged whether this activity was due to a specific form of  $\beta$ -galactosidase that was induced at senescence, or if it was attributable to increased lysosomal content, and thus increased  $\beta$ -galactosidase enzyme. It was later confirmed that senescent cells displayed increased abundance of lysosomal  $\beta$ -gal enzyme as a result of increased lysosomal mass (Kurz et al. 2000; Debacq-Chainiaux et al. 2009). This phenomenon continues to be referred to as SA- $\beta$ -gal activity, and has been frequently used as a readout of senescence in cultured cells and occasionally *in vivo* (Matthews et al. 2006).

#### **1.4.3.4. Senescence-associated Gene Markers**

Several genes associated with the ECM, DNA damage/repair and cell-cycle progression are affected in cells that have become senescent. Senescent cells display an expression profile that results in matrix degradation rather than matrix elaboration (Cristofalo et al. 2004). This includes elevated levels of tissue plasminogen activator (West et al. 1996) and matrix metalloproteinases (MMP) (Millis et al. 1992). There is also a concomitant decrease in the tissue inhibitor of matrix metalloproteinases (TIMP)

**Figure 1.4.** Schematic depicting the interactions that take place between cell-cycle proteins in response to a senescence stimulus. Stimuli that promote cellular senescence, such as critical telomere shortening, DNA double strand breaks, elevated reactive oxygen species or other sub-optimal environmental conditions can activate several different molecular pathways. P53 is activated in response to DNA damage (the result of excessive UV exposure, H<sub>2</sub>O<sub>2</sub>, harmful chemical agents), oxidative damage or excessive oncogene expression. Activated p53 induces expression of p21<sup>CIP1</sup> resulting in G<sub>1</sub>-S cell cycle arrest. Normally, p53 is inactive as a result of bound MDM2. Increased levels of p14<sup>ARF</sup> in humans or p19<sup>ARF</sup> in mice, as a result of increased p53 activity or unregulated oncogene expression, bind MDM2 resulting in a further increase in p53 activity. Critical telomere shortening or DNA double strand breaks trigger a p16<sup>INK4A</sup> mediated response in the cell. P16<sup>INK4A</sup> is a known CDK inhibitor of the cyclin D/CDK4 complex. Inhibition of this complex prevents the phosphorylation of retinoblastoma protein, allowing it to become activated. Both p21<sup>CIP1</sup> and active, hypophosphorylated retinoblastoma protein inhibit E2F and the cyclin E/CDK2 complex. This ultimately results in G<sub>1</sub>-S cell cycle arrest, or senescence.



(West et al. 1989) and mRNA levels of elastin, laminin and type I and type III collagen (Linskens et al. 1995).

Genes involved in cell-cycle progression can also be examined when assessing for cellular senescence (Figure 1.4). It is widely known that cells undergo a four-part cell cycle. Initially, the cell is in the G<sub>1</sub> phase, during which the majority of cell growth takes place. In particular, most organelles and structural proteins are synthesized in order to prepare the cell for division. Subsequently, the cell enters S or synthesis phase. During the S phase, DNA replication takes place. During the G<sub>2</sub> phase, the cell undergoes rapid growth in order to prepare for mitosis. Finally, M phase is the phase in which mitosis actually occurs. Cyclin dependent kinases (CDK) 4 and 6 are commonly regulated by cyclin D1, D2 and D3 and as complexes are essential for the transition of a dividing cell from G<sub>1</sub> into S phase (Blagosklonny et al. 2002). The cyclin D/CDK4/6 complex directly phosphorylates retinoblastoma protein (pRb), relieving the inhibitory effect of pRb on E2F. E2F that is no longer sequestered can then facilitate in the activation of downstream cell-cycle progression genes required for entry into S phase (Ohtani 1999). The activity of CDK-complexes can be inhibited by cyclin dependent kinase inhibitors (CDKI) such as p21<sup>CIP1</sup>, p16<sup>INK4A</sup> and p14<sup>ARF</sup>/p19<sup>ARF</sup>. Members of the CIP/KIP (CDK/kinase interacting protein) family, including p21<sup>CIP1</sup>, p27<sup>KIP1</sup> and p57<sup>KIP2</sup> are known to bind to cyclin D/CDK4/6 and cyclin E/CDK2 complexes. During mitogen-stimulated growth, CIP/KIP proteins remain bound to cyclin D/CDK4/6 complex. However, upon mitogen removal cyclin D is degraded and CIP/KIP proteins bind to and inhibit the actions of cyclin E/CDK2 complexes resulting in growth arrest (Sherr 2000).

A number of studies examining the relationship between p21<sup>CIP1</sup> and p53, a known tumour suppressor protein, established the value of p21<sup>CIP1</sup> as one indicator of senescence. A lung carcinoma cell line defective in p53 expression and overexpressing p21<sup>CIP1</sup> undergoes premature senescence (Wang et al. 1999), whereas human diploid fibroblasts defective in p21<sup>CIP1</sup> expression do not undergo replicative senescence (Brown et al. 1997). Similar experiments have also been demonstrated in mouse embryonic fibroblasts (MEFs) (Xu et al. 1998). Thus, p21<sup>CIP1</sup>, a downstream target of p53, is a player in cell-cycle arrest and is found in increased levels in senescent cells.

P16<sup>INK4A</sup> is an inhibitor of cyclin D/CDK4 complex catalytic activity (Serrano et al. 1993) resulting in hypophosphorylation of pRb (Alcorta et al. 1996). Cyclin D2-deficient MEFs are susceptible to premature senescence (Bouchard et al. 1999). Furthermore, inactivation of p16<sup>INK4A</sup> in MEFs induces extended lifespan via undisturbed pRb phosphorylation (Carnero et al. 2000). Also, human keratinocytes that have undergone replicative senescence exhibit high levels of p16<sup>INK4A</sup> expression (Munro et al. 1999). Expression of p16<sup>INK4A</sup> is thus also used as a cellular marker of senescence.

In addition to p16<sup>INK4A</sup>, the *Ink4a* locus encodes an unrelated transcript, p14<sup>ARF</sup> in humans and p19<sup>ARF</sup> in mice. P14/p19<sup>ARF</sup> binds mdm-2, preventing it from facilitating the degradation of p53. This results in increased levels of p53 expression and subsequent p53-p21<sup>CIP1</sup> mediated cell-cycle arrest (Marcotte et al. 2002). Furthermore, normal MEFs undergo replicative senescence in culture marked by an increase in p19<sup>ARF</sup> expression, but this is bypassed in MEFs lacking p19<sup>ARF</sup> (Kamijo et al. 1997). Therefore, an analysis of the expression profile of p16<sup>INK4A</sup>, p21<sup>CIP1</sup> and p14/p19<sup>ARF</sup> collectively can suggest senescence.

#### **1.4.3.5. Telomere Length**

Critical shortening of telomeres, whether it is the result of extensive proliferation or oxidative damage, can lead to senescence. In general, telomere shortening or damage is a process similar to DNA double-strand breaks. Markers associated with DNA damage such as phosphorylation of histone H2AX, and DNA repair and damage factors such as 53BP1, MDC1 and NBS1 are detected in cells undergoing senescence as a result of critical telomere shortening (d'Adda di Fagagna et al. 2003). There are also several techniques for measuring the length of telomeres, including Terminal Restriction Fragment assay, Quantitative Fluorescent *in situ* hybridization, or PCR (Hathcock et al. 2004).

#### **1.4.3.6. Senescence-associated Heterochromatic Foci**

As noted above, pRb phosphorylation releases E2F to promote cell cycle progress. One of the functions of E2F is to act on histone acetyltransferases leading to subsequent decompacting of chromatin structure and expression of genes required for G<sub>1</sub>-S transition (Trimarchi et al. 2002). On the other hand, stable repression of E2F by hypophosphorylated pRb leads to a unique accumulation of DNA foci known as senescence-associated heterochromatic foci (SAHF) (Narita et al. 2003). SAHF are similar to transcriptionally inactive sites, or heterochromatin, and are only found in senescent (not merely quiescent) cells. Binding of HP1 $\gamma$  and K9M-H3, proteins involved in SAHF formation, to E2F-target gene promoters such as *cyclin A* and *PCNA* is increased in senescent cells (Narita et al. 2003) resulting in decreased expression of genes required for G<sub>1</sub>-S phase transition. IMR90 human diploid fibroblasts undergoing either

replicative senescence or SIPS exhibit characteristic changes in nuclear morphology and DNA structure. A large nucleolus and punctate DNA foci as visualized by DAPI staining has been observed in senescent cells and is thought to identify SAHF (Narita et al. 2003). Thus, accumulation of SAHF is another marker that can be used to detect senescence.

#### **1.4.4. Relevance of Senescent SMCs *in vivo***

Recently, *in vivo* evidence of vascular SMC senescence has been identified in atherosclerotic plaques (Matthews et al. 2006). Essential to the vascular remodelling process in atherosclerosis is the migration and proliferation of vascular SMCs from the media into fatty streaks in the intima. Proliferation of vascular SMCs in early atherosclerotic lesions is quite high compared to advanced atherosclerotic plaques (Lutgens et al. 1999). It is thought that as a result of proliferation, replicative senescence can ensue. This might be a cause of plaque instability, due to the resulting decreased proliferation, increased expression of pro-inflammatory genes such as ICAM-1 and IL-1 $\beta$  (Saito et al. 2001), and increased expression of matrix-degrading enzymes (Cristofalo et al. 2004). It is also well known that atherosclerotic plaques and the surrounding arterial wall harbour high levels of ROS (Hathaway et al. 2002) that act as oxidizing agents and can result in SIPS (Gorenne et al. 2006). What is not clear is the role that the ECM plays in the viability and functionality of vascular SMCs and there is no data on the role of the ECM in senescence.

### **1.5. Role of the Extracellular Matrix in Atherosclerosis**

The ECM of the normal artery is elaborated primarily by vascular SMCs and is comprised mainly of collagens, elastin, proteoglycans and microfibrillar proteins (Lee et al. 1997). Turnover of ECM proteins is generally slow, but in the case of arterial injury or the onset of atherosclerosis, degradation, synthesis and organization of elastin, type I and III collagen and other matrix components is greatly accelerated. Degradation of the ECM can be attributed to serine proteases, cysteine proteases and MMPs. MMPs are a family of proteases consisting of twelve members, each having a different target substrate and are regulated at the transcriptional level, at the level of proenzyme activation (Birkedal-Hansen et al. 1993) and by a series of inhibitors called tissue inhibitors of metalloproteinases (TIMPs) (De Clerck et al. 1994). MMPs are secreted in high levels during the degradation of the fibrotic cap. For example, a study examining the decreased stability of vulnerable human atherosclerotic plaques concluded that the thin fibrous cap which is prone to rupture is a result of increased collagenolysis due to increased expression of MMP-1 and MMP-13 (Sukhova et al. 1999). Another study performed on apolipoprotein E (apoE) deficient mice demonstrated that reducing the activity of MMP-8 results in a substantial reduction in atherosclerotic lesion formation (Laxton et al. 2009).

The inflammatory response, which is characterized by the accumulation of macrophages, results in the increased secretion of ECM-degrading proteins (Mach et al. 1997). The elevated levels of ECM-degrading proteins can also be attributed to the altered role of plaque SMCs. Under normal conditions, MMP-1 is expressed at very low levels by SMCs. However, in the presence of inflammatory molecules such as TNF- $\alpha$  or IL-1 $\beta$ , the synthesis of MMP-1 by SMCs is increased markedly (Lee et al. 1997). Thus,

in an atherosclerotic lesion it is thought that the increased presence and activity of macrophages results in the stimulation of SMCs to produce proteases that break down the surrounding ECM.

The primary components of the ECM of the atherosclerotic plaque are type I and type III collagen. With aging, type I collagen is more abundant in the intima (Stary et al. 1992). Therefore, it would be useful to examine what signals arising from the ECM, specifically type I collagen, are relevant to SMCs and where there is room for further study.

### **1.5.1. The Interplay Between the ECM and Vascular SMCs**

ECM, including collagen, is not simply a structural component of tissue, but can exert major influence on the behaviour of cells in which it is in contact with. One mechanism of this interaction is via integrins. Integrins are cell-surface receptors that mediate cellular signalling arising from the ECM and can play an essential role in survival and cell-cycle progression. This includes apoptosis and cyclin activity. Cyclin E/CDK2 activity in fibroblasts is dependent on integrin-associated cell anchorage (Meredith et al. 1993; Fang et al. 1996) and is thought to be mediated via the  $\beta 1$  and  $\beta 3$  integrin cytoplasmic domains (Radeva et al. 1997). Furthermore, it has been shown that binding of integrins to specific amino acid sequences commonly found in components of the ECM, such as arginine-glycine-aspartic acid (RGD), can regulate cell attachment and thus, influence cell proliferation (Hansen et al. 1994; Ruoslahti 1996). Therefore, the ECM is a major regulator of cell-cycle progression. However, to date, the relationship between the ECM and cellular senescence is not clearly understood.

### 1.5.2. Structure of Type I Collagen

Type I collagen is the most abundant collagen in the body, and the most abundant ECM protein in advanced atherosclerotic lesions. Type I collagen is a trimeric, structural protein made from three polypeptide chains. They are arranged in a triple helical structure consisting of two  $\alpha 1(I)$  chains and one  $\alpha 2(I)$  chain, each being 1050 amino acids in length (Figure 1.5). These triple stranded molecules are then arranged into larger polymers known as collagen fibrils which then assemble into even larger collagen fibres (Lodish 2003). Type I collagen is mainly found in the vasculature, skin, tendon and bone.

### 1.5.3. The Effect of Alterations in Type I Collagen on Vascular SMCs

Vascular SMCs suspended within a polymerized three-dimensional fibrillar type I collagen gel, or cultured on top of a two-dimensional fibrillar type I collagen gel display growth inhibition as a result of the upregulation of cell cycle inhibitors such as p27<sup>Kip1</sup> and p21<sup>CIP1</sup>. On the other hand, SMCs grown on type I collagen in its monomeric form, or its degraded form, do not see similar increases in cell cycle inhibitors (Koyama et al. 1996; Li et al. 2003). Thus, the form of collagen can have a major impact on cell-cycle regulation of the cells in contact with it.

Another type of collagen modification is glycation. Advanced glycation end products (AGE) within the ECM arise from high levels of cellular glucose, resulting in non-enzymatic glycation. This involves the reaction of the carbonyl group of a sugar with the amino group of a matrix protein forming a reversible Schiff's base, which reacts further into an Amadori product (Mentink et al. 2002). These products can then undergo further rearrangement resulting in the formation of AGE (Vlassara 1994). This can render

**Figure 1.5.** Type I collagen is a triple helical molecule found in connective and interstitial tissue consisting of two  $\alpha 1(1)$  chains and one  $\alpha 2(1)$  chain. The *Coll1a1* gene encodes the  $\alpha 1(1)$  chain and the *Coll1a2* gene encodes the  $\alpha 2(1)$  chain. Type I collagen is cleaved by MMP-1, MMP-8 and MMP-13 (collagenase-1, collagenase-2 and collagenase-3 respectively) between glycine and isoleucine/leucine at the 775<sup>th</sup> and 776<sup>th</sup> residues on the  $\alpha 1(1)/\alpha 2(1)$  chains resulting in two fragments,  $\frac{1}{4}$  and  $\frac{3}{4}$  the length of the molecule. A targeted mutation substituting proline for glutamine at the 774<sup>th</sup> residue, methionine for isoleucine at the 776<sup>th</sup> residue and proline for alanine at the 777<sup>th</sup> residue of the  $\alpha 1(1)$  chain results in resistance to collagenase cleavage. The presence of normal  $\alpha 1(1)$  cleavage is required for cleavage of the  $\alpha 2(1)$  chain. It is known that type I collagen undergoes an aging process overtime which includes progressive intermolecular cross-linking and as a result reduced susceptibility to proteolysis. In this thesis, I use this collagenase-resistant type I collagen (*Coll1a1<sup>r/r</sup>*) as a model to study age-related modifications of the molecule.

molecules such as type I collagen, less susceptible to proteolysis (Singh et al. 2001). A study on the effect of glycated type I collagen on young human umbilical vein endothelial cells revealed that exposure to this altered collagen promotes premature senescence. This was detected by increased p53 and p14<sup>ARF</sup> expression, and elevated apoptosis

rates (Chen et al. 2002). Thus, alterations of type I collagen can have an effect on cells that are

### 1.5.4. Aged Type I Collagen

Structural changes in type I collagen have the potential to affect SMC growth and viability (Chen et al. 2002). It is well recognized for over 30 years that fibrillar collagen ages over time

(Hamlin et al. 1971; Zwolinski et al. 1976) due to progressive collagen

intermolecular crosslinking of the fibrils (Vassalli 1979) accompanied by a progressive

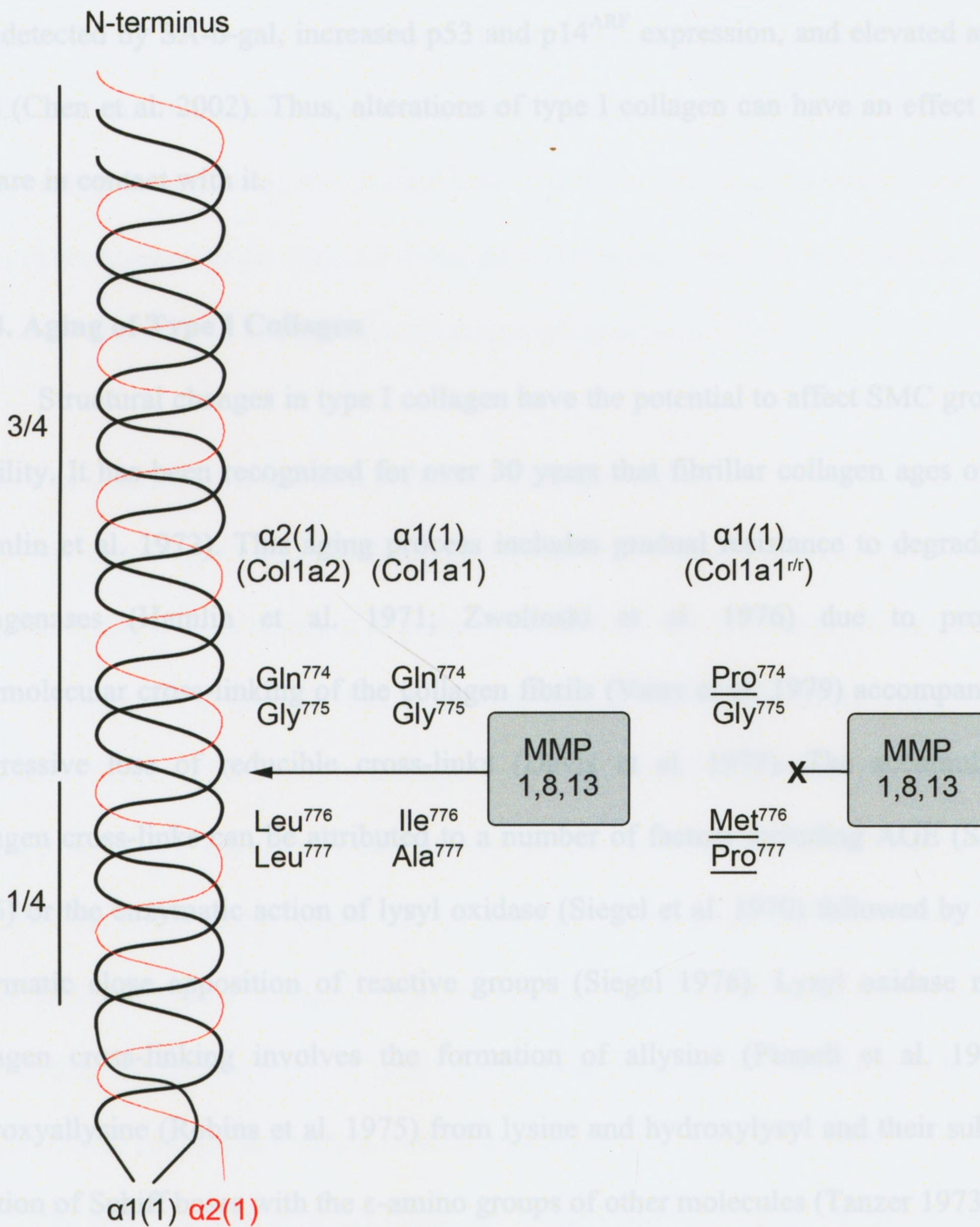
collagen crosslinking (a number of factors including AGEs) (Sell et al. 2005). The

action of lysyl oxidase (Siegel et al. 1970) followed by the non-enzymatic

oxidation of reactive groups (Siegel 1976). Lysyl oxidase mediated collagen crosslinking involves the formation of allysine (Panzell et al. 1968) and hydroxyallysine (Panzell et al. 1975) from lysine and hydroxylysyl and their subsequent

creation of crosslinks with the  $\epsilon$ -amino groups of other molecules (Tanzer 1973). Native, undenatured type I collagen at neutral pH can only be cleaved by the

following three MMPs: fibroblast collagenase or MMP-1; polymorphonuclear cell-derived collagenase or MMP-8 (Birkedal-Hansen et al. 1993); and collagenase-3 or



molecules such as type I collagen less susceptible to proteolysis (Singh et al. 2001). A study on the effect of glycated type I collagen on young human umbilical vein endothelial cells revealed that exposure to this altered collagen promotes premature senescence. This was detected by SA- $\beta$ -gal, increased p53 and p14<sup>ARF</sup> expression, and elevated apoptosis rates (Chen et al. 2002). Thus, alterations of type I collagen can have an effect on cells that are in contact with it.

#### **1.5.4. Aging of Type I Collagen**

Structural changes in type I collagen have the potential to affect SMC growth and viability. It has been recognized for over 30 years that fibrillar collagen ages over time (Hamlin et al. 1972). This aging process includes gradual resistance to degradation by collagenases (Hamlin et al. 1971; Zwolinski et al. 1976) due to progressive intermolecular cross-linking of the collagen fibrils (Vater et al. 1979) accompanied by a progressive loss of reducible cross-links (Davis et al. 1975). The accumulation of collagen cross-links can be attributed to a number of factors including AGE (Sell et al. 2005) or the enzymatic action of lysyl oxidase (Siegel et al. 1970) followed by the non-enzymatic close apposition of reactive groups (Siegel 1976). Lysyl oxidase mediated collagen cross-linking involves the formation of allysine (Pinnell et al. 1968) and hydroxyallysine (Robins et al. 1975) from lysine and hydroxylysyl and their subsequent creation of Schiff bases with the  $\epsilon$ -amino groups of other molecules (Tanzer 1973).

Native, undenatured type I collagen at neutral pH can only be cleaved by the following three MMPs: fibroblast collagenase or MMP-1; polymorphonuclear cell-derived collagenase or MMP-8 (Birkedal-Hansen et al. 1993); and collagenase-3 or

MMP-13 (Freije et al. 1994). Near the NH<sub>2</sub> terminus of the  $\alpha$ 1(I) chain, there is a cleavage site that is recognized by rodent collagenase (homologous to human MMP-13). It is thought that this cleavage site at the N-telopeptide domain is sufficient for collagen turnover during embryonic development but is not adequate enough to maintain the proper balance of synthesis and degradation required for collagen turnover (Liu et al. 1995). A highly conserved site at Gly<sup>775</sup>/Ile<sup>776</sup> in the  $\alpha$ 1(I) chain and Gly<sup>775</sup>/Leu<sup>776</sup> in the  $\alpha$ 2(I) chain located  $\frac{3}{4}$  the distance from the N-terminus serves as the cleavage site most commonly used by the collagenases (Birkedal-Hansen et al. 1993).

#### **1.5.5. The Colla1<sup>r/r</sup> Mouse as a Model of Collagen Aging**

As noted, type I collagen undergoes progressive intermolecular cross-linking over time, rendering it more resistant to proteolytic editing. This resistance can be emulated in type I collagen by artificially inducing cross-link formation via tissue transglutaminase incubation (Zhou et al. 2006) or through the formation of AGE via D-glucose incubation (Chen et al. 2001). Another model that can be used is an animal model that has been in existence for about fifteen years. Colla1 and Colla2 are genes that encode the  $\alpha$ 1(I) and  $\alpha$ 2(I) chains of type I collagen respectively. The highly conserved consensus sequence surrounding the cleavage site of type I collagen is required to be intact in order to allow for successful collagenase action. Substitutions of Pro<sup>774</sup> for Gln<sup>774</sup>, Met<sup>776</sup> for Ile<sup>776</sup> and Pro<sup>777</sup> for Ala<sup>777</sup> in the gene encoding the  $\alpha$ 1(I) chain (Colla1<sup>r/r</sup>) in mouse fibroblasts rendered the  $\alpha$ 1(I) chain resistant to collagenase activity (Wu et al. 1990) (Figure 1.5) It was also found that normal cleavage of the  $\alpha$ 1(I) was required for  $\alpha$ 2(I) chain cleavage. Liu et al injected the Colla1<sup>r/r</sup> gene into the pronuclei of mouse embryos in an attempt to

create a transgenic animal. This resulted in embryonic lethality that was thought to be caused by overexpression of the mutated gene. Subsequently, the  $Coll1a1^{r/r}$  mutation was introduced into embryonic stem cells that were injected into C57BL/6 or BALB/c blastocysts. These mice were then backcrossed to C57BL/6 or BALB/c mice and offspring were genotyped to ensure germline transmission. The heterozygous offspring were then intercrossed in order to produce viable homozygous  $Coll1a1^{tm1Jae}$  ( $Coll1a1^{r/r}$ ) mice (Liu et al. 1995). This resulted in a mouse expressing endogenous  $Coll1a1$  harbouring a targeted mutation at the site of collagenase cleavage rendering it resistant to proteolysis.

Although  $Coll1a1^{r/r}$  mice do not exhibit gross abnormalities during development, with age the effect of collagenase-resistance becomes apparent. The mice develop marked fibrosis of the dermis due to accumulation of dense collagen fibres beneath the skin and females reveal severely impaired reproductive potential due to improper uterine development (Liu et al. 1995). Wound healing is severely impaired in  $Coll1a1^{r/r}$  mice as a result of the impediment of reepithelialization, delayed wound contraction and the persistence of inflammatory cells (Beare et al. 2003). The bone remodelling process is also affected including the diminishment of bone resorption (Zhao et al. 1999), the increased presence of lacunae as a result of increased osteocyte and osteoblast apoptosis, and excessive bone deposition (Zhao et al. 2000). Another study examining the effect of vascular pressure overload provided evidence for possible stiffening of the left ventricle, due to impaired transition to dilation following normal hypertrophy (Lindsey et al. 2003). Further studies revealed that  $Coll1a1^{r/r}$  mice also exhibit ocular hypertension (Aihara et al. 2003). A study that examined the progression of atherosclerotic plaques in  $Coll1a1^{r/r}$  mice

crossed with apoE<sup>-/-</sup> mice revealed a significant reduction in intimal SMCs and an accumulation of intimal collagen in the atherosclerotic lesions (Fukumoto et al. 2004).

In order to determine whether there is a direct effect of mutant non-degradable type I collagen on cells, acid-soluble collagen purified from the tails of wild-type and Colla1<sup>r/r</sup> mice was coated on cell culture plates. Myofibroblastic-activated hepatic stellate cells were then grown on Colla1<sup>r/r</sup> collagen and displayed a reduction in thymidine incorporation and proliferating cell nuclear antigen, along with increased p21<sup>CIP1</sup> expression (Zhou et al. 2006). Thus, the accumulation of proteolysis-resistant type I collagen is compatible with survival but results in an abnormal phenotype in mice. Furthermore, there seems to be a link between Colla1<sup>r/r</sup> collagen and cell proliferation.

## **1.6. Hypothesis and Thesis Objectives**

Vascular SMCs play a major functional and structural role in the regulation of vascular repair and disease progression. The overall health and reparative ability of the arterial wall is largely dependent on the ability of vascular SMCs to survive so that they can migrate, proliferate and turnover ECM molecules. One pathway by which SMCs may lose their functional attributes is by becoming senescent. Type I collagen, the predominant ECM molecule found in the arterial wall, undergoes progressive intermolecular cross-linking over time rendering it more resistant to collagenase cleavage. Previous findings support the notion that modifications of the ECM can impact cell signalling. To date however, no studies have linked aging of type I collagen to aging of the cell. Similarly, the extent to which aged collagen leads to the aging of an organism is unknown.

**I hypothesize that vascular smooth muscle cell lifespan is determined by the extent to which the surrounding type I collagen can be proteolytically modified.**

The objectives of my study were:

- 1) To determine if the accumulation of type I collagen with reduced susceptibility to proteolysis is associated with features of accelerated aging in mice.
- 2) To determine if proteolysis-resistant type I collagen promotes replicative and/or stress-induced premature senescence in cultured human vascular smooth muscle cells.
- 3) To determine if cultured mouse embryonic fibroblasts expressing proteolysis-resistant type I collagen are more susceptible to premature senescence.

To address the hypothesis and these objectives, I made use of  $Coll1a1^{r/r}$  mice. Several phenotypic endpoints of mouse aging were studied including survival, body composition, and body structure to determine the age-related consequences of proteolysis-resistant type I collagen. I then examined the vasculature of the  $Coll1a1^{r/r}$  mouse since the artery wall is a known site of type I collagen aging. This included the examination of ECM formation in the aortic wall and indications of senescent SMCs in the aortic arch. To determine if there was a direct effect of proteolysis-resistant type I collagen on aging, I examined senescence-related endpoints, of vascular SMCs grown on  $Coll1a1^{r/r}$  type I collagen *in vitro*. Finally, experiments utilizing  $Coll1a1^{r/r}$  MEFs were undertaken to examine the behaviour of endogenous proteolysis-resistant type I collagen production on susceptibility to premature senescence.

## **Chapter 2**

### **Materials and Methods**

## 2.1. Animals

Previously developed  $Col1a1^{r/r}$  mice (Liu et al. 1995) obtained from Jackson Laboratories (Bar Harbor, Maine) were backcrossed in either C57BL/6J or 129s mice for 5 generations to breed progeny yielding homozygous mutant (n=28) and homozygous wild type mice (n=23) (heterozygotes were not used in these studies). Mice were housed at Health Sciences Animal Care Facility (London, ON) in accordance with the Canadian Guide for the Care and Use of Laboratory Animals. All experiments were approved by the Animal Care Committee at the University of Western Ontario (Protocol #2006-064-08). Only data pertaining to male mice were reported in order to control for possible sex-related differences. For longevity experiments, mice were followed until their natural death, unless there was undue suffering at which point they were sacrificed. For measurements of kyphosis, adipose tissue content and bone mineral density, eight wild-type/ $Col1a1^{r/r}$  littermates (a mixture of five 129s background littermates and three C57BL/6 background littermates) 7-13 months of age were used.

In order to perform a serological screen, anesthetized mice had blood drawn via cardiac puncture. The blood was allowed to coagulate and was spun at 3000 rpm for 30 minutes to separate the serum from the white blood cells and red blood cells. Isolated blood serum of mice aged 3, 7, and 17 months was then sent for diagnosis by Charles River Animal Diagnostic Services (Wilmington, MA).

## 2.2. Data Acquired From Micro-CT Scans

Micro-CT imaging was performed in the Imaging Research Laboratories, Robarts Research Institute. Animals were scanned using a cone-beam, volumetric, micro-CT

scanner (GE eXplore Locus Ultra, GE Healthcare). Mice were scanned 6 times each, as this has been previously identified as sufficient to obtain a 95% confidence in calculated precision value of bone mineral density (Gluer et al. 1995).

Kyphotic index of mice was measured by obtaining two measurements from micro-CT micrographs of skeletal structure. The first measurement (x) is the distance along the spine from the seventh cervical vertebra to the sixth lumbar vertebra. The second measurement (y) is the distance from that line to the farthest point of the vertebral body (where the highest arch of the spine is located). Kyphotic index was defined as  $y/x$ .

CT imaging is capable of differentiating body composition based on grey-scale intensity (Hounsfield Units) of measured voxels, due to differences in tissue density. I was able to generate three grey-scale thresholds corresponding to lean tissue, adipose tissue and bone, in order to assign each voxel to a tissue type. Next, the total number of voxels (in this study, each voxel had a volume of  $0.0308 \text{ cm}^3$ ) within each threshold were accounted for, and used to calculate the total volume of each tissue type.

Bone-mineral content was calculated based on the known linear relationship between CT number and amount of mineral content by using calibrators placed within each micro-CT image. One calibrator was a tissue-equivalent plastic with zero bone-mineral content and the other was a bone-mimicking epoxy (SB3) known to have 1100 mg of hydroxy apatite per  $\text{cm}^3$ . Thus, total bone-mineral content was calculated based on the following equation, where  $N_{\text{ST}}$  represents the number of skeletal tissue voxels,  $\Delta x^3$  represents the volume of 1 voxel ( $0.0308 \text{ cm}^3$ ),  $\text{CT}_{\text{TE}}$  represents the CT value of the tissue-equivalent calibrator,  $\text{CT}_{\text{SB3}}$  represents the CT value of the SB3 calibrator, and the

second half of the equation is a weighted representation of CT values on a voxel by voxel basis (Granton et al. 2009):

$$\text{Bone-mineral content} = N_{ST} \times \Delta x^3 [1100 / (CT_{SB3} - CT_{TE})] \sum_{i=1}^{N_{ST}} [(CT_i - CT_{TE}) / N_{ST}]$$

### 2.3. Histological Assessment of Mouse Aorta

In order to assess for elastin structure, 4% paraformaldehyde fixed aortas of 22-month old littermates were sectioned at 5  $\mu\text{m}$  onto glass coverslips and stained with elastin-trichrome.

To assess for propensity of vascular cells to express senescence-associated  $\beta$ -galactosidase (SA- $\beta$ -gal) activity *in vivo*, mice were administered angiotensin II (Sigma) (1.4 mg/kg/day) continuously for 28 days through the implantation of an osmotic pump. This manipulation is known to impose a hemodynamic and receptor-mediated stress on the vessel wall (Ishizaka et al. 1997; Yanagitani et al. 1999). Aortic cryosections were assessed for SA- $\beta$ -gal activity as previously described (Dimri et al. 1995). Specifically, mice were antegrade perfused via the left ventricle with PBS followed by SA- $\beta$ -Gal solution [(1 mg/ml X-Gal (Invitrogen), stock = 20 mg/ml in dimethylformamide), 40 mM citric acid, sodium phosphate (pH 6.0), 5 mM potassium ferrocyanide, 5 mM potassium ferricyanide, 150 mM NaCl, 2 mM MgCl<sub>2</sub>]. Mouse aortas were then harvested and incubated in X-Gal solution at 37°C, no CO<sub>2</sub>, overnight. Tissue sections were then assessed for SA- $\beta$ -gal activity according to the abundance of positively stained blue cells by light microscopy.

#### **2.4. Harvesting of Mouse Type I Collagen**

Type I collagen was employed that is resistant to degradation by the interstitial collagenases (MMP1, MMP8, and MMP13) by virtue of a targeted mutation at the collagenase cleavage site, substituting proline for glutamine at the 774<sup>th</sup> residue, methionine for isoleucine at the 776<sup>th</sup> residue and proline for alanine at the 777<sup>th</sup> residue of the  $\alpha 1(I)$  chain (Dimri et al. 1995). Collagen was harvested from the tails of mice harbouring this mutation and their wild-type littermates. All steps were performed at 4°C. Tail tendons were excised and kept in 0.1 M glacial acetic acid for one day. Insoluble tendon pieces were removed and collagen was precipitated to a final concentration of 1.7 M NaCl. The precipitate was resuspended in 0.1 M acetic acid and re-precipitated to a final concentration of 1.7 M NaCl. This process was repeated a total of three times. Collagen was then dialysed against 0.18 M acetic acid for 3-5 days to remove all NaCl. The final collagen concentration was quantified by Lowry assay (Bio Rad). In order to coat dish surfaces with a collagen monolayer, cell culture dishes were incubated for three hours at room temperature with the designated collagen solution (0.1 mg/ml in acetic acid), then washed three times with phosphate-buffered saline (PBS).

#### **2.5. Isolation of Primary Human Vascular SMCs**

Primary cultures of human vascular SMCs were derived from internal thoracic arteries (ITA) of patients undergoing coronary artery bypass surgery, as previously described (Pickering et al. 1992). In each case, the ITA was isolated from surrounding connective tissue, split open, and the adventia and intima were removed by gentle scraping. The ITA was then cut into 2 mm segments and placed, intimal side up, onto a

fibronectin-coated tissue culture dish with supplemented M199 medium. After 1-2 weeks, explanted SMCs that had adhered to the culture dish were removed with the application of trypsin-EDTA (Invitrogen) and amplified by serial passage. SMCs studied for replicative longevity were grown on plastic for the first two cell passages following tissue explant, after which the cells were subcultured onto collagen until growth arrest.

## **2.6. Isolation of Primary Mouse Embryonic Fibroblasts.**

Primary MEFs were isolated as previously described (Xu 2005). MEFs were isolated at embryonic day 13.5 (E13.5) from both wild-type and *Coll1a1<sup>tr</sup>* mice. Female mice bearing offspring at E13.5 were euthanized and dissected in order to remove the uterus. The uterus was washed several times in PBS and subsequently the uterine wall and yolk sac were incised in order to dissect out the intact fetuses. Fetal liver, heart, brain and as much blood as possible was removed from the fetuses. The fetus was then minced into fine pieces and incubated in trypsin-EDTA (3 ml per embryo) in a tube at 4°C overnight. The next morning, trypsin-EDTA was aspirated, leaving an amount equivalent to approximately two volumes of tissue. MEF culture media was added and the tissue was pipetted up and down vigorously allowing for the digested tissue to break up into a cell suspension. The supernatant containing the cell suspension was then transferred to another tube. More MEF culture media was added to the tissue as before, vigorously pipetted, then supernatant was added to the cell suspension already collected. This cell suspension was transferred to tissue culture plates, and MEFs were then serially passaged.

## 2.7. Cell Culture

Cell culture experiments were performed using primary human vascular SMCs or MEFs, the latter derived from wild-type and *Colla1<sup>tr</sup>* mice. Cells were cultured at 37°C in a humidified atmosphere of 5% CO<sub>2</sub>. SMCs were maintained in Medium 199 (M199) (Invitrogen), supplemented with 1% penicillin G, 1% streptomycin, 1% L-glutamine and 10% fetal bovine serum (FBS) unless otherwise specified. MEFs were maintained in Dulbecco's Modified Eagle's Medium (DMEM) (Sigma) supplemented with 1% penicillin G, 1% streptomycin, 1% L-glutamine, 10% FBS and 0.1 mM beta-mercaptoethanol. Cell media was changed every 48 hours.

Cells were grown to 90-95% confluence and serially passaged at 4500 cells/cm<sup>2</sup> until growth arrest. This was determined by the inability of cultured cells to reach confluence, indicating a cessation of growth. Cumulative population doublings were assessed by counting cells prior to subculture using a hemocytometer and expressed as:

$$\log_{10}[(\text{number of cells harvested})/(\text{number of cells seeded})]/\log_{10}2.$$

SIPS was triggered by serum-withdrawal. Cells previously grown on plastic dishes were plated onto a collagen monolayer. Following three days of growth, SMCs were serum-deprived (0.5% FBS) for 3 days and then assessed for various senescence-related endpoints, as described in Sections 2.9 and 2.11.

## **2.8. Determination of Matrix Production by MEFs**

I used circular polarization microscopy to evaluate for the presence of type I collagen fibrils in culture. MEFs grown on glass coverslips were administered fresh ascorbate (100  $\mu$ M) every 48 hours for up to two weeks in order to improve triple helical structure stabilization of procollagen. Cells were fixed with 4% paraformaldehyde for 20 minutes. Picosirius Red Stain Kit (Polysciences) was used to stain collagen fibrils as follows: Cells were incubated for two minutes with phosphomolybdic acid hydrate; cells were then stained for 60 minutes with Picosirius Red solution; finally cells were incubated for two minutes with hydrochloric acid. Cells on coverslips were then dehydrated in an ascending gradient of ethanol and mounted on slides using Cytoseal 60 (Thermo Scientific). Imaging was performed as described in Section 2.12.

## **2.9. Assessment of Senescence-associated $\beta$ -galactosidase Activity in Cultured Cells**

Upon reaching ~70% confluence, cells were assessed for SA- $\beta$ -gal activity, as previously described (Dimri et al. 1995). SMCs were fixed with 2% formaldehyde/0.2% glutaraldehyde in PBS for 3 minutes. SMCs were then washed with PBS and incubated at 37°C with fresh SA- $\beta$ -gal solution overnight as described above. Cells were counterstained with Hoechst 33258 (2.5  $\mu$ l/ml) and the proportion of SA- $\beta$ -gal positive cells was quantified by counting approximately 1000 cells.

MEFs were assessed for SA- $\beta$ -gal activity using a slightly modified protocol as follows (Yang et al. 2000). MEFs were fixed with 0.5% glutaraldehyde in PBS for 10 minutes. MEFs were then washed with PBS (pH 6.0, supplemented with 1 mM  $MgCl_2$ ) and incubated overnight at 37°C with fresh modified SA- $\beta$ -gal solution (0.5 mg/ml X-gal,

0.12 mM potassium ferrocyanide, 0.12 mM potassium ferricyanide, 1 mM MgCl<sub>2</sub> at a pH of 6.0 in PBS).

## **2.10. Quantitative Real-time Reverse Transcription – Polymerase Chain Reaction**

SMCs in culture were trypsinized and centrifuged into a tightly packed pellet that was washed three times with PBS. SMCs were then lysed via incubation with Trizol (Invitrogen) reagent for 5 minutes at room temperature. Two hundred microlitres of chloroform per 1 ml of Trizol was added to the mixture and allowed to incubate for three minutes at room temperature. The mixture was then centrifuged at 12,200 rpm for 15 minutes at 4°C resulting in a discarded organic phase consisting of DNA and protein, and an aqueous phase containing nearly all the RNA. RNA was precipitated by 70% ethanol and subsequently washed using the QiaGen RNeasy Kit and protocol. In brief, precipitated RNA was collected in an RNeasy mini column, and subsequently washed using Buffer RW1 and RPE, then eluted using RNase-free water. Total RNA concentration was quantified by UV spectrophotometry using a NanoDrop ND-1000 (Thermo Scientific).

Multiscribe Reverse Transcriptase (Applied Biosystems) was used to synthesize cDNA from single stranded mRNA. In brief, the RNA sample, 1X RT Buffer, 1X dNTP mix, 1X random primers and Multiscribe Reverse Transcriptase (2.5 U/μl) were incubated at 25°C for 10 minutes, 37°C for 120 minutes and 85°C for 5 seconds in order to allow for thorough reverse transcription. Transcript abundance of human p21<sup>CIP1</sup> (Hs00355782\_m1), human p16<sup>INK4A</sup> (custom primer/probe set using the following sequence: forward primer – CCAACGCACCGAATAGTTACG; reverse primer –

CGCTGCCCATCATCATGAC; probe - TCGGAGGCCGATCCAG), and human GAPDH (Hs00266705\_g1) as an endogenous loading control was assessed by a Taqman-based primer/probe set (Applied Biosystems). A total of 30  $\mu$ g of generated cDNA was subjected to 40 cycles of PCR. Signal detection was performed by the ABI 7900HT Fast Real-time PCR apparatus and analyzed by the Sequence Detection System software (Applied Biosystems). Relative quantification of mRNA abundance based on critical threshold (CT) was assessed with the following method:

Relative difference in mRNA abundance:

$$=2^{-\Delta\Delta CT}$$

$$=2^{-(\Delta CT[\text{condition A}] - \Delta CT[\text{condition B}])}$$

$$=2^{-((CT[\text{target condition A}] - CT[\text{reference condition A}]) - (CT[\text{target condition B}] - CT[\text{reference condition B}])))}$$

For example, in order to determine relative abundance of p21<sup>CIP1</sup> in SMCs grown on Coll1a1<sup>r/r</sup> collagen for 9 CPDs the following was used: target condition A = p21<sup>CIP1</sup> signal for SMCs grown on Coll1a1<sup>r/r</sup> collagen for 9 CPDs; target condition B = p21<sup>CIP1</sup> signal for SMCs grown on wild-type collagen for 3 CPDs (these cells were used as the baseline in all assessments); reference condition A = GAPDH signal for SMCs grown on Coll1a1<sup>r/r</sup> collagen for 9 CPDs; reference condition B = GAPDH signal for SMCs grown on wild-type collagen for 3 CPDs.

## 2.11. Western Blot Analysis

Protein expression was determined by Western Blot analysis. Cells grown on cell culture dishes were washed with PBS, trypsinized and centrifuged. Cells were lysed with

RIPA buffer (50 mM Tris, 150 mM NaCl, 1% Igepal (Sigma), 0.5% sodium deoxycholate, 0.1% SDS) containing 1% protease inhibitor cocktail (Sigma). Cell lysate was centrifuged at 12,000 RPM at 4°C for 10 minutes in order to separate the insoluble cell membrane fraction from the soluble intracellular protein. Final total protein concentration was quantified by colorimetry with a BCA Protein Assay Reagent kit (Thermo Scientific) and quantified with a Multiskan Ascent plate reader (Thermo Electron Corporation).

Equal protein quantities (40 µg) were resolved by SDS-polyacrylamide gel electrophoresis using a 15% gel. Resolved protein was then electrophoretically transferred onto an Immobilon-P polyvinylidene difluoride (PVDF) membrane (Millipore). In order to reduce non-specific binding, membranes were incubated in blocking buffer (Tris-buffered saline containing 5% non-fat dry milk and 0.1% Tween-20) for 1 hour at room temperature. Membranes were probed for protein of interest by incubating with primary antibody diluted in blocking buffer overnight. Primary antibodies, along with dilution factor used were as follows: human and mouse p21<sup>CIP1</sup>, 1:1000 (sc-756, Santa Cruz); human p16<sup>INK4A</sup>, 1:500 (51-1325GR, BD Biosciences); mouse p16<sup>INK4A</sup>, 1:500 (sc-1207, Santa Cruz); human p14<sup>ARF</sup> and mouse p19<sup>ARF</sup>, 1:500 (sc-1063, Santa Cruz); human and mouse α-Tubulin, 1:30000 (T5168, Sigma-Aldrich). Membranes were then washed and probed with secondary antibody, a horseradish peroxidase conjugated anti-mouse IgG (from sheep) or anti-rabbit IgG (from donkey) (Amersham Biosciences). Bound secondary antibody was detected using the Super Signal West Pico chemiluminescent substrate (Pierce) and visualized by exposure on Amersham

Hyperfilm (GE Healthcare). Relative protein abundance was quantified with Quantity One imaging software (Bio-Rad) and normalized to endogenous reference  $\alpha$ -tubulin.

## **2.12. Microscopy and Image Analysis**

Cell morphology was assessed from images acquired using a Zeiss Axiovert S100 microscope (Carl Zeiss Microimaging Inc.) equipped with Hoffman Modulation Contrast Plan objectives and model TCT condenser (Modulation Optics Inc.), cooled QICAM Mono Fast 1394 camera (QImaging Inc.), and Northern Eclipse image analysis software (Empix Imaging Inc.).  $\beta$ -gal-stained cells were imaged using an Olympus BX-50 microscope with an Olympus BH2-RFL-T3 illuminator, UPlan objective lenses (Olympus Optical Co. Ltd.), Hitachi HV-F22 camera (Hitachi Ltd.) and Northern Eclipse image analysis software. Vascular histology section images were acquired using an Olympus BX-51 microscope, UPlan objective lenses, cooled Retiga EXi Mono Fast 1394 camera (QImaging Inc.), and Northern Eclipse image analysis software. Collagen fibril formation images were acquired using an Olympus BX51 microscope, UPlan objective lenses, Abrio CCD camera, Olympus BX series liquid crystal compensator, Olympus BX series circular polarizer/interference filter optic and Abrio image analysis software (Cambridge Research & Instrumentation, Inc.)

## **2.13. Data Analysis**

All values are expressed as mean  $\pm$  standard error (SE) unless otherwise indicated. Statistical analysis was performed using GraphPad Prism software (Version 5.0b, Graphpad Software Inc.). Kaplan-Meier Survival analysis was analyzed using a log-

rank and Wilcoxon test. All other comparisons were made using Student's t-test, as each analysis was made with respect to the effect of wild-type versus  $\text{Colla1}^{\text{tr}}$  collagen. Statistical significance was set at  $p < 0.05$ .

## **Chapter 3**

### **Results**

### 3.1. $Coll1a1^{r/r}$ Mice Display Impaired Weight Gain

To determine if the accumulation of type I collagen with reduced susceptibility to proteolysis is associated with accelerated aging, I made use of a strain of mice harbouring a mutation that renders endogenous type I collagen resistant to proteolytic editing ( $Coll1a1^{r/r}$ ). These mice have been previously studied and found to have thickened skin and associated patchy hair loss (Liu et al. 1995). I also observed this phenotype in our colonies (Figure 3.1A). However, no studies to date have evaluated phenotypic changes in these mice as they age. To further evaluate the consequences of this collagen mutation, I first assessed attributes of young adult mice as a baseline. Mice 2-5 months of age homozygous for the mutation weighed slightly less than their wild-type littermates with a mean weight of  $22.9 \text{ g} \pm 0.5 \text{ g}$  versus  $26.9 \text{ g} \pm 0.6 \text{ g}$  respectively ( $p < 0.01$ ) (Figure 3.1B). To determine whether the reduced body weight could be attributed to differences in food consumption, the dietary intake of three pairs of littermates was observed for 46 days in the first two pairs and 56 days in the third pair. No significant differences in food consumption, relative to body weight, were found between littermates in the three pairs of mice ( $p = \text{NS}$ ) (Figure 3.1C).

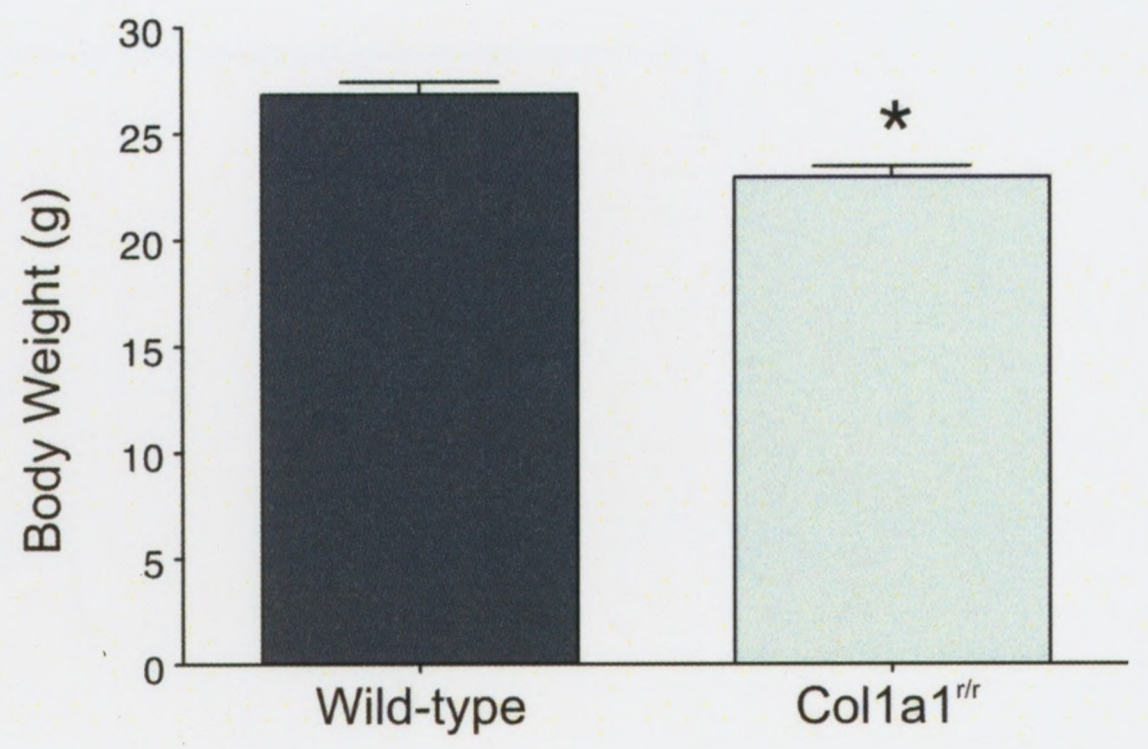
### 3.2. $Coll1a1^{r/r}$ Mice Exhibit Decreased Lifespan

To determine if there were differences in the lifespan of the mice, I followed 23 wild-type mice and 28  $Coll1a1^{r/r}$  mice for up to 2 and half years. By 26 months, all wild-type mice were still alive, while only 11  $Coll1a1^{r/r}$  mice remained alive. Kaplan-Meier survival analysis confirmed that  $Coll1a1^{r/r}$  mice died prematurely, particularly during the second year ( $p < 0.05$ ) (Figure 3.2). In an effort to determine if this increased mortality

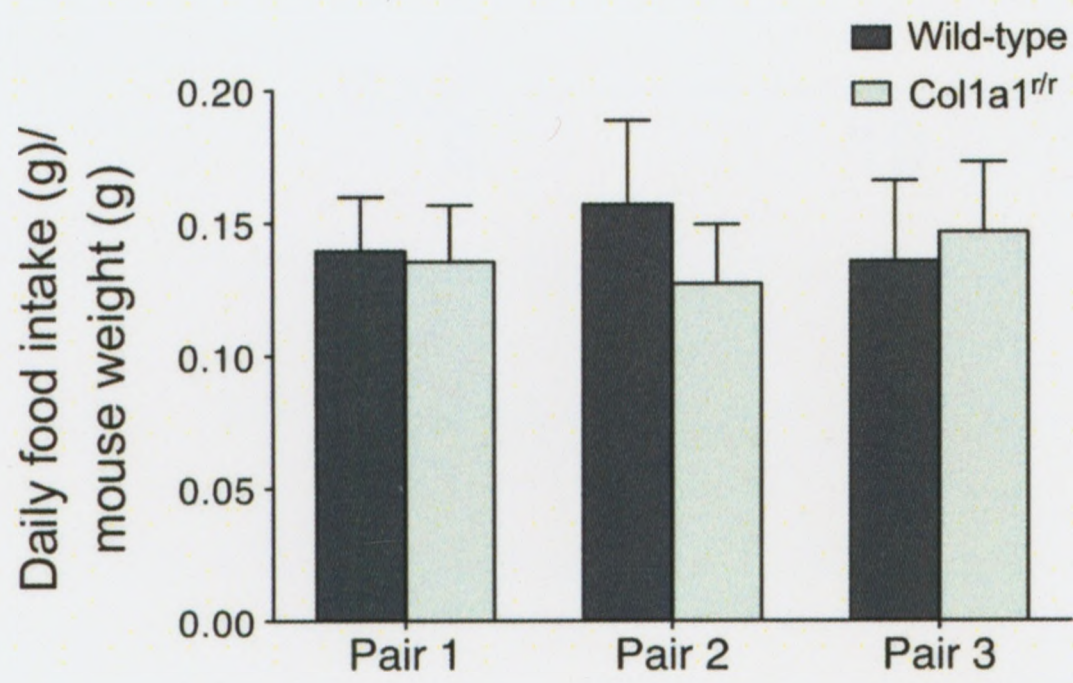
**Figure 3.1.**  $Coll1a1^{r/r}$  mice display impaired weight gain and decreased lifespan. *A*, Images of a C57BL/6  $Coll1a1^{r/r}$  mouse and its wild-type littermate at 12 months of age are shown. The  $Coll1a1^{r/r}$  mouse is noticeably smaller and is losing hair on its back. *B*, A bar graph depicting the average weights of littermates of C57BL/6, 129s, and mixed 129s x C57BL/6 background is shown. Wild-type (n=28) and  $Coll1a1^{r/r}$  (n=14) littermates were weighed at 2-5 months of age. Wild-type mice had an average weight of  $26.9 \text{ g} \pm 0.6 \text{ g}$  and  $Coll1a1^{r/r}$  mice had an average weight of  $22.9 \text{ g} \pm 0.5 \text{ g}$ . Statistical analysis revealed a significant difference ( $p < 0.01$ ). *C*, A bar graph displaying the average daily dietary intake of three different pairs of littermates [Pair 1 – 129 x C57BL/6 (n=46 days); Pair 2 – 129s (n=46 days); Pair 3 – 129s (n=56 days)] corrected for body weight. Error bars indicate standard deviation of the mean. No significant difference in food intake relative to body weight was revealed between  $Coll1a1^{r/r}$  mice and wild-type mice.



A



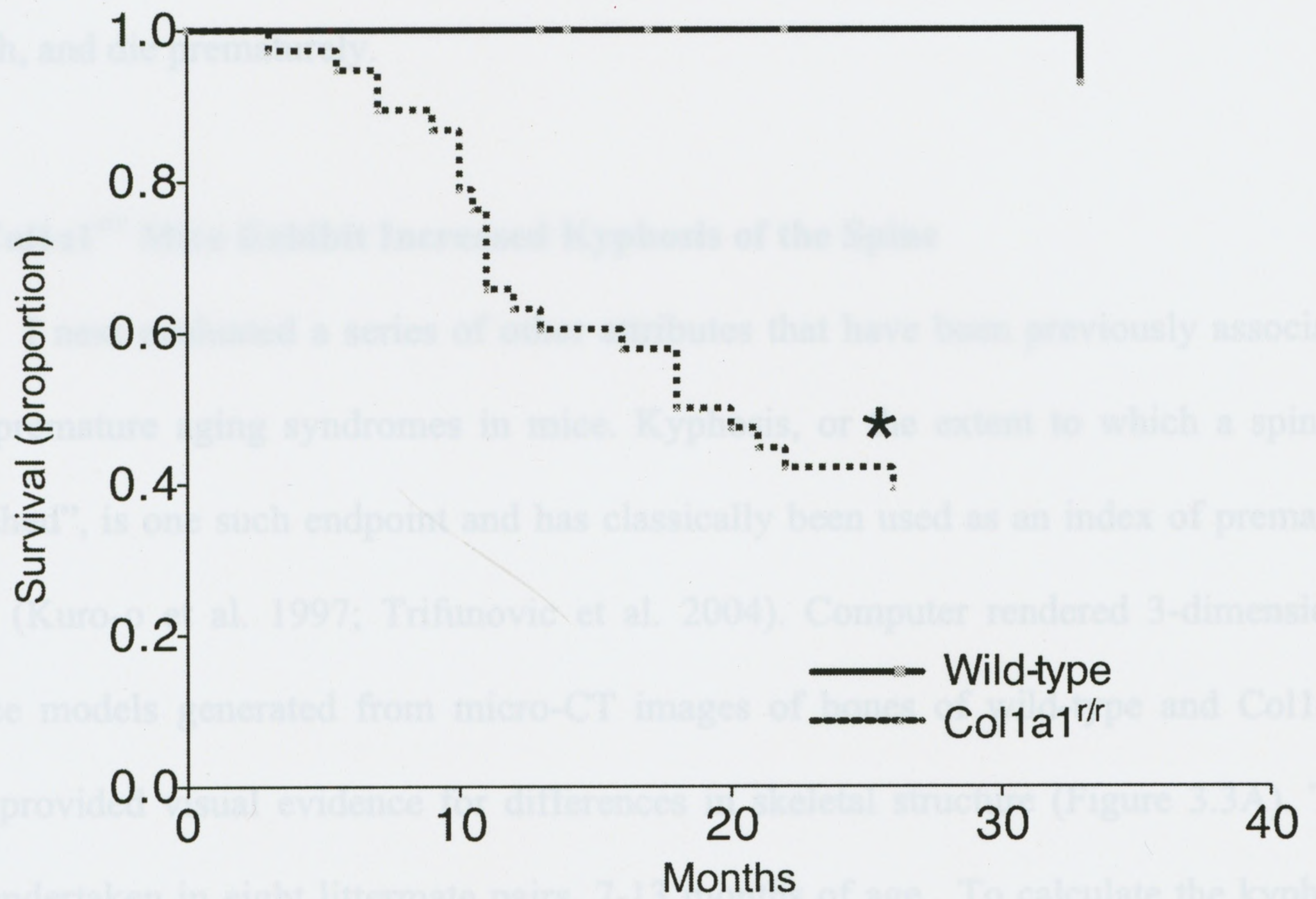
B



C

**Figure 3.2.** Kaplan-Meier Survival Analysis was performed on wild-type (n=23) and  $\text{Colla1}^{r/r}$  (n=28) mice over a period of 33 months. Log-rank and Wilcoxon tests revealed a significant decrease in survival of  $\text{Colla1}^{r/r}$  mice ( $p < 0.05$ ).

was due to specific organ failure, I performed a serological screen on mice at 3, 7 and 17 months of age. Specific organ dysfunction was not evident from this screen, as shown by the lack of significant differences seen in urea, creatinine, aspartate transaminase, alanine transaminase, alkaline phosphatase, bilirubin, albumin, glucose,  $\text{Na}^+$ ,  $\text{K}^+$  and  $\text{Cl}^-$  levels between wild-type and  $\text{Col1a1}^{\text{fl/fl}}$  mice ( $n=1$ ) ( $p=\text{NS}$ ) (Table 3.1). Thus it is observed that, despite normal serology,  $\text{Col1a1}^{\text{fl/fl}}$  mice display impaired early-stage weight gain and growth, and



was due to specific organ failure, I performed a serological screen on mice at 3, 7 and 17 months of age. Specific organ dysfunction was not evident from this screen, as shown by the lack of significant differences seen in urea, creatinine, aspartate transaminase, alanine transaminase, alkaline phosphatase, bilirubin, albumin, glucose, Na<sup>+</sup>, K<sup>+</sup> and Cl<sup>-</sup> levels between wild-type and *Coll1a1<sup>r/r</sup>* mice (n=1) (p=NS) (Table 3.1). Thus it is observed that, despite normal serology, *Coll1a1<sup>r/r</sup>* mice display impaired early-stage weight gain and growth, and die prematurely.

### **3.3. *Coll1a1<sup>r/r</sup>* Mice Exhibit Increased Kyphosis of the Spine**

I next evaluated a series of other attributes that have been previously associated with premature aging syndromes in mice. Kyphosis, or the extent to which a spine is “hunched”, is one such endpoint and has classically been used as an index of premature aging (Kuro-o et al. 1997; Trifunovic et al. 2004). Computer rendered 3-dimensional surface models generated from micro-CT images of bones of wild-type and *Coll1a1<sup>r/r</sup>* mice provided visual evidence for differences in skeletal structure (Figure 3.3A). This was undertaken in eight littermate pairs, 7-13 months of age. To calculate the kyphotic index, the distance from the 7<sup>th</sup> cervical vertebrae to the 6<sup>th</sup> lumbar vertebrae was compared to the greatest height of the curve in the mice (Figure 3.3B). *Coll1a1<sup>r/r</sup>* mice exhibited a 46.2% ± 0.1% increase in kyphosis relative to wild-type mice (n=8) (p<0.01) (Figure 3.3C).

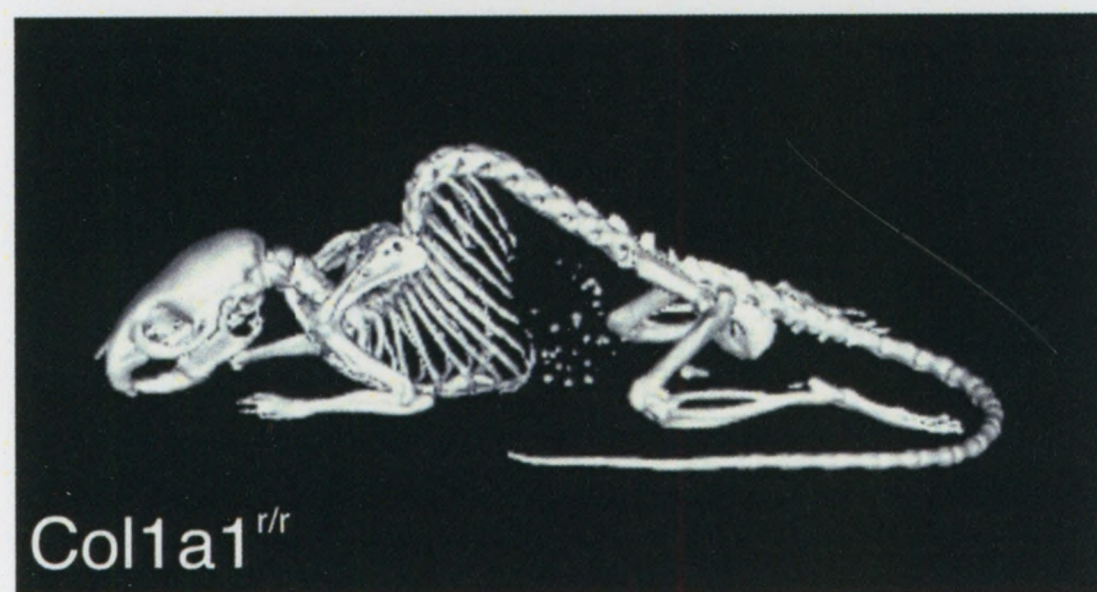
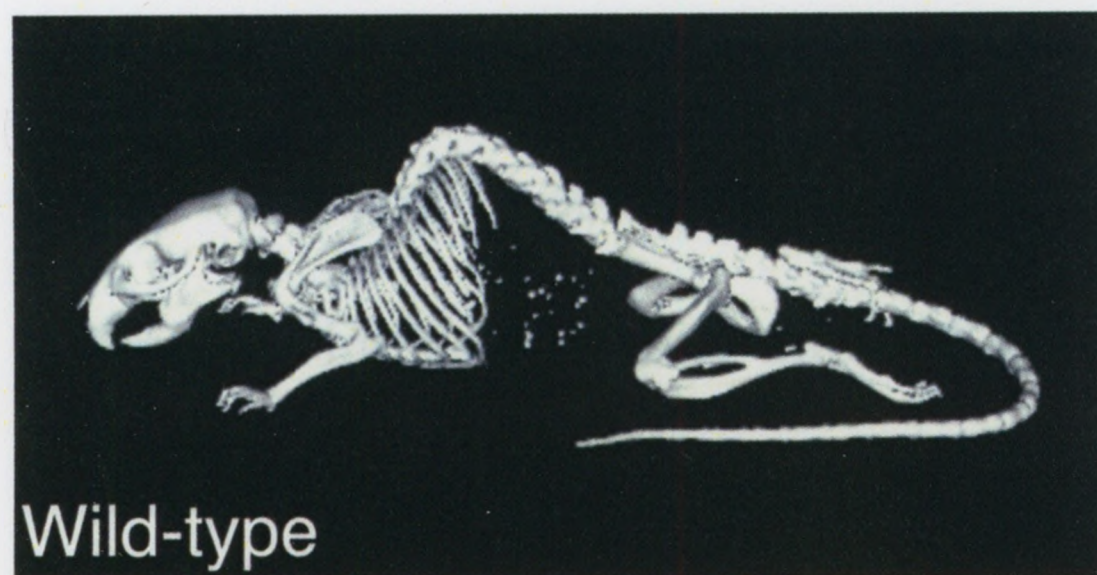
**Table 3.1.** Colla1<sup>r/r</sup> mice display normal serology. A table displaying serological screening results of wild-type and Colla1<sup>r/r</sup> littermates at 3 months, 7 months and 17 months of age is shown (n=1). Anesthetized mice had blood drawn via cardiac puncture. Blood serum was isolated and sent to Charles River Animal Diagnostic Services for analysis. Statistical analysis reveals no significant difference between wild-type and Colla1<sup>r/r</sup> mice across all results. QNS indicates that the quantity of serum was not sufficient for analysis.

Mouse ID#	PB25N4	PB25M2	PB24G3	PB24H5	PB21W7	PB21W5
Genotype	Wild-type	Colla1 <sup>rr</sup>	Wild-type	Colla1 <sup>rr</sup>	Wild-type	Colla1 <sup>rr</sup>
Age	3 months	3 months	7 months	7 months	17 months	17 months
Cholesterol (mg/dl)	145	120	152	104	98	42
Triglycerides (mg/dl)	162	94	164	113	139	124
Alanine aminotransferase (u/l)	57	40	58	37	39	36
Aspartate aminotransferase (u/l)	153	71	68	93	108	149
Alkaline phosphatase (u/l)	86	92	69	75	48	80
Bilirubin (total) (mg/dl)	0.4	0.2	0.3	0.2	0.2	0.3
Glucose (mg/dl)	258	226	237	207	152	134
Inorganic phosphate (mg/dl)	9.3	7.9	8.9	8.8	9	8.6
Total protein (g/dl)	5.9	5.8	6.1	6.1	5.2	4.7
Calcium (mg/dl)	10.3	11	11.1	10.9	10.4	9.6
Blood urea nitrogen (mg/dl)	22	24	25	20	21	24
Creatinine (mg/dl)	0.4	0.4	0.4	0.3	0.3	0.2
Albumin (g/dl)	3.4	3.3	3.4	3.2	2.7	2.4
Sodium (meq/l)	QNS	159.5	159	122.6	153.3	160.5
Potassium (meq/l)	QNS	7.87	6.82	6.44	9.91	8.93
Chloride (meq/l)	QNS	118.3	115.6	91.9	114.3	119.3

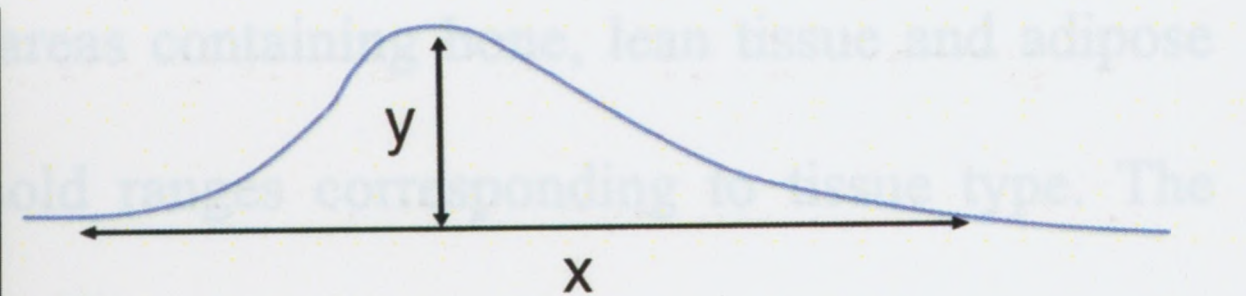
**Figure 3.3.**  $Coll1a1^{r/r}$  mice display increased kyphosis of the spine. *A*, Computer rendered 3D surface models of micro-CT images of 17-month old wild-type and  $Coll1a1^{r/r}$  129s x C57BL/6 littermates are shown. Exaggerated spinal curvature is evident in the  $Coll1a1^{r/r}$  mouse. *B*, A schematic depicting the method of kyphotic index measurement. Kyphotic index was determined by  $y/x$  ( $x$  = distance from the 7<sup>th</sup> cervical vertebrae to the 6<sup>th</sup> lumbar vertebrae;  $y$  = distance from the greatest height of the spinal curve). *C*, A bar graph revealing a significant increase ( $1.46 \pm 0.08$  fold) in the average kyphotic index of  $Coll1a1^{r/r}$  mice ( $p < 0.01$ ) is shown. 129s and C57BL/6  $Coll1a1^{r/r}$  mice ( $n=8$ ) 7-13 months of age were measured to determine the kyphotic index and this was normalized to the corresponding wild-type littermates.

### 3.4. *Col1a1*<sup>fl/fl</sup> Mice Exhibit Decreased Body Fat

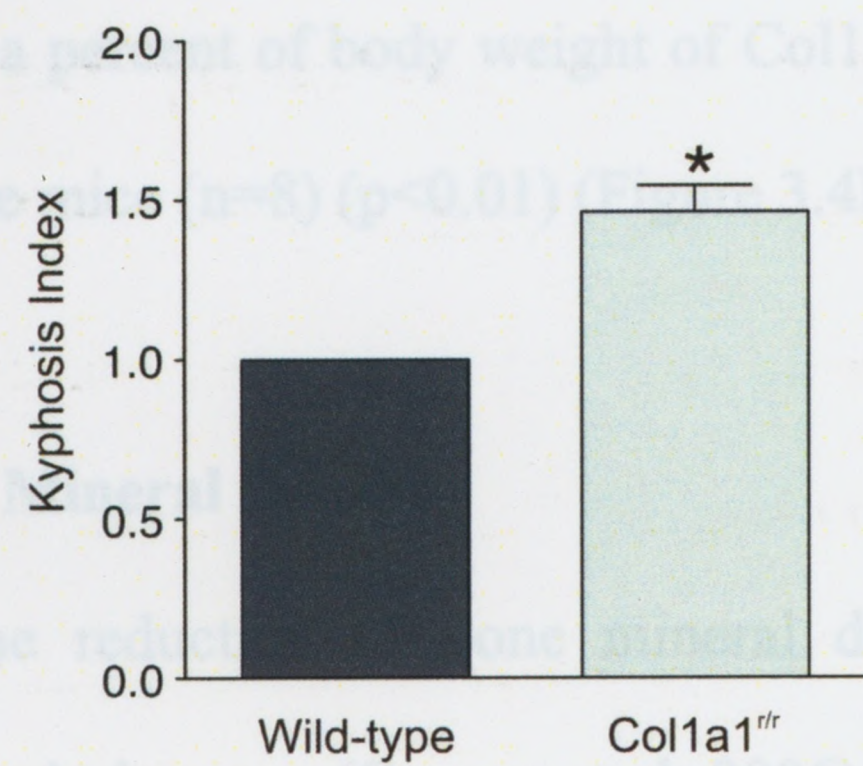
Reduction of body fat is a common characteristic in elderly humans (Mott et al. 1999). Mice that are prematurely aging also display decreased body fat composition (Trifunovic et al. 2004). To determine whether *Col1a1*<sup>fl/fl</sup> mice had decreased body fat content, whole-body micro-CT imaging was implemented in the mice (Figure 3.4A).



A



B



C

Other commonly found characteristic in elderly humans (Casper et al. 2006) and mice (Kuro-o et al. 1997). Cylindrical calibration samples were included in each micro-CT scan, the first being a tissue-equivalent plastic with zero bone-mineral content and the second being a bone-mimicking epoxy (SB3) containing an equivalent of 1.1 grams of hydroxy apatite per  $\text{cm}^3$ . CT grey-scale intensities were measured when acquiring micro-CT images of the mice and bone-mineral content was calculated by comparing unknown CT numbers to the calibration samples. Skeletal bone-mineral density of *Col1a1*<sup>fl/fl</sup> mice ( $0.99 \pm 0.002$  grams of hydroxy apatite per  $\text{cm}^3$ ) was significantly lower than that of

### 3.4. $Coll1a1^{r/r}$ Mice Exhibit Decreased Body Fat

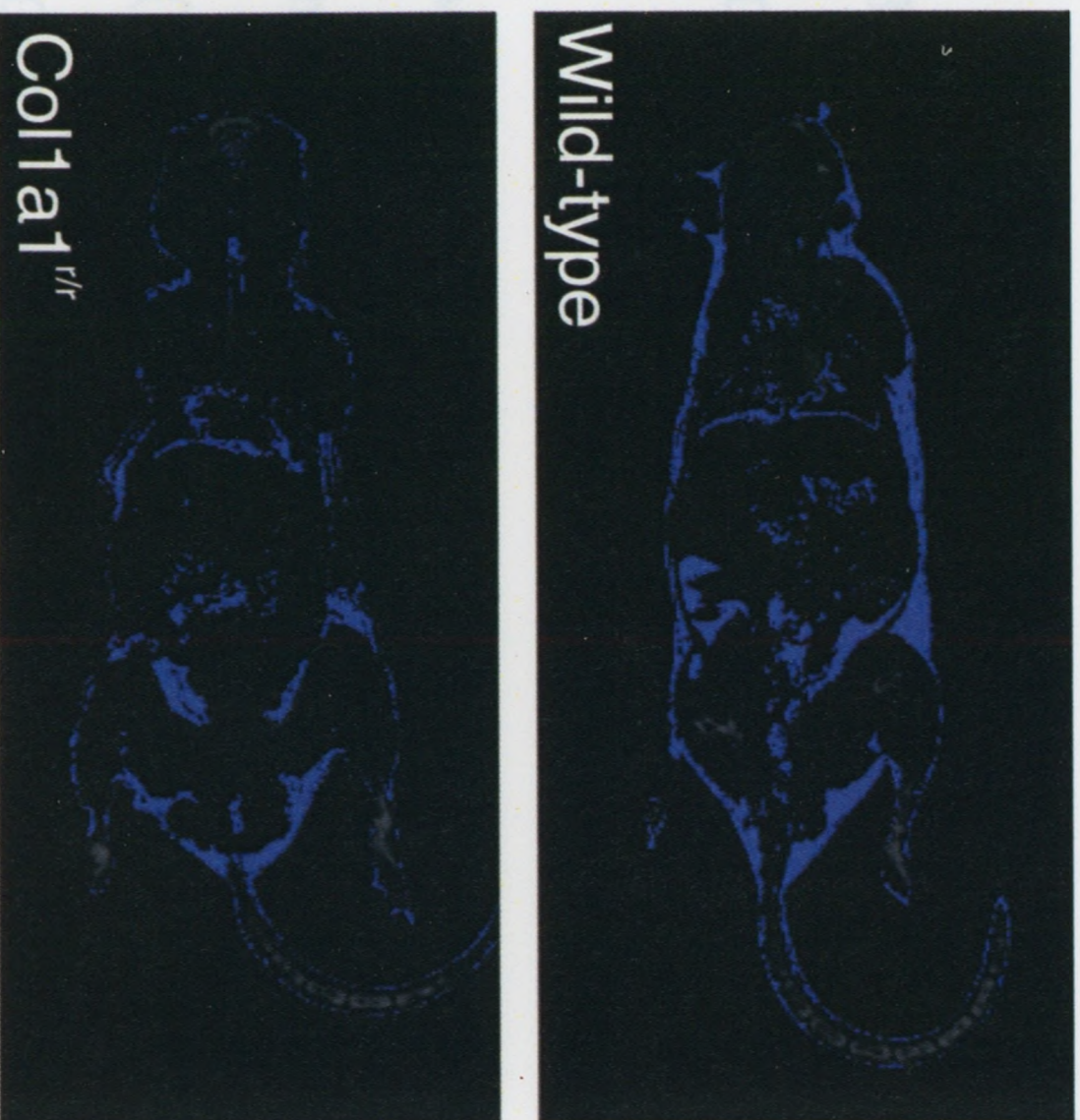
Reduction of body fat is a common characteristic in elderly humans (Mott et al. 1999). Mice that are prematurely aging also display decreased body fat composition (Trifunovic et al. 2004). To determine whether  $Coll1a1^{r/r}$  mice had decreased body fat content, whole-body micro-CT imaging was implemented in the mice (Figure 3.4A). Gray scale intensity of voxels in known areas containing bone, lean tissue and adipose tissue was used to establish three threshold ranges corresponding to tissue type. The differences in tissue density allowed us to differentiate between imaged bone, lean tissue and adipose tissue. Adipose tissue content as a percent of body weight of  $Coll1a1^{r/r}$  mice was  $68.7\% \pm 2.5\%$  lower than that of wild-type mice ( $n=8$ ) ( $p<0.01$ ) (Figure 3.4B).

### 3.5. $Coll1a1^{r/r}$ Mice Exhibit Decreased Bone Mineral Density

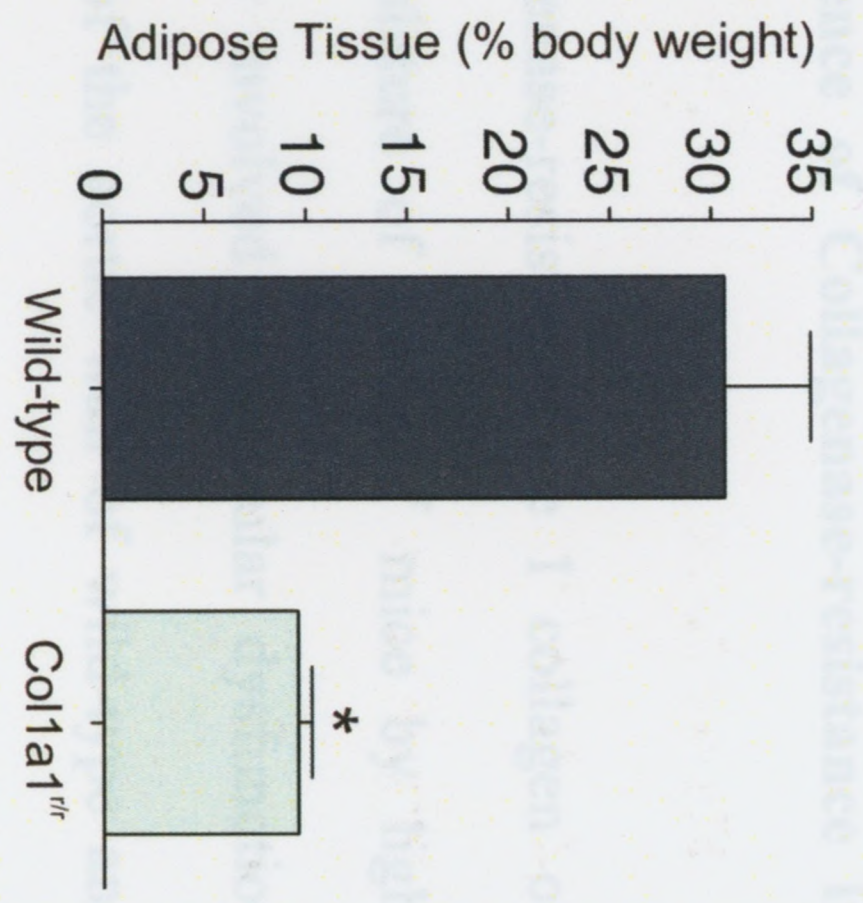
Osteoporosis, a disease involving the reduction of bone mineral density, is another commonly found characteristic in elderly humans (Cooper et al. 2006) and mice (Kuro-o et al. 1997). Cylindrical calibration samples were included in each micro-CT scan, the first being a tissue-equivalent plastic with zero bone-mineral content and the second being a bone-mimicking epoxy (SB3) containing an equivalent of 1.1 grams of hydroxy apatite per  $cm^3$ . CT grey-scale intensities were measured when acquiring micro-CT images of the mice and bone-mineral content was calculated by comparing unknown CT numbers to the calibration samples. Skeletal bone-mineral density of  $Coll1a1^{r/r}$  mice ( $0.99 \pm 0.002$  grams of hydroxy apatite per  $cm^3$ ) was significantly lower than that of

**Figure 3.4.**  $Coll1a1^{r/r}$  mice exhibit decreased body fat and reduced bone mineral density.

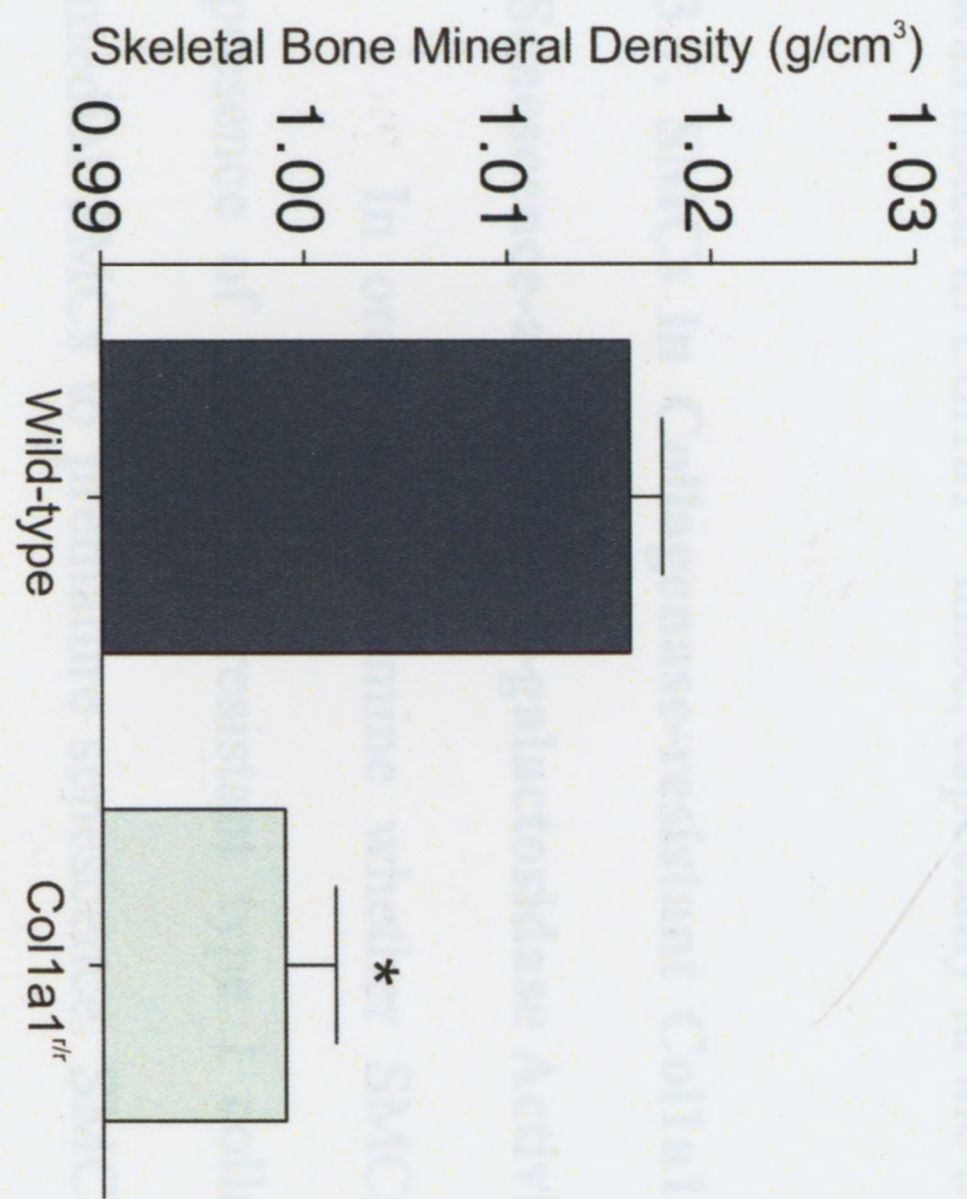
*A*, Reconstructed micro-CT image slices of a wild-type and  $Coll1a1^{r/r}$  129 x C57BL/6 littermate overlaid with adipose tissue composition are shown. Based on three pre-established voxel intensity thresholds corresponding to lean tissue, adipose tissue and skeletal tissue, an overlay with voxel density corresponding to adipose tissue is highlighted in blue. *B*, A bar graph revealing that 7-13 month old  $Coll1a1^{r/r}$  mice (C57BL/6J and 129s) had a significantly lower average proportion of adipose tissue ( $30.7\% \pm 4.2\%$ ) than their wild-type littermates ( $9.6\% \pm 0.7\%$ ) ( $n=8$ ) ( $p<0.01$ ) as assessed by micro-CT analysis is shown. CT number of tissue was measured and compared to recognized CT number of adipose tissue in order to determine tissue composition. *C*, A bar graph revealing that 7-13 month old  $Coll1a1^{r/r}$  mice (C57BL/6J and 129s) had significantly lower average bone mineral density ( $1.016 \pm 0.002$  grams of hydroxy apatite per cubic centimetre) than their wild-type littermates ( $0.99 \text{ g HA/cm}^3 \pm 0.002 \text{ g HA/cm}^3$ ) ( $n=8$ ) ( $p<0.01$ ) is shown. This was determined by plotting CT numbers of bones of unknown mineral density from mice against a curve generated from the CT numbers of a tissue-equivalent plastic ( $0 \text{ g HA/cm}^3$ ) and bone-mimicking epoxy material (SB3) ( $1.1 \text{ g HA/cm}^3$ ).



A



B



C

Left internal carotid artery and the aortic arch was investigated based on  $\beta$ -galactosidase activity. Mice were perfused with fresh SA- $\beta$ -gal solution (1 mg of X-Gal per ml stock + 20 mg/ml 1-dimethylformamide)/40 mM citric acid/0.1 M phosphate buffer, pH 6.0/5 mM potassium ferrioxalate/5 mM potassium ferricyanide/150 mM NaCl/2 mM

wild-type mice ( $1.016 \pm 0.002$  grams of hydroxy apatite per  $\text{cm}^3$ ) ( $n=8$ ) ( $p<0.01$ ) (Figure 3.4C).

### **3.6. Disrupted Elastin is a Vascular Consequence of Collagenase-resistance in $\text{Coll1a1}^{r/r}$ mice**

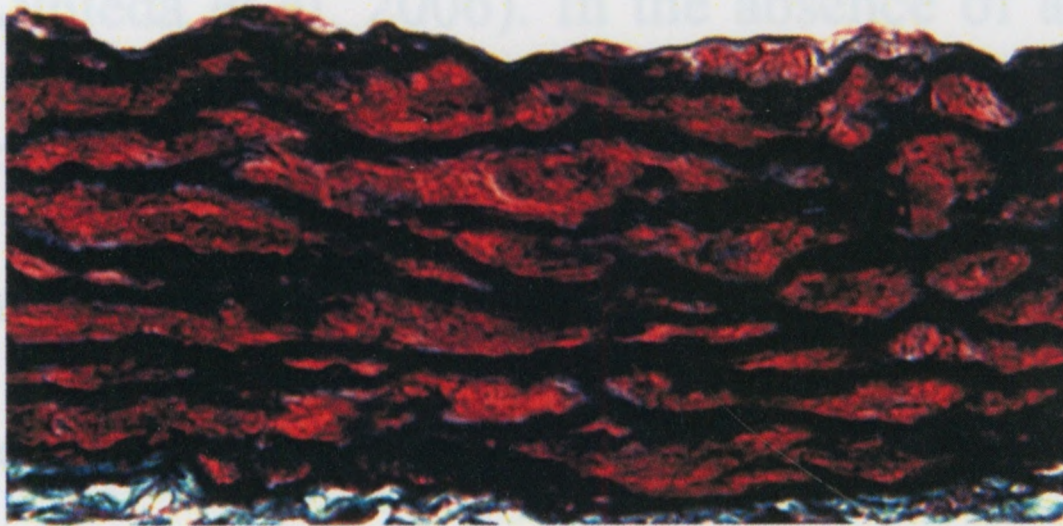
To determine the consequences of collagenase-resistant type I collagen on vascular health and aging I examined the vasculature of  $\text{Coll1a1}^{r/r}$  mice by light microscopy. Elastin disruption is a known factor involved in vascular dysfunction (MacSweeney et al. 1994). Histological analysis of the aortic wall of wild-type and  $\text{Coll1a1}^{r/r}$  mice stained with elastin trichrome revealed a normal elastin lamellae in wild-type mice, while  $\text{Coll1a1}^{r/r}$  mice displayed broken elastin lamellae. As well, more fibrosis was noted in  $\text{Coll1a1}^{r/r}$  mice, especially in the outer media (Figure 3.5).

### **3.7. SMCs in Collagenase-resistant $\text{Coll1a1}^{r/r}$ Mice are Predisposed to Expressing Senescence-associated $\beta$ -galactosidase Activity in the Artery Wall**

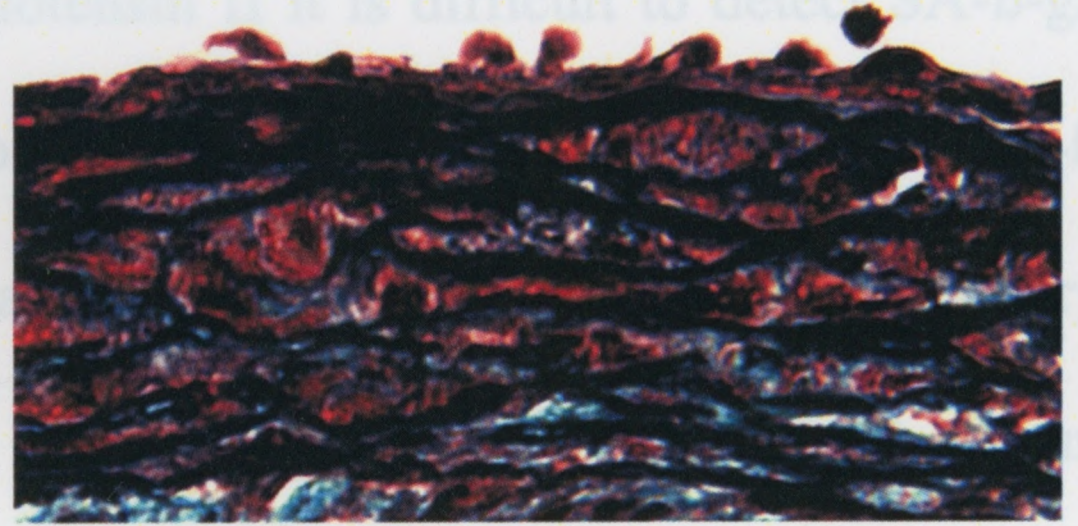
In order to determine whether SMCs in the aortic wall are affected by the presence of proteolysis-resistant type I collagen, I investigated the susceptibility of medial SMCs to premature senescence. SMC senescence in the brachiocephalic artery, the left internal carotid artery and the aortic arch was investigated based on  $\beta$ -galactosidase activity. Mice were perfused with fresh SA- $\beta$ -gal solution (1 mg of X-Gal per ml (stock = 20 mg/ml in dimethylformamide)/40 mM citric acid/sodium phosphate, pH 6.0/5 mM potassium ferrocyanide/5 mM potassium ferricyanide/150 mM NaCl/2 mM

**Figure 3.5.**  $Coll1a1^{r/r}$  mice exhibit disrupted elastin in the aortic wall. Images using bright field microscopy of ascending aorta of 22-month old littermates stained with elastin trichrome are shown. There are noticeable changes in the ECM, specifically the disruption of elastin (in black) and increased fibrosis (in blue) in the medial layer of the aorta in the  $Coll1a1^{r/r}$  mouse.

MgCl<sub>2</sub>) followed by overnight incubation in fresh SA- $\beta$ -gal at 37°C. Under these conditions, I was unable to detect SA- $\beta$ -gal activity in SMCs in the artery wall. Therefore, in order to impose stress, mice were administered angiotensin II via mini-pump at a concentration of 1.4 mg/kg body weight/day for 28 days. Angiotensin II is a known inducer of ROS production in cultured vascular SMCs resulting in both telomere dependent and telomere independent SPS as assessed by elevated  $\beta$ -gal activity and increased p53 and p21<sup>CIP1</sup> expression (Herbert et al. 2008). Angiotensin II has also been shown to significantly increase SA- $\beta$ -gal activity and p21<sup>CIP1</sup> expression in ApoE<sup>-/-</sup> mice (Kawabuchi et al. 2006). In the absence of angiotensin II it is difficult to detect SA- $\beta$ -gal



Wild-type

Col1a1<sup>r/r</sup>

3.6B) closer at the ascending aorta. In Col1a1<sup>r/r</sup> mice, senescent cells were specifically detected in the outer layers of the media. In contrast, there were no senescent SMCs found in the ascending aortas of wild-type littermates (Figure 3.6B).

Results examining Col1a1<sup>r/r</sup> mouse survivability, weight, adipose tissue content, kyphosis, and bone mineral density provide strong evidence for the notion that the inability to cleave type I collagen in mice results in a phenotype reminiscent of accelerated aging. Our findings in the vasculature provide further evidence for aging in the aortic wall.

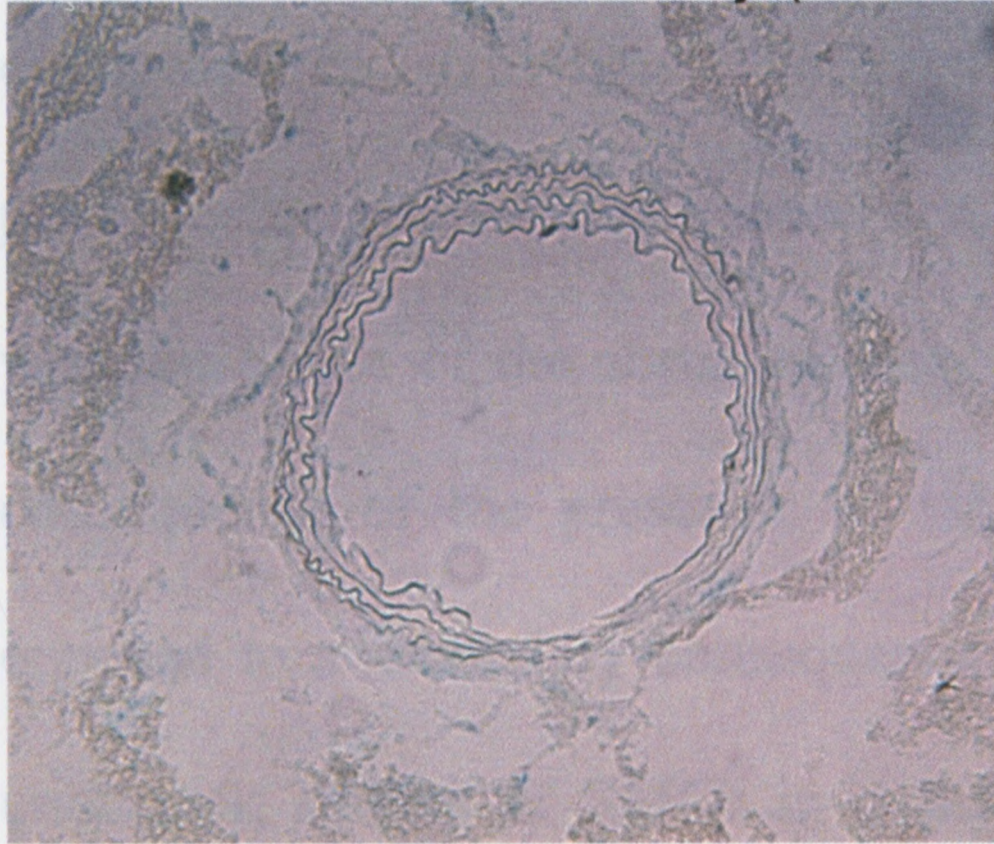
MgCl<sub>2</sub>) followed by overnight incubation in fresh SA-β-gal at 37°C. Under these conditions, I was unable to detect SA-β-gal activity in SMCs in the artery wall. Therefore, in order to impose stress, mice were administered angiotensin II via mini-pump at a concentration of 1.4 mg/kg body weight/day for 28 days. Angiotensin II is a known inducer of ROS production in cultured vascular SMCs resulting in both telomere dependent and telomere independent SIPS as assessed by elevated β-gal activity and increased p53 and p21<sup>CIP1</sup> expression (Herbert et al. 2008). Angiotensin II has also been shown to significantly increase SA-β-gal activity and p21<sup>CIP1</sup> expression in ApoE<sup>-/-</sup> mice (Kunieda et al. 2006). In the absence of angiotensin II it is difficult to detect SA-β-gal activity *in vivo*. Sections of a 13-month-old Coll1a1<sup>r/r</sup> mouse show that there was no SA-β-gal activity in either the brachiocephalic artery or the left internal carotid artery. However, senescent cells were detected in the ascending portion of the aortic arch (Figure 3.6A). Looking closer at the ascending aorta of Coll1a1<sup>r/r</sup> mice, senescent cells were specifically detected in the outer layers of the media. In contrast, there were no senescent SMCs found in the ascending aortas of wild-type littermates (Figure 3.6B).

Results examining Coll1a1<sup>r/r</sup> mouse survivability, weight, adipose tissue content, kyphosis, and bone mineral density provide strong evidence for the notion that the inability to cleave type I collagen in mice results in a phenotype reminiscent of accelerated aging. Our findings in the vasculature provide further evidence for aging in the aortic wall.

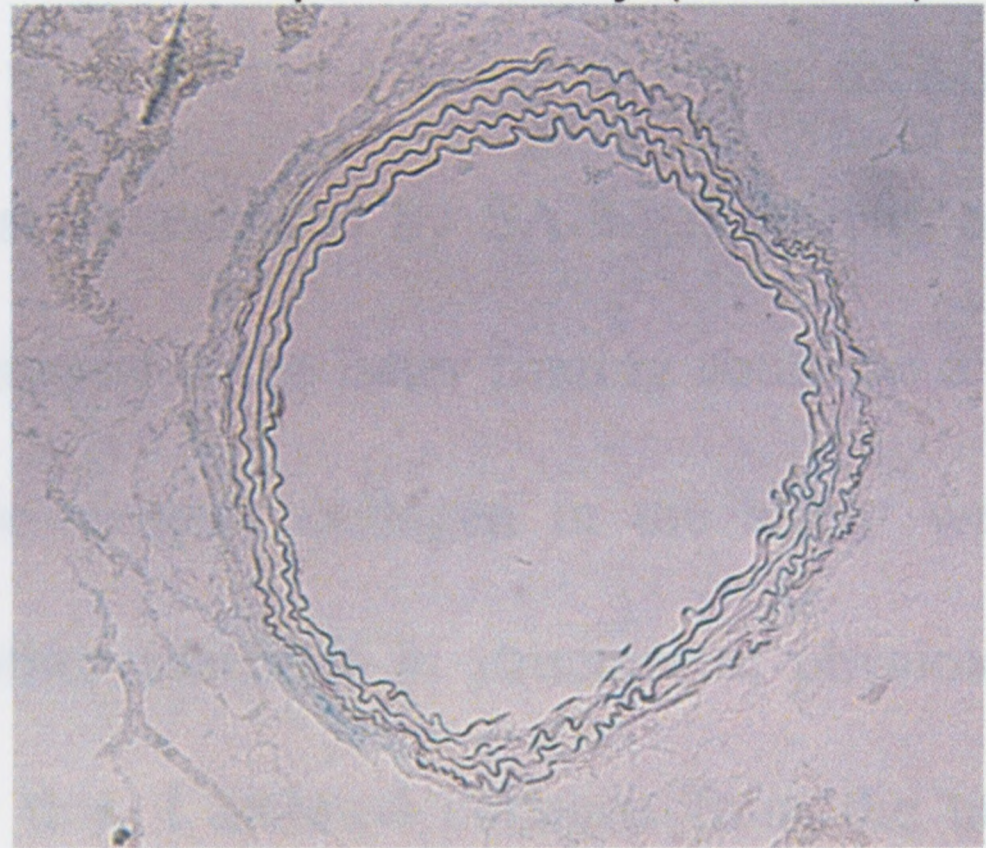
**Figure 3.6.** SMCs in the ascending aorta display more SA- $\beta$ -gal activity in  $Coll1a1^{tr}$  mice than wild-type mice. *A*, Phase-contrast images of left internal carotid artery, braciocephalic artery, aortic arch and ascending aorta of  $Coll1a1^{tr}$  mice. Littermates were infused with angiotensin II for a period of 28 days followed by cryosectioning of arteries. *Top*, No senescent SMCs were detected in the left internal carotid artery or the braciocephalic artery of  $Coll1a1^{tr}$  mice as assessed by SA- $\beta$ -gal activity. *Bottom*, Senescent SMCs were detected in the media of the outer wall of the aortic arch of  $Coll1a1^{tr}$  mice. *B*, Phase-contrast images display senescent SMCs in the outer media of the ascending aortic wall of angiotensin II infused  $Coll1a1^{tr}$  mice as indicated by  $\beta$ -gal staining. Senescent SMCs were not detected in the aortic wall of their wild-type littermates.

### 3.8. Human SMCs Replicating on Collagen Derived From Col1a1<sup>+/+</sup> Mice Reach Growth Arrest Sooner Than SMCs Replicating on Wild-type Collagen

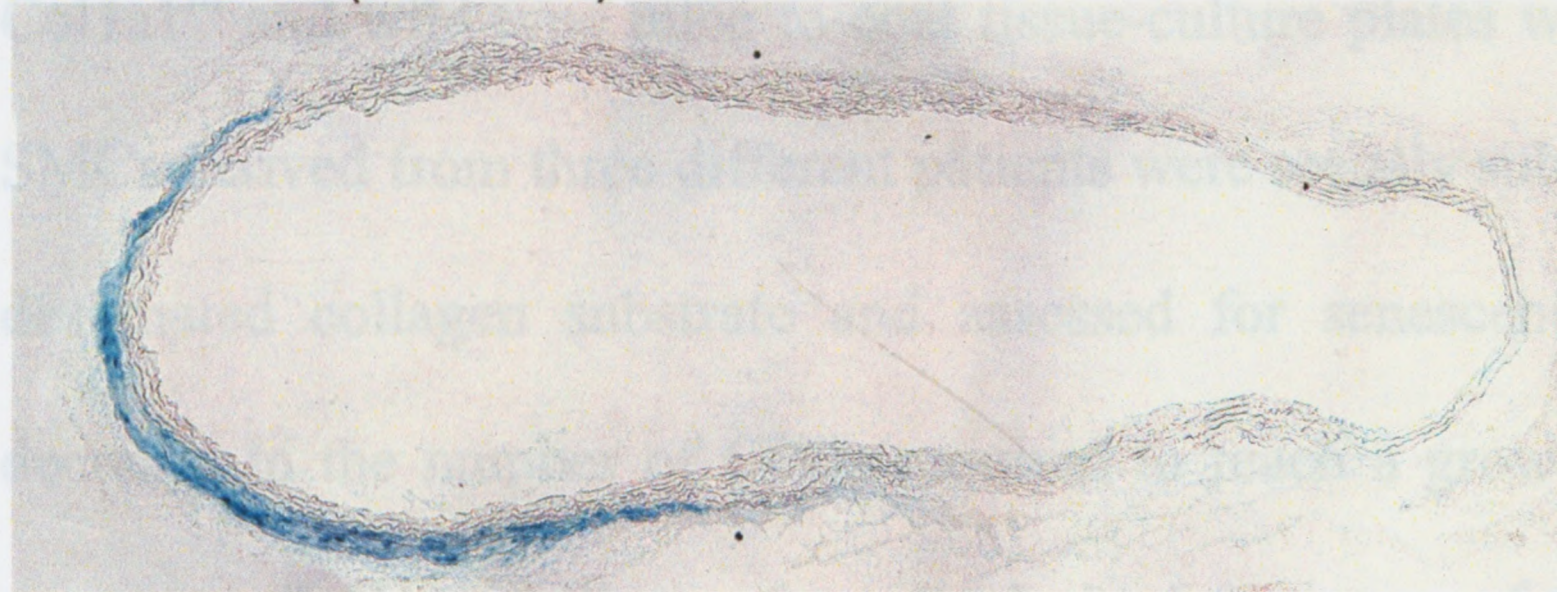
Left Internal Carotid Artery (Col1a1<sup>r/r</sup>)



Brachiocephalic Artery (Col1a1<sup>r/r</sup>)

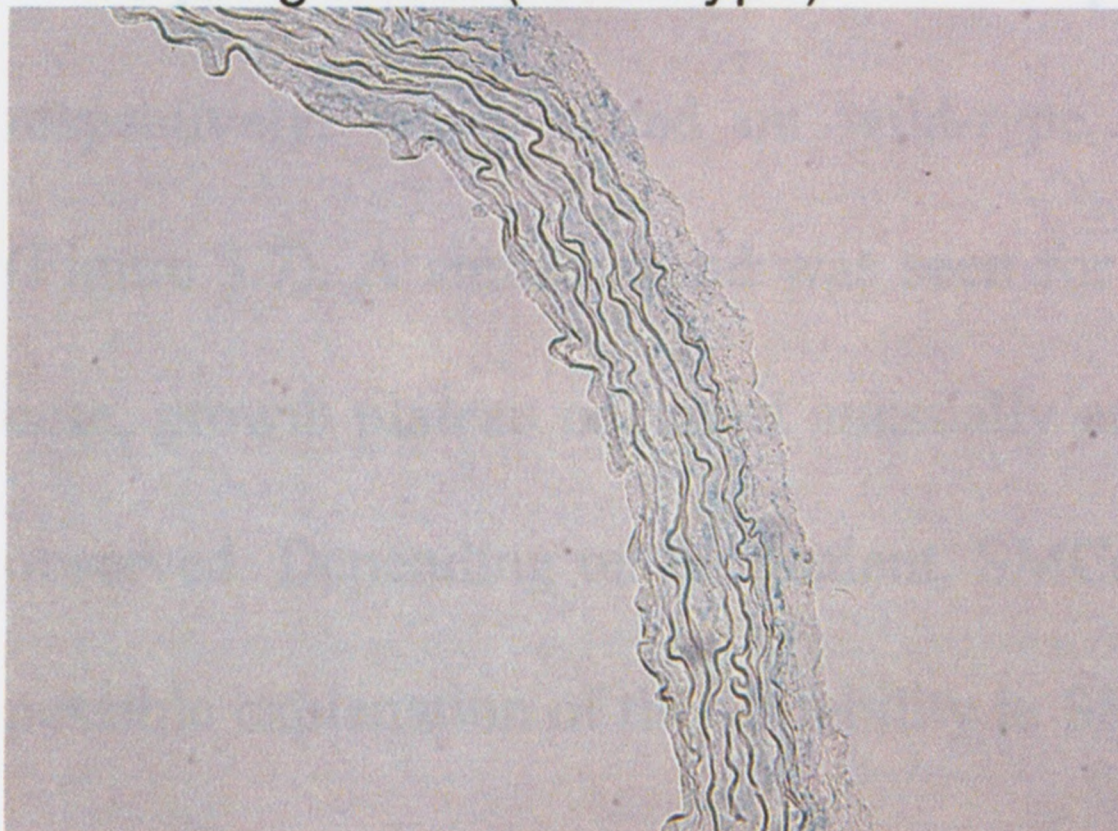


Aortic Arch (Col1a1<sup>r/r</sup>)

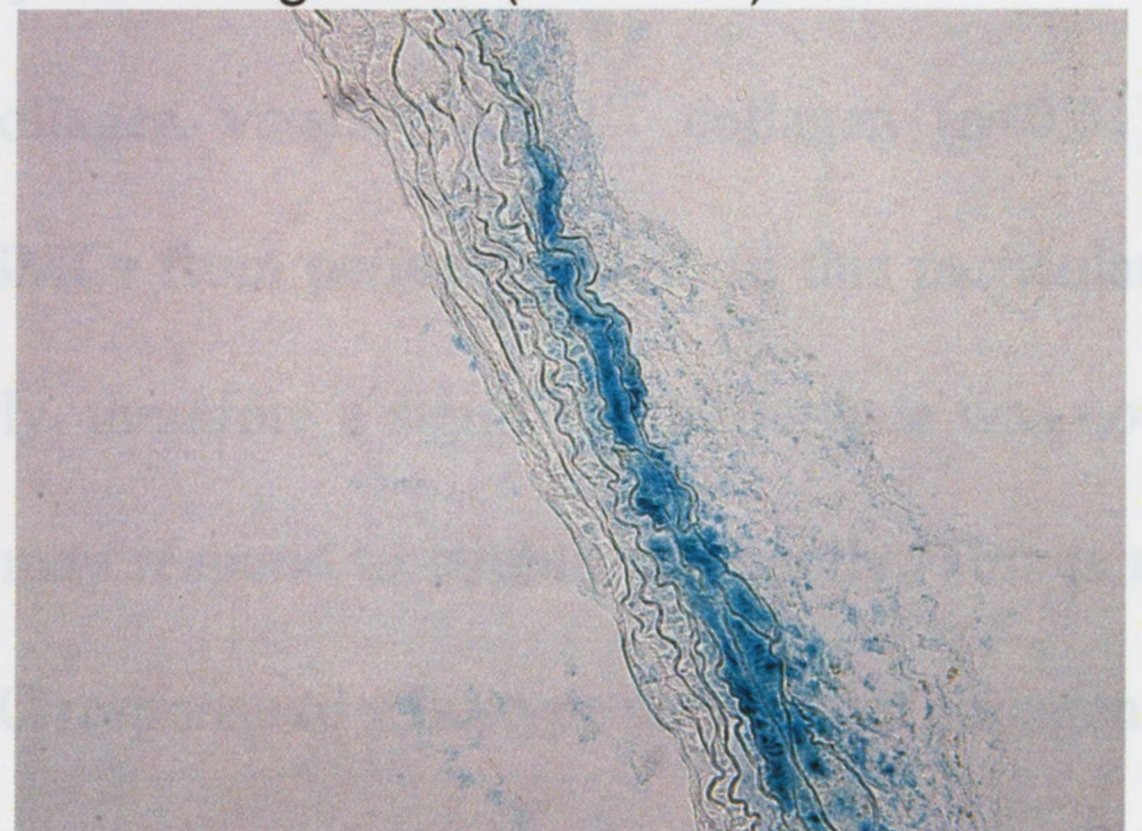


A

Ascending Aorta (Wild Type)



Ascending Aorta (Col1a1<sup>r/r</sup>)



B

These observations support the notion that SMCs grown on collagenase-resistant type I collagen cannot replicate in culture as many times as SMCs grown on normal type I collagen.

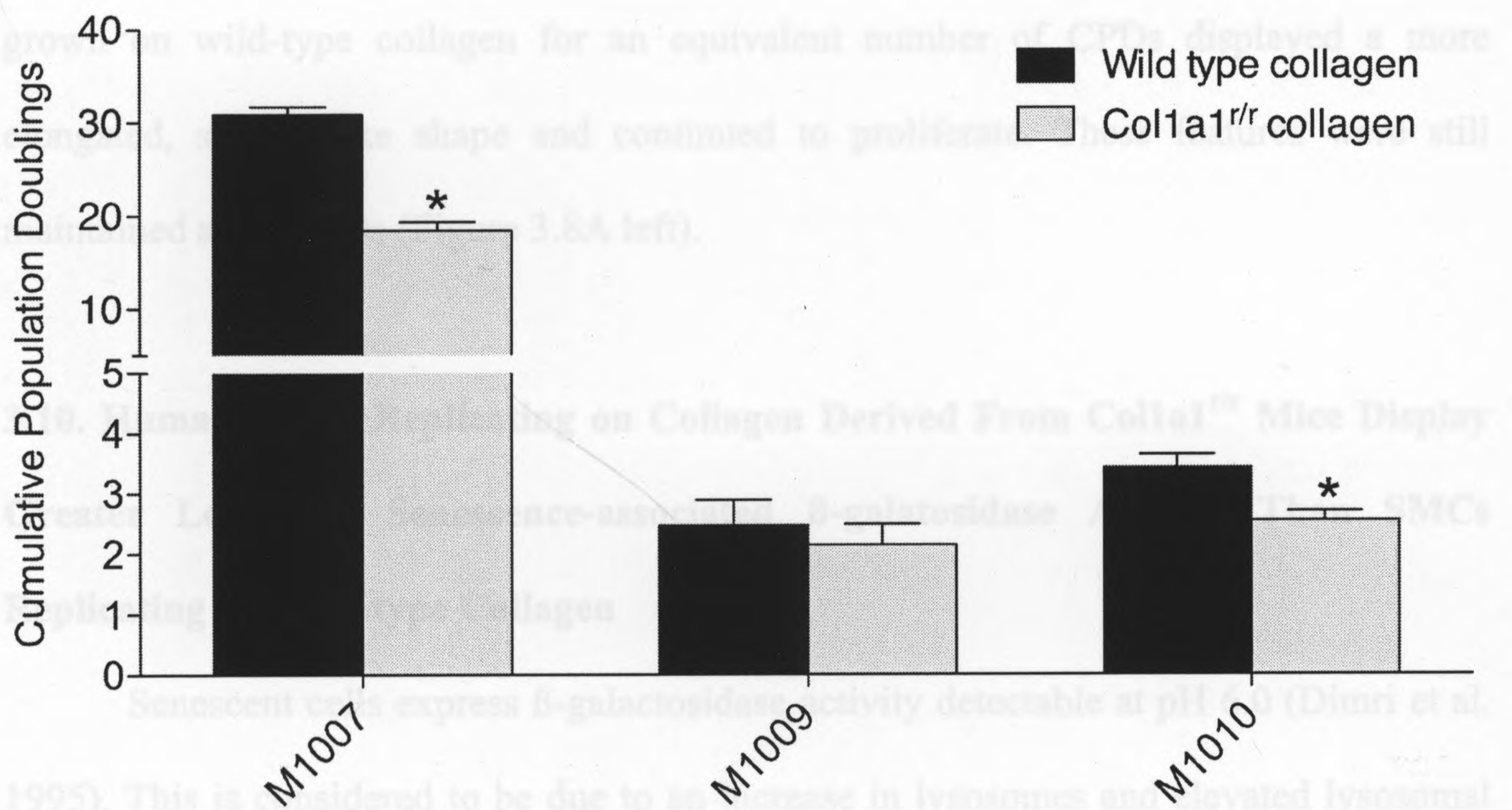
### **3.8. Human SMCs Replicating on Collagen Derived From $Coll1a1^{r/r}$ Mice Reach Growth Arrest Sooner Than SMCs Replicating on Wild-type Collagen**

The foregoing analysis of  $Coll1a1^{r/r}$  mice suggested that the presence of collagenase-resistant type I collagen leads to accelerated aging in mice, including a predisposition to cellular senescence, at least as assessed by SA- $\beta$ -gal activity among vascular SMCs of the aorta. In order to determine if the latter finding could be a direct consequence of the presence of collagenase-resistant collagen in the artery wall, as opposed to a secondary consequence of another alteration in structure or physiology, I undertook studies of SMCs in culture. For this, I isolated collagen from the tails of  $Coll1a1^{r/r}$  and wild-type mice to coat tissue-culture plates with. Primary human vascular SMCs derived from three different patients were serially subcultured onto a monolayer of designated collagen substrate and assessed for senescence. There was a significant decrease in the number of CPDs required to reach a growth plateau when SMCs were grown on  $Coll1a1^{r/r}$  collagen for cells derived from two of the three patients. The SMCs from patients M1007 and M1010 displayed a 1.68 fold and 1.34 fold increase respectively, when plated on wild-type collagen versus  $Coll1a1^{r/r}$  collagen ( $p < 0.01$ ) (Figure 3.7). A similar trend was seen for SMCs from patient M1009. In this particular case, growth plateau occurred unusually early, therefore a significant difference was not observed. Depending on the patient, SMCs may respond to stimuli differently. This is a possible explanation of the variability in SMC response to wild-type and mutant collagen. These observations support the notion that SMCs grown on collagenase-resistant type I collagen cannot replicate in culture as many times as SMCs grown on normal type I collagen.

**Figure 3.7.** Human SMCs replicating on collagen derived from  $\text{Coll1a1}^{r/r}$  mice reach growth arrest more rapidly than SMCs replicating on wild-type collagen as assessed by growth curves. A bar graph displaying the average number of CPDs by human vascular SMCs *in vitro* before growth arrest. SMCs were serially subcultured onto either a wild-type or  $\text{Coll1a1}^{r/r}$  collagen monolayer. The period at which SMC growth plateau occurred is measured in CPDs. SMCs from patient M1007 ( $30.9 \pm 0.8$  CPDs on wild-type collagen vs.  $18.4 \pm 0.9$  CPDs on  $\text{Coll1a1}^{r/r}$  collagen) and M1010 ( $3.4 \pm 0.2$  CPDs on wild-type collagen vs.  $2.5 \pm 0.1$  CPDs on  $\text{Coll1a1}^{r/r}$  collagen) experienced a significantly lower number of CPDs when grown on  $\text{Coll1a1}^{r/r}$  collagen (n=7) ( $p < 0.01$ ).

### 3.9. Human SMCs Replicating on Collagen Derived From Col1a1<sup>fl/fl</sup> Mice Show Senescent-like Morphology Earlier Than SMCs Replicating on Wild-type Collagen

Senescent cells exhibit specific morphological changes including an enlarged, round and flattened appearance (Goldstein 1990); pronounced stress fibres (Cho et al. 2004); and enlarged or split nuclei (Matsumura 1980). After 9.6 CPDs, morphology consistent with a senescent phenotype was observed in SMCs grown on Col1a1<sup>fl/fl</sup> collagen as evidenced by the large round shape displayed (Figure 3.8A left). SMCs



grown on wild-type collagen for an equivalent number of CPDs displayed a more elongated, spindle shape and continued to proliferate (Figure 3.8A left). SMCs grown on Col1a1<sup>fl/fl</sup> collagen displayed a more rounded, flattened morphology and a senescent-like morphology was observed in SMCs replicating on Collagen Derived From Col1a1<sup>fl/fl</sup> Mice Display Senescent-like Morphology Earlier Than SMCs Replicating on Wild-type Collagen. Senescent cells express  $\beta$ -galactosidase activity detectable at pH 6.0 (Dimri et al. 1995). This is considered to be due to an increase in lysosomes and elevated lysosomal activity in senescent cells (Robbins et al. 1970; Cristofalo et al. 2004). This is relatively specific for senescent cells and thus, SA- $\beta$ -gal activity can be used as an indicator of cellular senescence. SMCs were grown on glass coverslips pre-coated with the designated type I collagen substrate. They were fixed in 2% formaldehyde/0.2% glutaraldehyde and incubated at 37°C with fresh SA- $\beta$ -gal solution overnight (no CO<sub>2</sub>). Cells were then visualized by bright field microscopy (Figure 3.8A right). The proportion of positively stained SMCs was compared in young cells (0-5 CPDs) versus old cells (8-13 CPDs).

### **3.9. Human SMCs Replicating on Collagen Derived From *Coll1a1<sup>r/r</sup>* Mice Show Senescent-like Morphology Earlier Than SMCs Replicating on Wild-type Collagen**

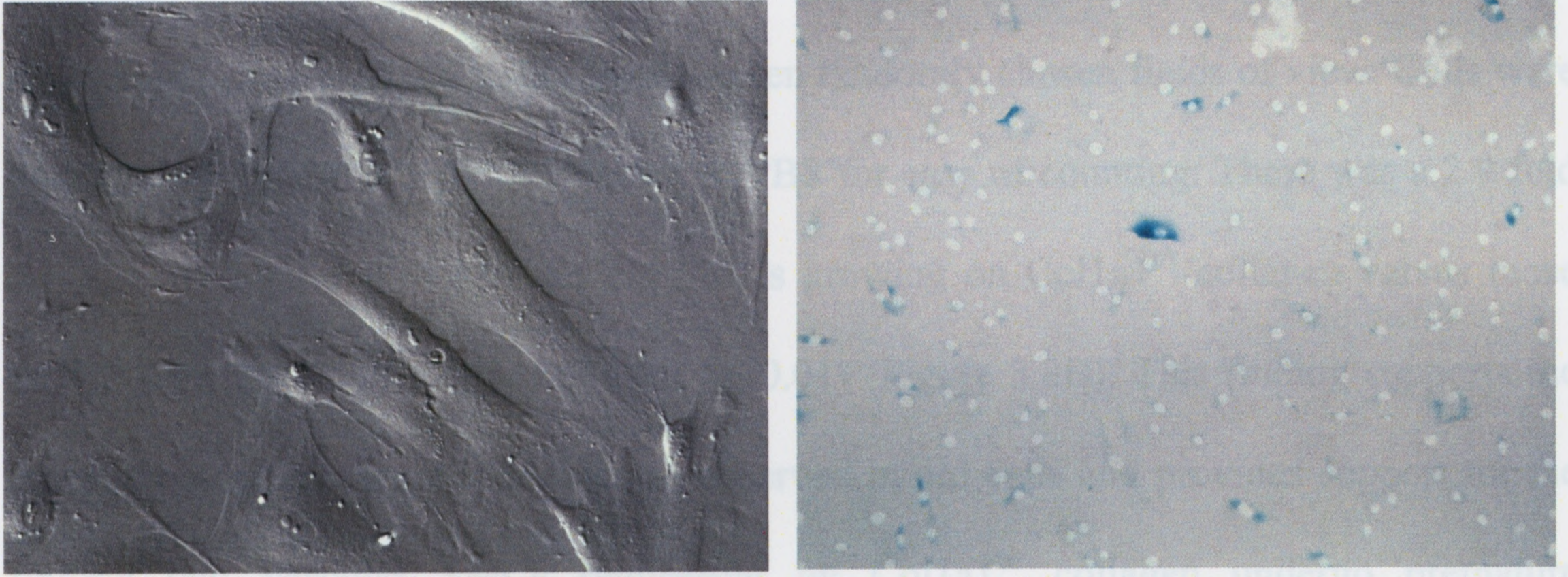
Senescent cells exhibit specific morphological changes including an enlarged, round and flattened appearance (Goldstein 1990); pronounced stress fibres (Cho et al. 2004); and enlarged or split nuclei (Matsumura 1980). After 9.6 CPDs, morphology consistent with a senescent phenotype was observed in SMCs grown on *Coll1a1<sup>r/r</sup>* collagen as evidenced by the large round shape displayed (Figure 3.8A left). SMCs grown on wild-type collagen for an equivalent number of CPDs displayed a more elongated, spindle-like shape and continued to proliferate. These features were still maintained at 12 CPDs (Figure 3.8A left).

### **3.10. Human SMCs Replicating on Collagen Derived From *Coll1a1<sup>r/r</sup>* Mice Display Greater Levels of Senescence-associated $\beta$ -galactosidase Activity Than SMCs Replicating on Wild-type Collagen**

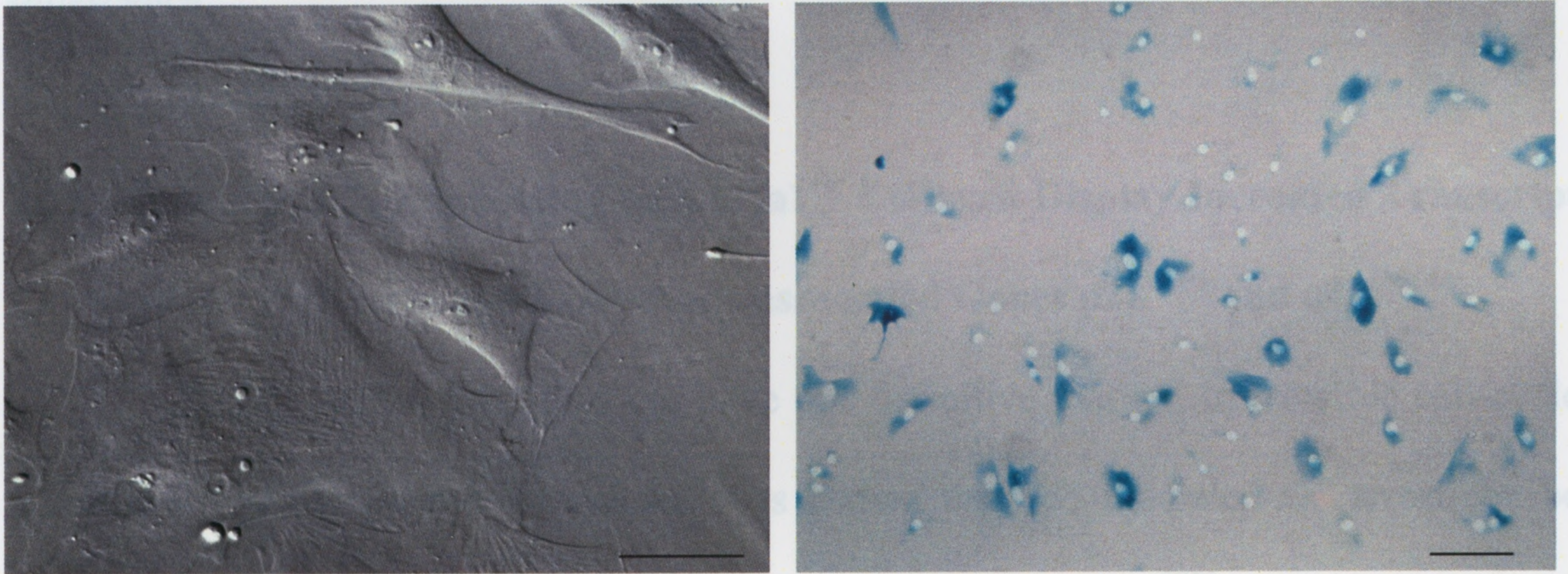
Senescent cells express  $\beta$ -galactosidase activity detectable at pH 6.0 (Dimri et al. 1995). This is considered to be due to an increase in lysosomes and elevated lysosomal activity in senescent cells (Robbins et al. 1970; Cristofalo et al. 2004). This is relatively specific for senescent cells and thus, SA- $\beta$ -gal activity can be used as an indicator of cellular senescence. SMCs were grown on glass coverslips pre-coated with the designated type I collagen substrate. They were fixed in 2% formaldehyde/0.2% glutaraldehyde and incubated at 37°C with fresh SA- $\beta$ -gal solution overnight (no CO<sub>2</sub>). Cells were then visualized by bright field microscopy (Figure 3.8A right). The proportion of positively stained SMCs was compared in young cells (0-5 CPDs) versus old cells (8-13 CPDs).

**Figure 3.8.** Human SMCs replicating on Coll1a1<sup>r/r</sup> collagen show senescent-like morphological changes and increased SA- $\beta$ -gal activity earlier than SMCs replicating on wild-type collagen. *A, Left*, Hoffman-modulated contrast images of SMCs from patient M1007 are shown. SMCs serially subcultured on wild-type collagen were imaged after 12 CPDs and SMCs serially subcultured on Coll1a1<sup>r/r</sup> collagen were imaged after 9.6 CPDs. SMCs grown on Coll1a1<sup>r/r</sup> collagen substrate display morphology consistent with a senescent phenotype. This is characterized by a large, round and flattened appearance and the presence of stress fibres. Bar denotes 100 microns. *Right*, Bright field images of SMCs stained overnight for SA- $\beta$ -gal activity. SMCs were grown on glass coverslips pre-coated with wild-type or Coll1a1<sup>r/r</sup> type I collagen substrate for 12 or 9.6 CPDs respectively, fixed and stained for SA-  $\beta$ -gal activity. The increase in  $\beta$ -galactosidase activity can be visualized in the SMCs grown on Coll1a1<sup>r/r</sup> collagen. Cells were counterstained with Hoechst for quantification purposes. Bar denotes 200 microns. *B*, A bar graph displaying the average proportion of positively stained SMCs upon use of  $\beta$ -gal as described comparing young cells (0-5 CPDs) and old cells (8-13 CPDs) is shown. In old cells, an average of 10.7%  $\pm$  0.8% of SMCs grown on wild-type collagen stained positively for  $\beta$ -gal activity as opposed to an average of 31.4%  $\pm$  3.1% of SMCs grown on Coll1a1<sup>r/r</sup> collagen. This difference was statistically significant (n=4) (p<0.01).

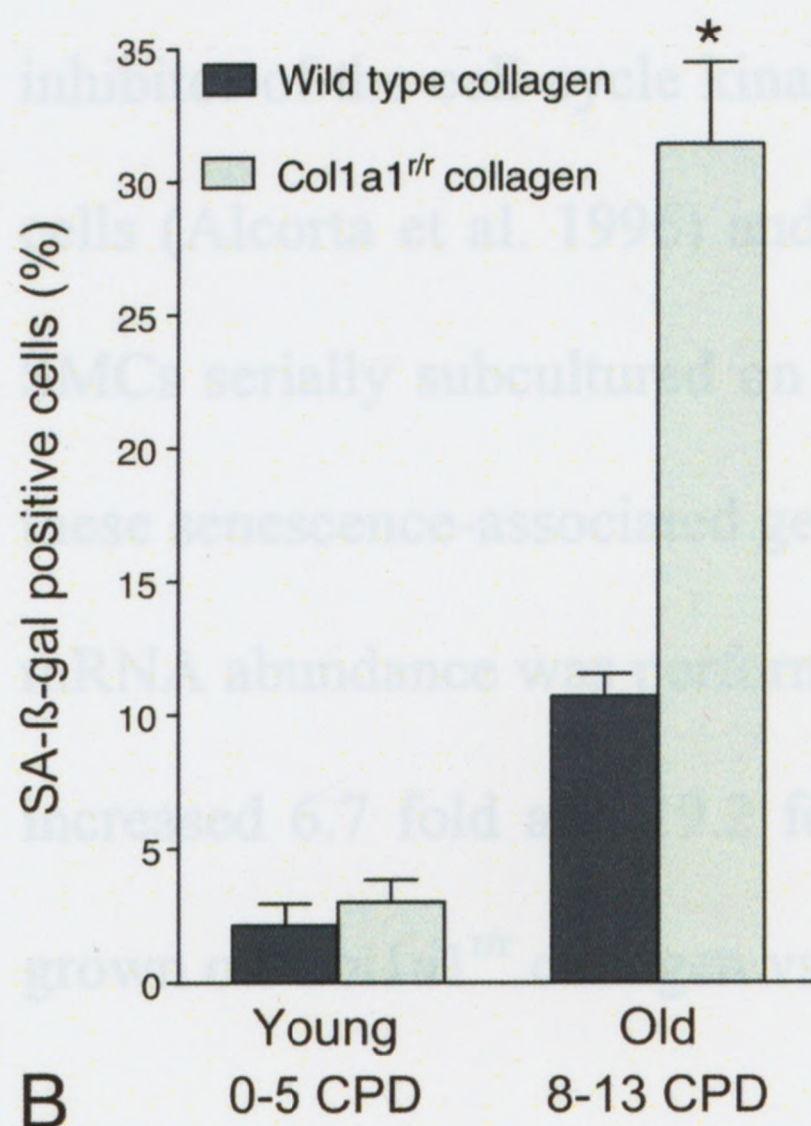
SMCs grown on wild type collagen after 12 cumulative population doublings



SMCs grown on Col1a1<sup>tr</sup> collagen after 9.6 cumulative population doublings



A



The number of positively stained cells was counted along with the total number of cells (approximately 1000 cells) from sixteen randomly chosen fields of view. Cells were counterstained with 0.5  $\mu$ l/ml Hoechst in PBS for ease of counting. There was a 2.9 fold increase in  $\beta$ -gal staining in the old SMCs growing on  $\text{Coll1a1}^{\text{tr}}$  collagen versus those SMCs growing on wild-type collagen ( $p < 0.01$ ) (Figure 3.8B). This finding supports the morphological senescent-like changes observed in old cells and provides support for the finding that vascular SMCs replicating on  $\text{Coll1a1}^{\text{tr}}$  collagen undergo premature senescence.

### **3.11. Human SMCs Replicating on $\text{Coll1a1}^{\text{tr}}$ Collagen Display Increased Transcript Levels of the Cell-cycle and Senescence-associated Genes $\text{p21}^{\text{CIP1}}$ and $\text{p16}^{\text{INK4A}}$**

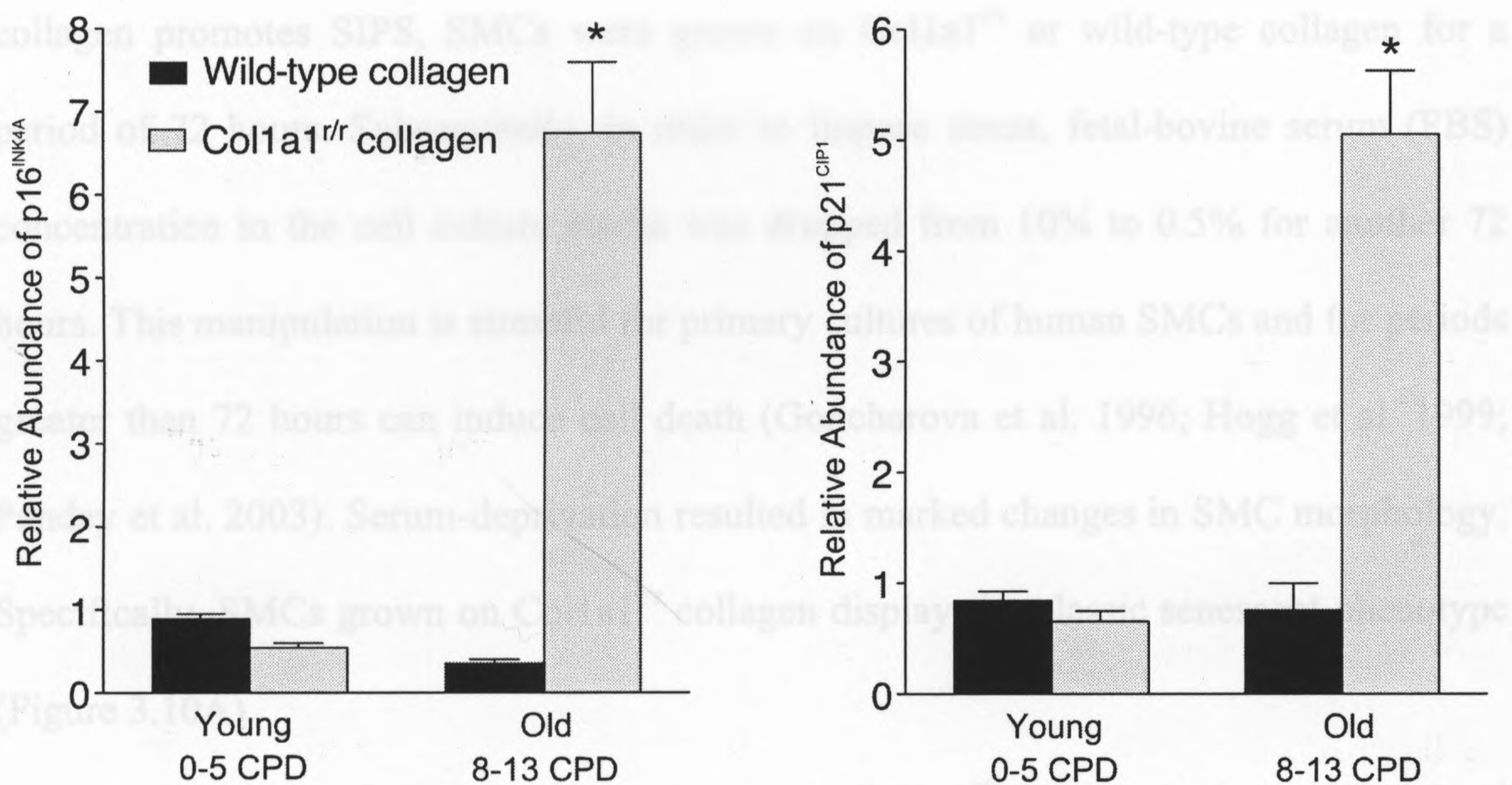
Although senescence does not have one definitive marker, irreversible cell-cycle arrest is a key component. In culture, it is known that p53-mediated G1 arrest can be caused by the cyclin-dependent kinase inhibitor  $\text{p21}^{\text{CIP1}}$ . This leads to hypophosphorylation of pRb (Levine 1997). Increased levels of  $\text{p16}^{\text{INK4A}}$ , a known inhibitor of the cell-cycle kinases CDK4 and CDK6, has also been detected in senescent cells (Alcorta et al. 1996) and causes pRb hypophosphorylation. To determine whether SMCs serially subcultured on  $\text{Coll1a1}^{\text{tr}}$  collagen displayed increased transcript levels of these senescence-associated genes, real-time RT-PCR assessment of  $\text{p21}^{\text{CIP1}}$  and  $\text{p16}^{\text{INK4A}}$  mRNA abundance was performed. Mean expression of  $\text{p21}^{\text{CIP1}}$  and  $\text{p16}^{\text{INK4A}}$  in old SMCs increased 6.7 fold and 19.2 fold relative to baseline GAPDH levels respectively when grown on  $\text{Coll1a1}^{\text{tr}}$  collagen vs. those grown on wild-type collagen ( $p < 0.01$ ) (Figure 3.9).

**Figure 3.9.** Human SMCs replicating on Colla1<sup>tr</sup> collagen display increased transcript levels of p16<sup>INK4A</sup> and p21<sup>CIP1</sup>. Bar graphs depicting the average abundance of p16<sup>INK4A</sup> and p21<sup>CIP1</sup> mRNA relative to baseline levels as assessed by quantitative real-time RT-PCR are shown. The average abundance of each gene relative to GAPDH (loading control) in SMCs grown on wild-type collagen for three CPDs was used as a baseline. Relative expression of p16<sup>INK4A</sup> in old SMCs (8-13 CPDs) grown on wild-type collagen was  $0.35 \pm 0.05$  and relative expression of p16<sup>INK4A</sup> in similar passage cells grown on Colla1<sup>tr</sup> collagen was  $6.74 \pm 0.86$ . Relative expression of p21<sup>CIP1</sup> in old SMCs grown on wild-type collagen was  $0.76 \pm 0.24$  and relative expression of p21<sup>CIP1</sup> in similar passage cells grown on Colla1<sup>tr</sup> collagen was  $5.05 \pm 0.57$ . The increase in transcript levels of p16<sup>INK4A</sup> and p21<sup>CIP1</sup> in old SMCs grown on Colla1<sup>tr</sup> was statistically significant (n=6) (p<0.01). There was no significant increase in transcript levels of p16<sup>INK4A</sup> or p21<sup>CIP1</sup> in young cells growing on Colla1<sup>tr</sup> collagen over young cells growing on wild-type collagen.

This increase was not seen in young cells, however overall abundance of p21<sup>CIP1</sup> and p16<sup>INK4A</sup> increased in old cells over young cells irrespective of collagen substrate.

### 3.12. Col1a1<sup>fl/fl</sup> Collagen Promotes Stress-induced Premature Senescence

Cell senescence can be induced in the absence of cell replication by external stressors, a phenomenon referred to as SIPS. To determine if collagenase resistant



To determine whether SMCs grown on Col1a1<sup>fl/fl</sup> displayed elevated SA- $\beta$ -gal activity in the presence of stress, SMCs were grown on a collagen substrate as described above. It was observed that SMCs on Col1a1<sup>fl/fl</sup> collagen exposed to 72 hours of serum-deprivation displayed a 1.8 fold increase in SA- $\beta$ -gal activity versus SMCs on wild-type collagen ( $p < 0.01$ ) ( $n = 11$ ) (Figure 3.10B). In the absence of serum-deprivation, there was no difference in SA- $\beta$ -gal activity between SMCs on Col1a1<sup>fl/fl</sup> and wild-type collagen ( $p = \text{NS}$ ) ( $n = 3$ ). This implies that for SMCs on Col1a1<sup>fl/fl</sup> collagen, a superimposed stress of sub-optimal media conditions can elicit SIPS.

This increase was not seen in young cells, however overall abundance of p21<sup>CIP1</sup> and p16<sup>INK4A</sup> increased in old cells over young cells irrespective of collagen substrate.

### 3.12. Colla1<sup>r/r</sup> Collagen Promotes Stress-induced Premature Senescence

Cell senescence can be induced in the absence of cell replication by external stressors, a phenomenon referred to as SIPS. To determine if collagenase resistant collagen promotes SIPS, SMCs were grown on Colla1<sup>r/r</sup> or wild-type collagen for a period of 72 hours. Subsequently, in order to impose stress, fetal-bovine serum (FBS) concentration in the cell culture media was dropped from 10% to 0.5% for another 72 hours. This manipulation is stressful for primary cultures of human SMCs and for periods greater than 72 hours can induce cell death (Goncharova et al. 1996; Hogg et al. 1999; Pandey et al. 2003). Serum-deprivation resulted in marked changes in SMC morphology. Specifically, SMCs grown on Colla1<sup>r/r</sup> collagen displayed a classic senescent phenotype (Figure 3.10A).

To determine whether SMCs grown on Colla1<sup>r/r</sup> displayed elevated SA-β-gal activity in the presence of stress, SMCs were grown on a collagen substrate as described above. It was observed that SMCs on Colla1<sup>r/r</sup> collagen exposed to 72 hours of serum-deprivation displayed a 1.8 fold increase in SA-β-gal activity versus SMCs on wild-type collagen ( $p < 0.01$ ) ( $n = 11$ ) (Figure 3.10B). In the absence of serum-deprivation, there was no difference in SA-β-gal activity between SMCs on Colla1<sup>r/r</sup> and wild-type collagen ( $p = \text{NS}$ ) ( $n = 3$ ). This implies that for SMCs on Colla1<sup>r/r</sup> collagen, a superimposed stress of sub-optimal media conditions can elicit SIPS.

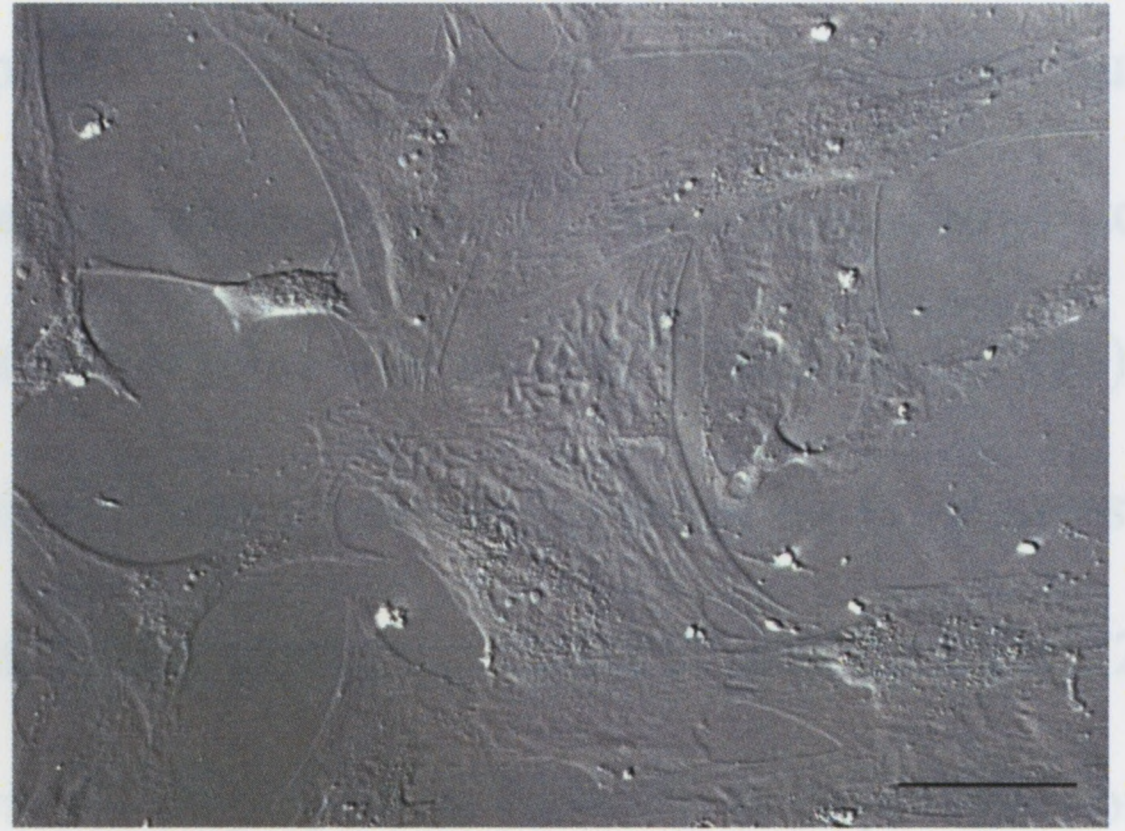
**Figure 3.10.** Human SMCs exposed to serum-deprivation are more susceptible to premature senescence in the presence of Colla1<sup>r/r</sup> collagen as indicated by morphological changes and increased SA- $\beta$ -gal activity. *A*, Hoffman-modulated contrast images of SMCs at cell passage six grown on wild-type or Colla1<sup>r/r</sup> collagen for six days are shown. SMCs were serum-deprived (0.5% FBS) for a period of three days prior to imaging. Morphological differences between SMCs grown on wild-type collagen and SMCs grown on Colla1<sup>r/r</sup> can be observed. These include enlarged cell size, round shape, and increased presence of stress fibres in SMCs grown on Colla1<sup>r/r</sup> collagen. Bar denotes 100 microns. *B*, A bar graph displaying the average proportion of positively stained SMCs upon use of  $\beta$ -Gal as described is shown. SMCs not exposed to stressful conditions (10% FBS in media was maintained) are compared to SMCs exposed to stressful conditions (0.5% FBS for three days). Although no significant increase in proportion of SMCs stained positively for  $\beta$ -gal activity is shown between SMCs grown on wild-type and Colla1<sup>r/r</sup> collagen in normal serum levels (n=3), there is a significant increase in serum-deprived conditions. In 0.5% FBS, 7.2%  $\pm$  0.3% of SMCs grown on wild-type collagen stained positive for  $\beta$ -gal activity as opposed to 12.9%  $\pm$  0.5% of SMCs grown on Colla1<sup>r/r</sup> collagen (n=11) (p<0.01).

### 3.13. Serum-deprived Human SMCs on Col1a1<sup>tr</sup> Collagen Display Increased Expression of the Cell-cycle and Senescence-associated Genes p21<sup>CIP1</sup>, p16<sup>INK4A</sup> and p14<sup>ARF</sup>

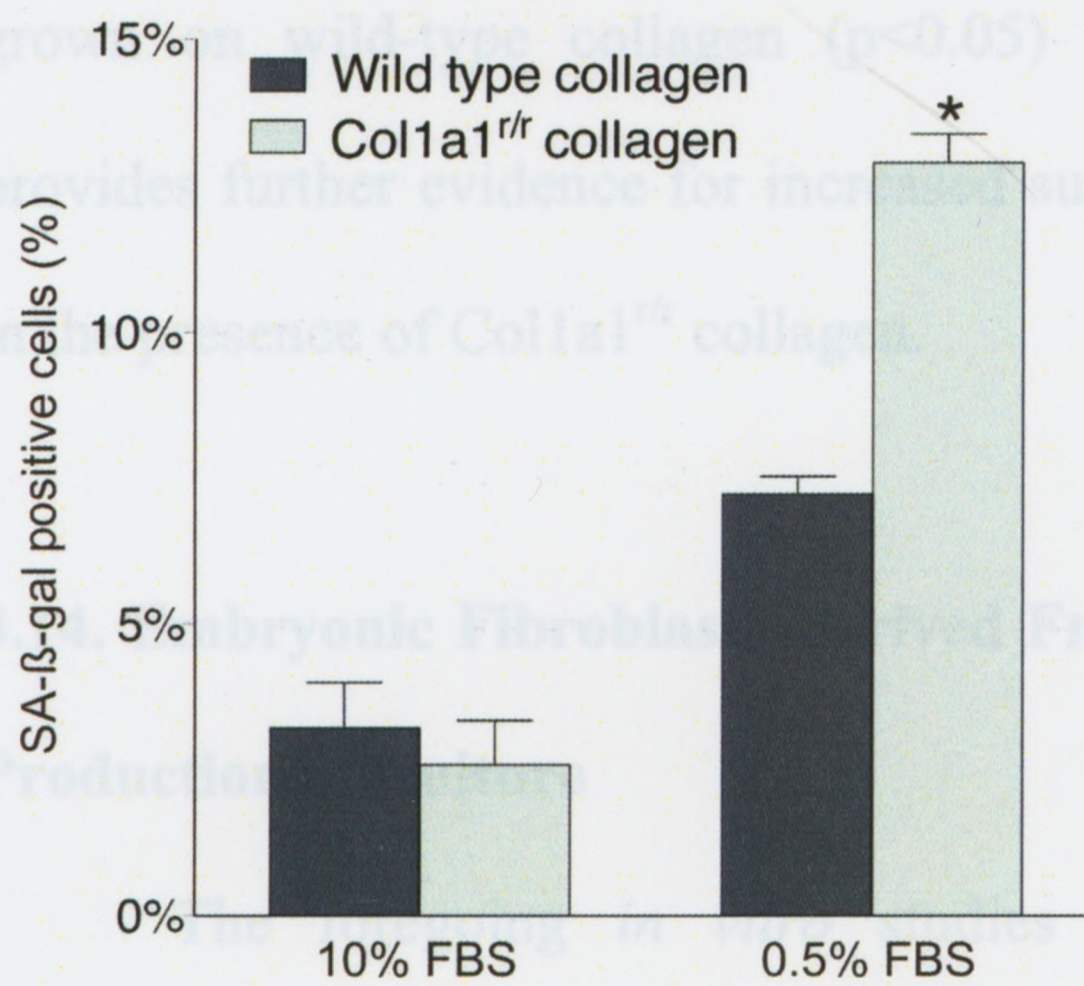
Wild Type



Col1a1<sup>tr</sup>



A



B

### **3.13. Serum-deprived Human SMCs on Colla1<sup>r/r</sup> Collagen Display Increased Expression of the Cell-cycle and Senescence-associated Genes p21<sup>CIP1</sup>, p16<sup>INK4A</sup> and p14<sup>ARF</sup>**

In addition to p16<sup>INK4A</sup> and p21<sup>CIP1</sup>, p14<sup>ARF</sup> is another commonly known senescence-associated protein. P14<sup>ARF</sup> and p16<sup>INK4A</sup> share a common second exon, but these two proteins are unrelated in structure. Increases in p14<sup>ARF</sup> have been shown to increase p53 activation due to MDM2 sequestration (Haupt et al. 1997; Stott et al. 1998). The subsequent activation of p53 results in p21<sup>CIP1</sup> upregulation followed by G<sub>1</sub>-S arrest (Wang et al. 1999). Western blot analysis of SMCs grown on Colla1<sup>r/r</sup> collagen for 72 hours followed by 72 hours of serum-deprivation displayed an increase in expression of p21<sup>CIP1</sup> (1.4 fold), p16<sup>INK4A</sup> (1.9 fold) and p14<sup>ARF</sup> (1.8 fold) when compared to SMCs grown on wild-type collagen (p<0.05) (Figure 3.11). This protein expression data provides further evidence for increased susceptibility to SIPS by human vascular SMCs in the presence of Colla1<sup>r/r</sup> collagen.

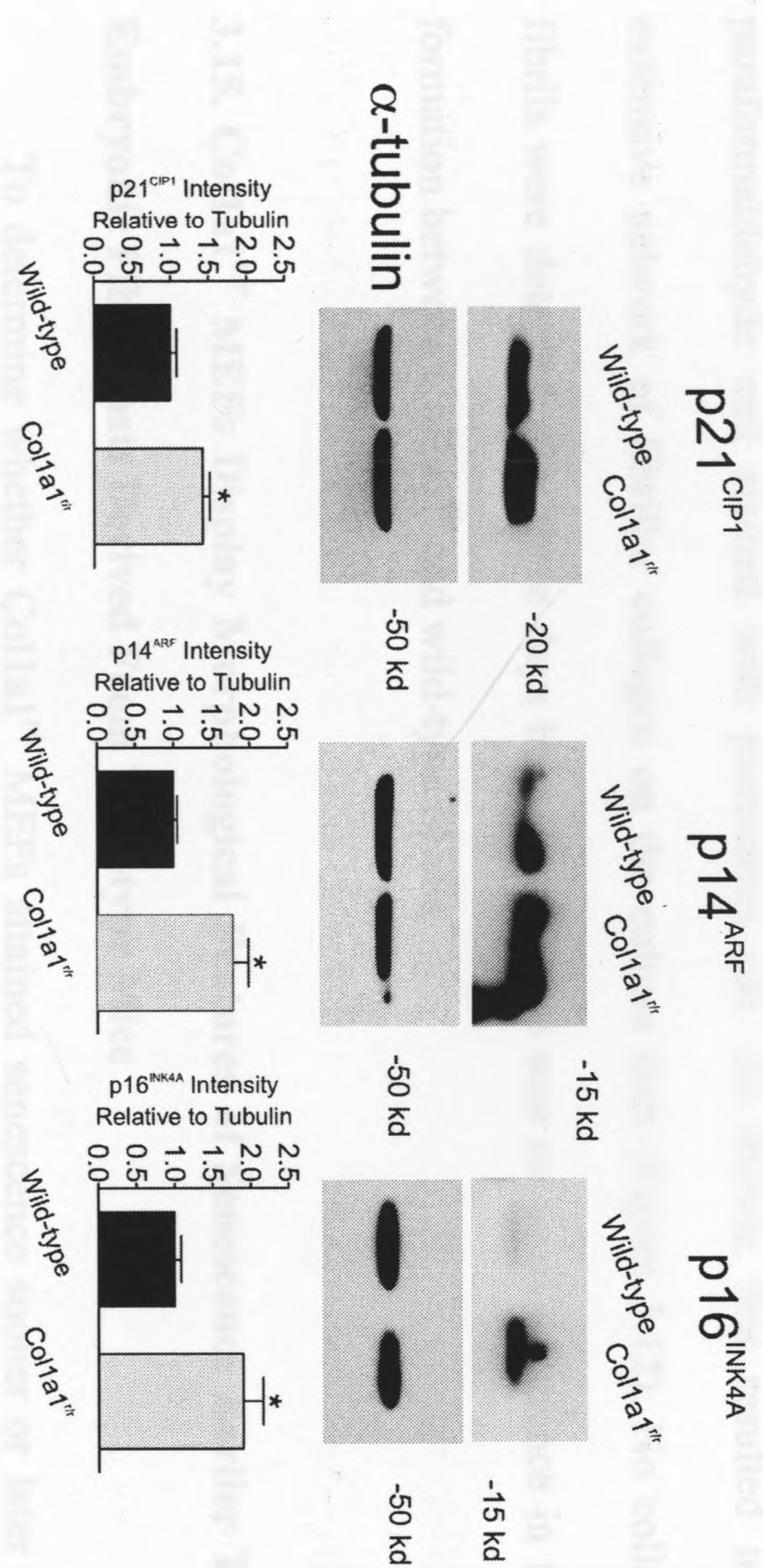
### **3.14. Embryonic Fibroblasts Derived From Colla1<sup>r/r</sup> Mice are Capable of Collagen Production in Culture**

The foregoing *in vitro* studies established that a 2-dimensional layer of collagenase-resistant collagen impacts SMC aging. However, the collagen solubilised from mouse tails and plated onto cell culture dishes may not mimic that which is endogenously secreted from the cell.

**Figure 3.11.** Serum-deprived human SMCs grown on  $\text{Coll1a1}^{r/r}$  collagen display increased protein expression of the cell-cycle and senescence-associated genes  $\text{p21}^{\text{CIP1}}$ ,  $\text{p14}^{\text{ARF}}$  and  $\text{p16}^{\text{INK4A}}$ . Western blots of the cell-cycle control genes  $\text{p21}^{\text{CIP1}}$ ,  $\text{p14}^{\text{ARF}}$  and  $\text{p16}^{\text{INK4A}}$  in SMCs grown on wild-type or  $\text{Coll1a1}^{r/r}$  collagen for six days and exposed to 0.5% FBS for the final three days are shown.  $\alpha$ -tubulin expression was used as a loading control. Quantification of average band intensity revealed an increase of  $\text{p21}^{\text{CIP1}}$  (1.4 fold),  $\text{p14}^{\text{ARF}}$  (1.8 fold) and  $\text{p16}^{\text{INK4A}}$  (1.9 fold) expression in SMCs grown on  $\text{Coll1a1}^{r/r}$  relative to SMCs grown on wild-type collagen and is displayed in bar graphs below (n=3) ( $p < 0.05$ ).

To study the latter scenario, I sought to evaluate cultured cells harvested from wild-type and Col1a1<sup>fl/fl</sup> mice. MEFs were selected due to their relative ease of harvesting and their known program of replicative senescence when grown in culture (Kohama 1981; Cozzani et al. 1995; Serrano et al. 1996). To ensure that harvested MEFs were capable of collagen production, assembly and secretion *in vitro*, I evaluated for the presence of type I collagen fibrils in culture using circular polarization microscopy. This technique specifically identifies fibrils based on their birefringence. Over the course of two weeks, MEFs were treated with fresh ascorbate (100  $\mu$ M) every 48 hours in order to improve triple helical structure maturation of pro-collagen. Cells were then fixed with 4% paraformaldehyde and were processed with immunoblotting for the phosphorylated serine residues p21<sup>CIP1</sup>, p14<sup>ARF</sup> and p16<sup>INK4A</sup> (Figure 3.13A).

Western blots and bar graphs show that p21<sup>CIP1</sup>, p14<sup>ARF</sup> and p16<sup>INK4A</sup> intensity was significantly increased in Col1a1<sup>fl/fl</sup> MEFs relative to wild-type MEFs. The bar graphs show the relative intensity of each protein normalized to tubulin. The asterisks indicate statistical significance (p < 0.05). The Western blots show the relative intensity of each protein normalized to tubulin. The asterisks indicate statistical significance (p < 0.05).



To study the latter scenario, I sought to evaluate cultured cells harvested from wild-type and *Coll1a1<sup>r/r</sup>* mice. MEFs were selected due to their relative ease of harvesting and their known program of replicative senescence when grown in culture (Rohme 1981; Conzen et al. 1995; Serrano et al. 1996). To ensure that harvested MEFs were capable of collagen production, assembly and secretion *in vitro*, I evaluated for the presence of type I collagen fibrils in culture using circular polarization microscopy. This technique specifically identifies fibres based on their birefringence. Over the course of two weeks, MEFs were treated with fresh ascorbate (100  $\mu$ M) every 48 hours in order to improve triple helical structure stabilization of procollagen. Cells were then fixed with 4% paraformaldehyde and stained with picosirius red. As shown, this resulted in an extensive network of fibrillar collagen on the culture dish (Figure 3.12). No collagen fibrils were detected after three days in culture. There was no overt difference in fibril formation between *Coll1a1<sup>r/r</sup>* and wild-type MEFs.

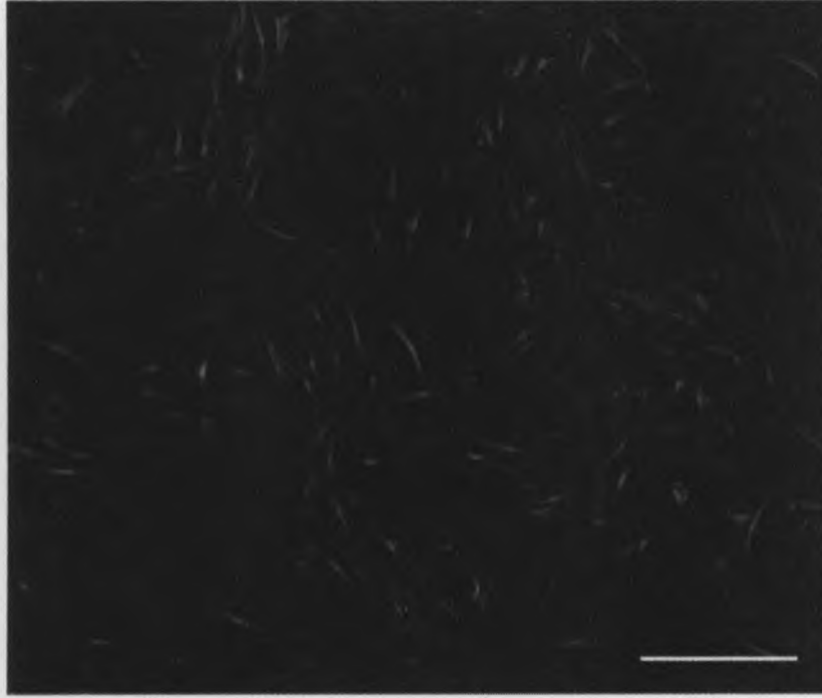
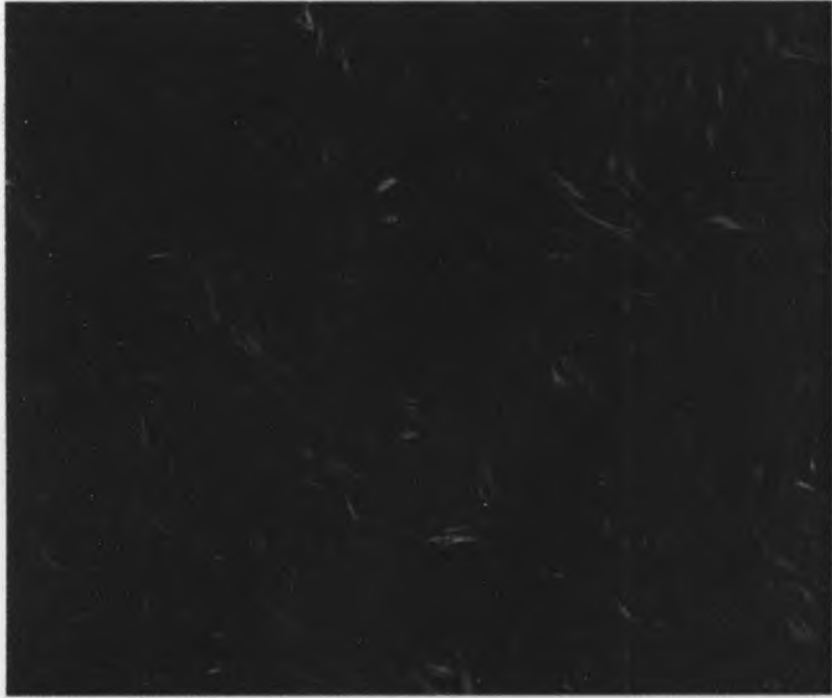
### **3.15. *Coll1a1<sup>r/r</sup>* MEFs Display Morphological Features of Senescence Earlier Than Embryonic Fibroblasts Derived From Wild-type Mice**

To determine whether *Coll1a1<sup>r/r</sup>* MEFs attained senescence sooner or later than wild-type MEFs, I examined serially subcultured cells with Hoffman-modulation contrast microscopy to characterize morphology over multiple subcultures. After six cell passages, MEFs derived from *Coll1a1<sup>r/r</sup>* mice displayed an enlarged round shape, suggestive of a senescent phenotype (Figure 3.13A).

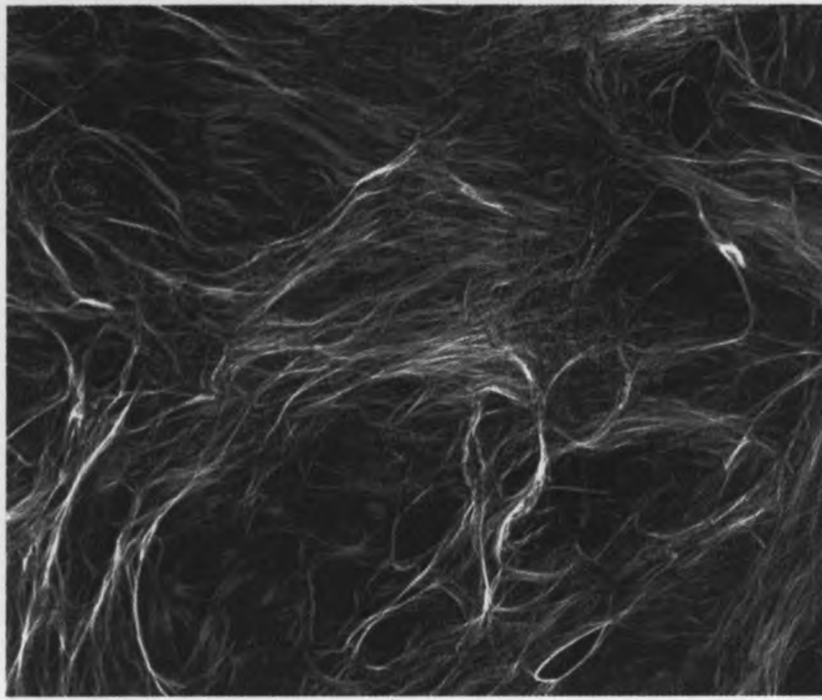
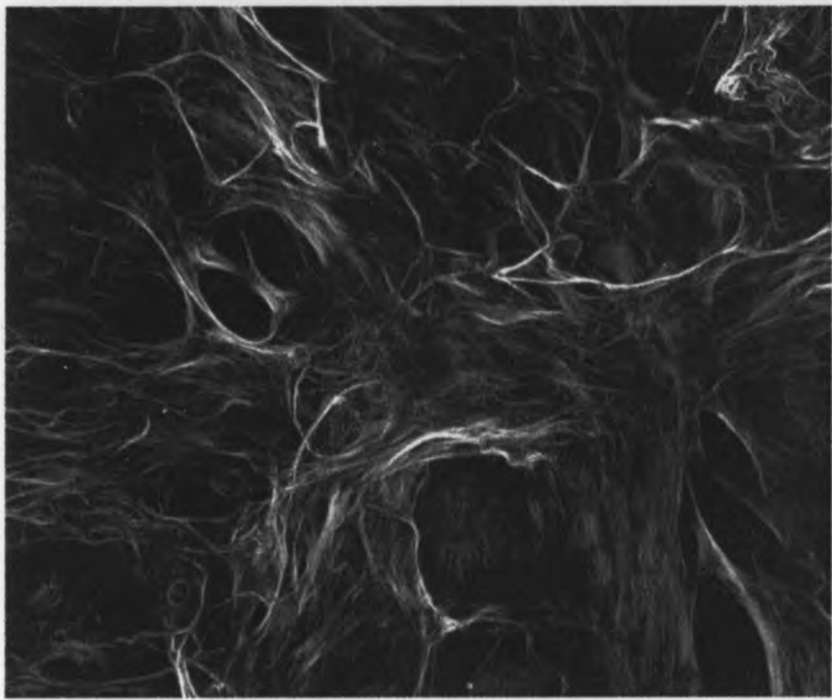
**Figure 3.12.** Mouse embryonic fibroblasts elaborate an extensive collagen fibril network as detected by circular polarization microscopy of cultures stained with picosirius red when grown in culture for two weeks. MEFs isolated at embryonic day 13.5 from wild-type and *Coll1a1<sup>tr</sup>* mice grown on plastic for three days or two weeks are shown. Fresh ascorbate (100  $\mu$ M) was administered every 48 hours. MEFs were fixed with 4% paraformaldehyde for thirty minutes then stained with picosirius red solution for two hours. Collagen fibril birefringence was detected using circular polarization microscopy. Bar denotes 200 microns.

Wild-type

Col1a1<sup>rr</sup>



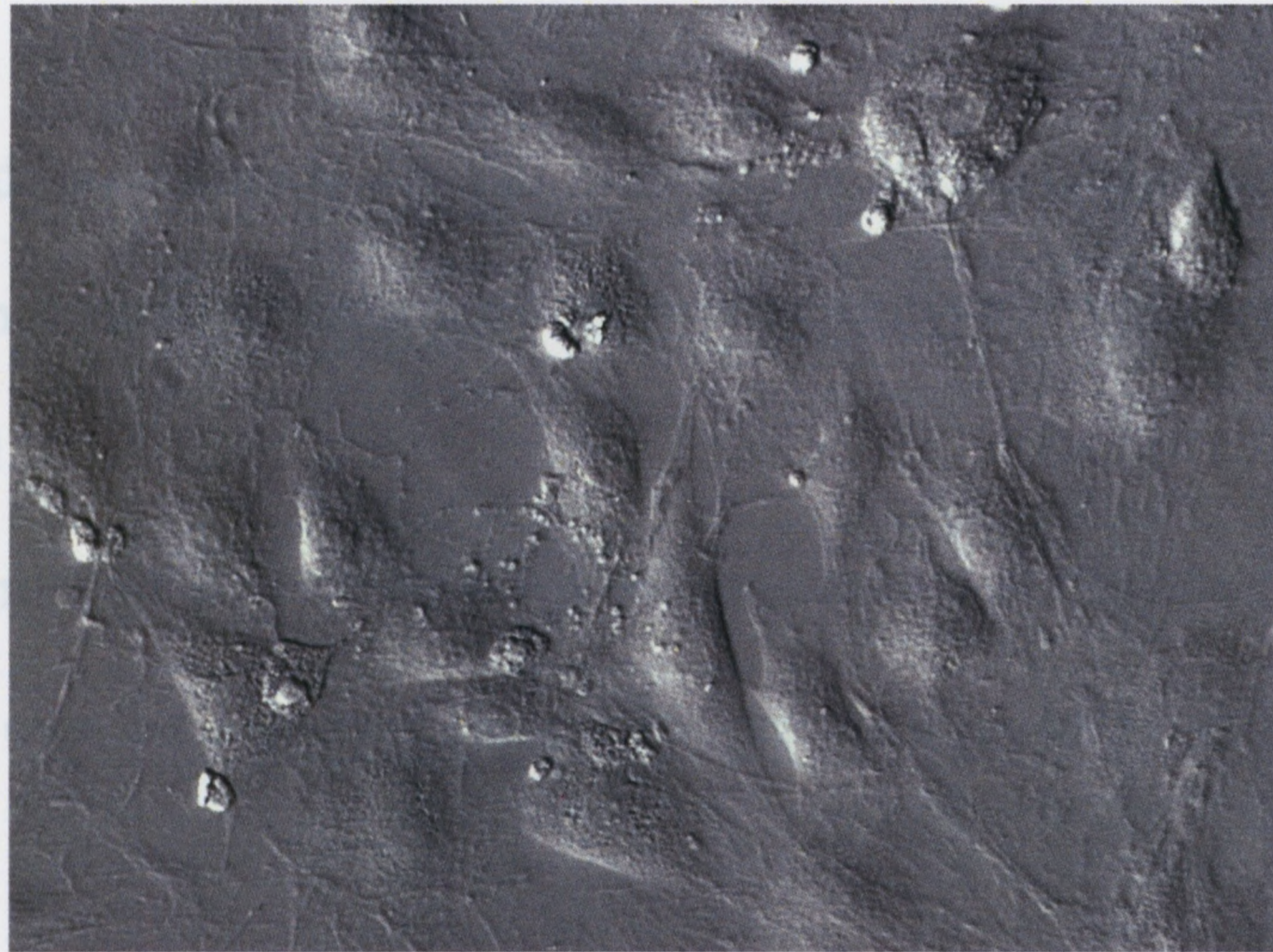
3 days in culture



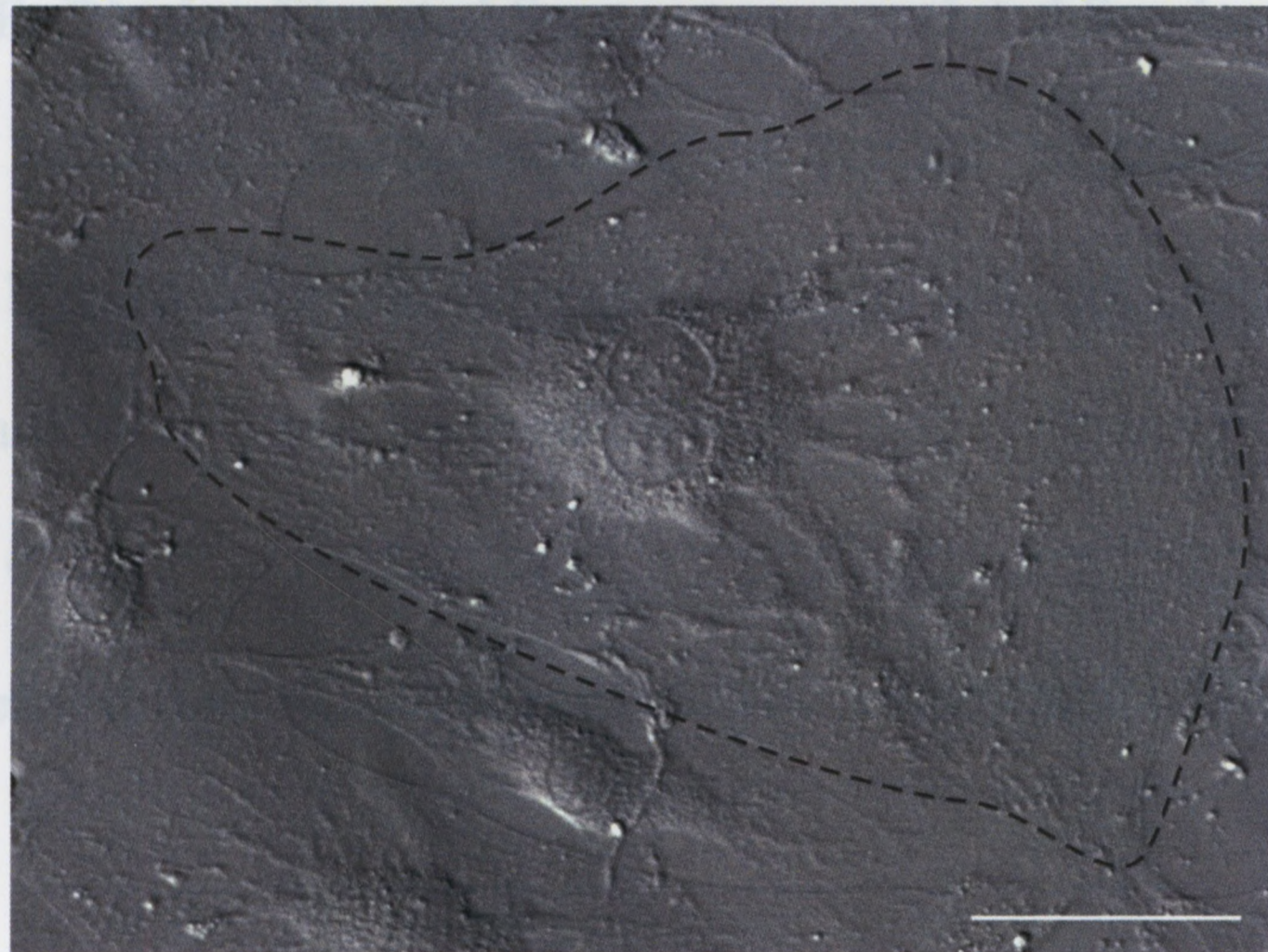
14 days in culture

**Figure 3.13.** Embryonic fibroblasts derived from  $Coll1a1^{r/r}$  mice display spread morphology and multinucleation earlier than embryonic fibroblasts derived from wild-type mice. *A*, Hoffman-modulation contrast images displaying MEFs derived from wild-type and  $Coll1a1^{r/r}$  mice at cell passage six are shown. It can be observed that MEFs derived from  $Coll1a1^{r/r}$  display spread and flattened morphology consistent with senescence, while wild-type MEFs are in a relatively healthy and proliferative state. A large multinucleated  $Coll1a1^{r/r}$  MEF is traced for visualization purposes. Bar denotes 100 microns. *B*, A bar graph displaying the average proportion of wild-type and  $Coll1a1^{r/r}$  multinucleated MEFs is shown. MEFs were grown for two weeks in culture in the presence of ascorbate. There was a significant increase in proportion of multinucleated MEFs derived from  $Coll1a1^{r/r}$  mice ( $10.5\% \pm 0.7\%$ ) over MEFs derived from wild-type mice ( $7.2\% \pm 0.9\%$ ) ( $n=9$ ) ( $p<0.05$ ).

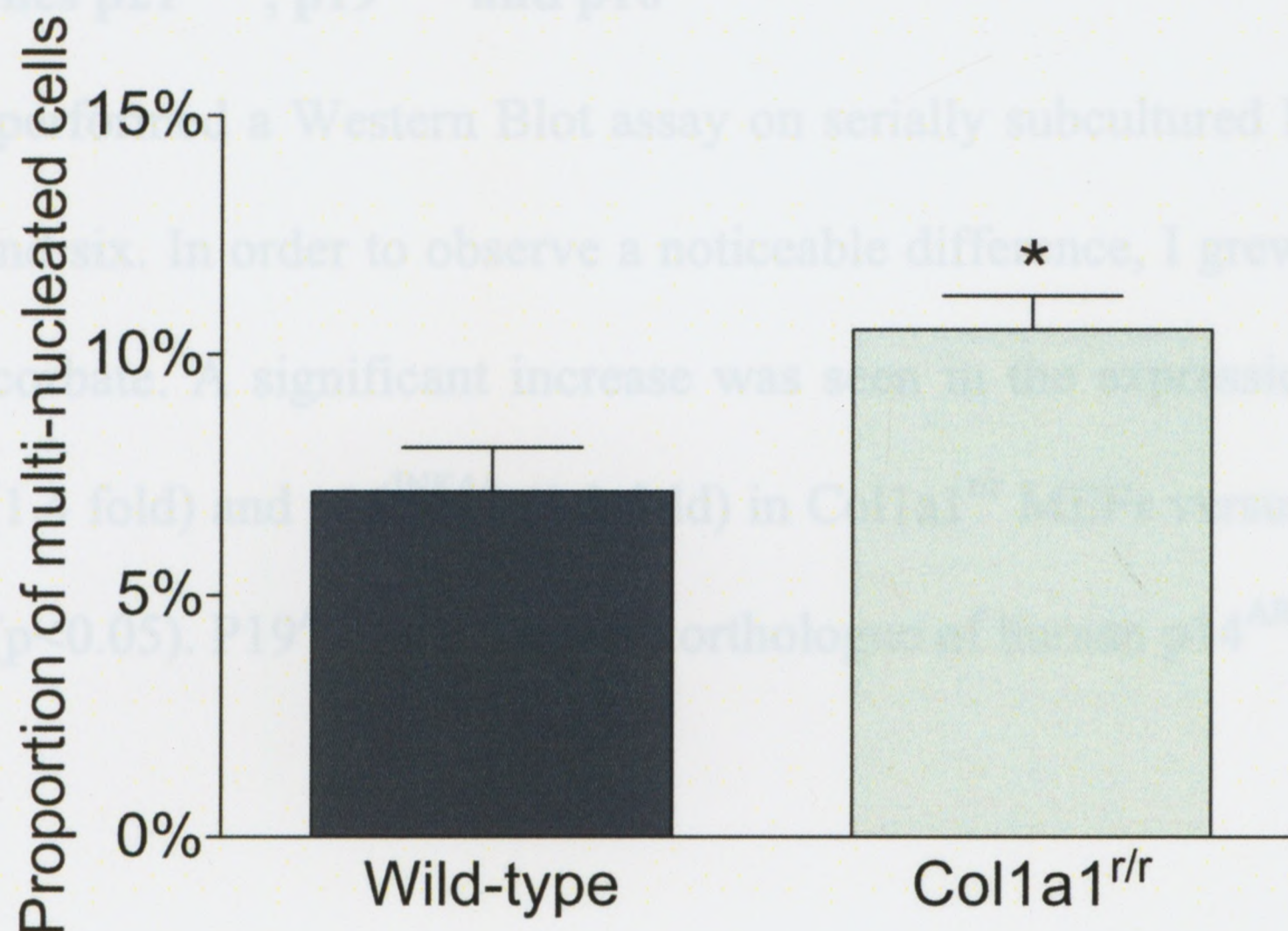
Wild-type  
cell passage 6



Col1a1<sup>r/r</sup>  
cell passage 6



A



B

I also noted an increase in the number of multinucleated cells, a feature commonly found in senescent cells and more noticeably the MEF populations I had cultured (Figure 3.13B). MEFs grown to cell passage six in the presence of ascorbate were assessed for multiple nuclei and a 1.5 fold increase was observed in cells derived from *Coll1a1<sup>r/r</sup>* mice over cells derived from wild-type mice ( $p < 0.05$ ) ( $n = 9$ ).

### **3.16. *Coll1a1<sup>r/r</sup>* MEFs Display Elevated Senescence-associated $\beta$ -galactosidase**

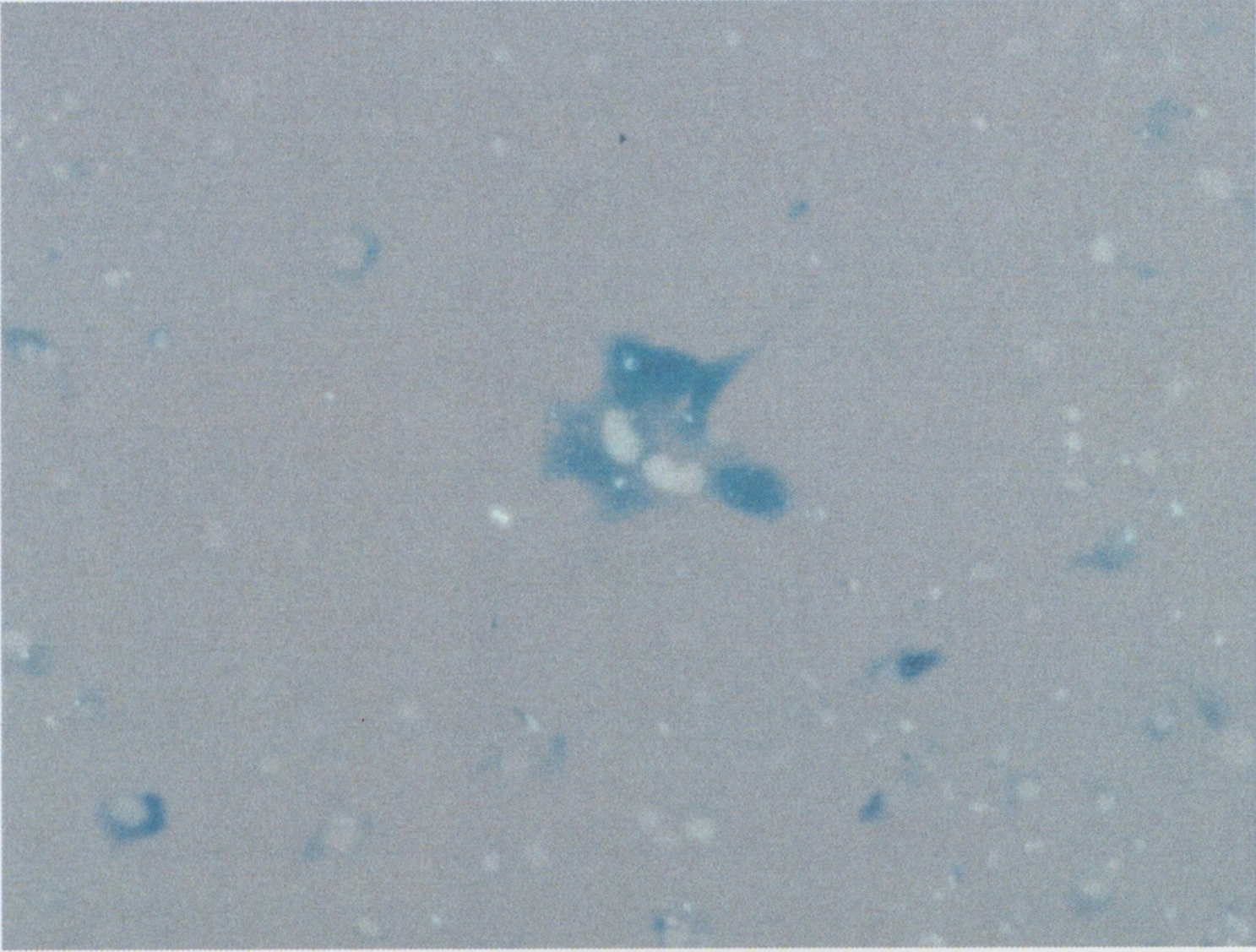
Reminiscent of human SMCs growing on *Coll1a1<sup>r/r</sup>* collagen, cultured MEFs derived from *Coll1a1<sup>r/r</sup>* also displayed increased SA- $\beta$ -gal activity. Cultured cells grown in the presence of ascorbate were observed by bright field microscopy (Figure 3.14A). MEFs derived from *Coll1a1<sup>r/r</sup>* mice displayed a 4.2 fold increase in positively stained cells compared to cells derived from wild-type mice (Figure 3.14B) ( $p < 0.05$ ) ( $n = 3$ ).

### **3.17. *Coll1a1<sup>r/r</sup>* MEFs Exhibit Increased Expression of the Cell-cycle and Senescence-associated Genes $p21^{CIP1}$ , $p19^{ARF}$ and $p16^{INK4A}$**

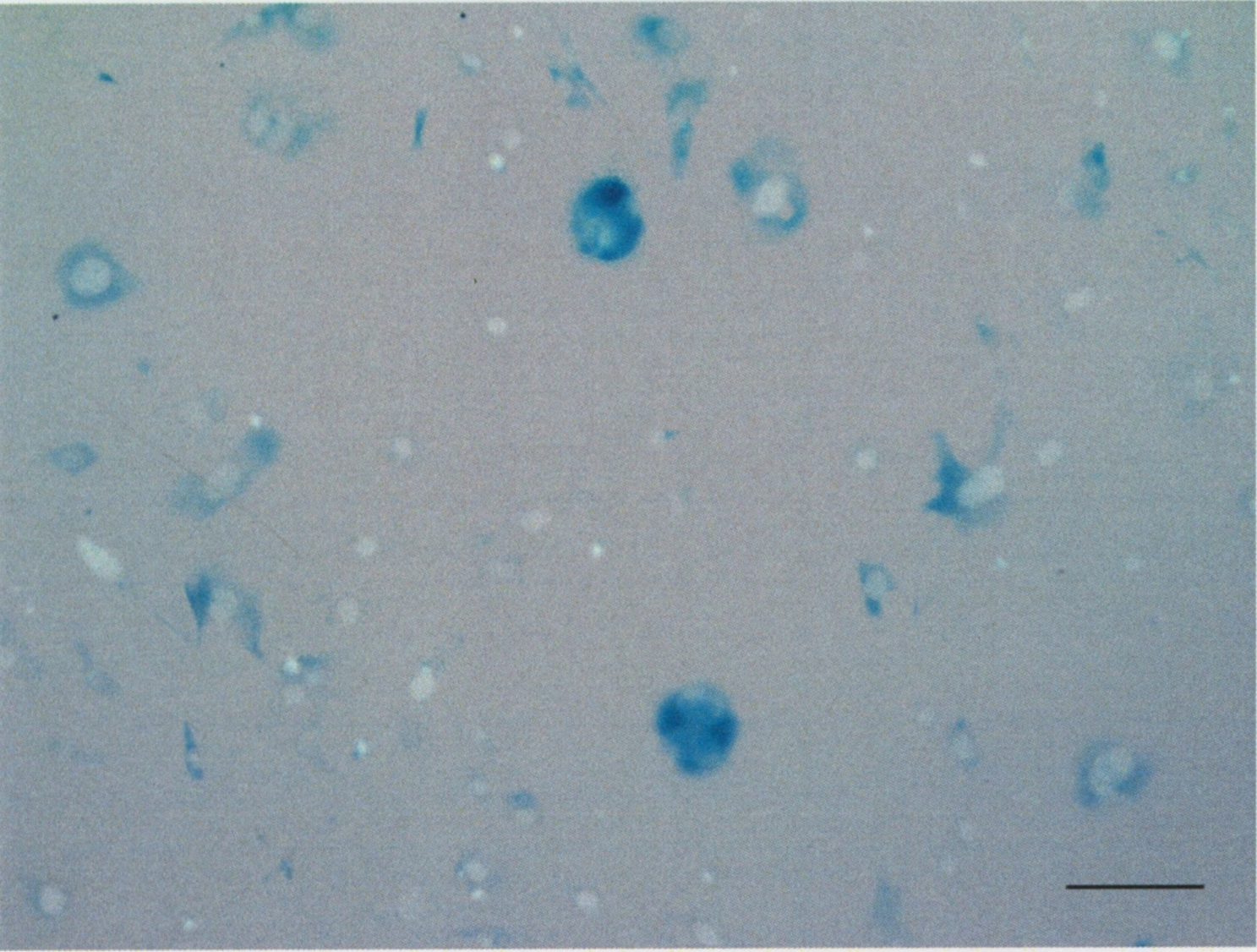
I next performed a Western Blot assay on serially subcultured MEFs at both cell passage five and six. In order to observe a noticeable difference, I grew the MEFs in the absence of ascorbate. A significant increase was seen in the expression of  $p21^{CIP1}$  (1.3 fold),  $p19^{ARF}$  (1.4 fold) and  $p16^{INK4A}$  (1.3 fold) in *Coll1a1<sup>r/r</sup>* MEFs versus wild-type MEFs (Figure 3.15) ( $p < 0.05$ ).  $p19^{ARF}$  is the mouse orthologue of human  $p14^{ARF}$ .

**Figure 3.14.** Serum-starved embryonic fibroblasts derived from  $Coll1a1^{tr}$  mice are more susceptible to premature senescence as indicated by increased SA- $\beta$ -gal activity. *A*, Bright field images of MEFs stained for SA- $\beta$ -gal activity and counterstained with Hoechst are shown. An increase in proportion of positively stained MEFs can be visualized. Bar denotes 200 microns. *B*, A bar graph depicting the average proportion of positively stained SMCs upon administration of  $\beta$ -Gal as described is shown. MEFs were grown for two weeks in culture in the presence of ascorbate. There was a significant increase in proportion of SMCs staining positive for SA- $\beta$ -gal activity in  $Coll1a1^{tr}$  MEFs ( $9.6\% \pm 1.8\%$ ) versus wild-type MEFs ( $2.3\% \pm 0.6\%$ ) ( $n=3$ ) ( $p<0.05$ ).

Wild-type  
cell passage 6



Col1a1<sup>r/r</sup>  
cell passage 6



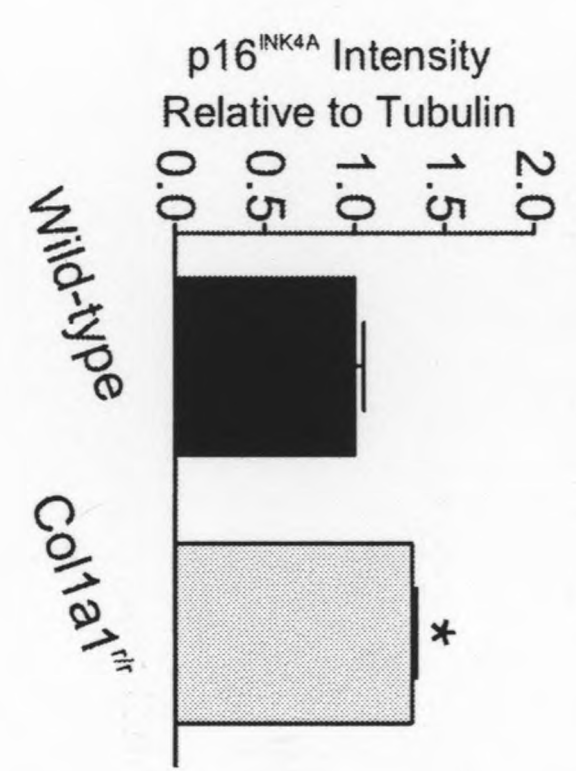
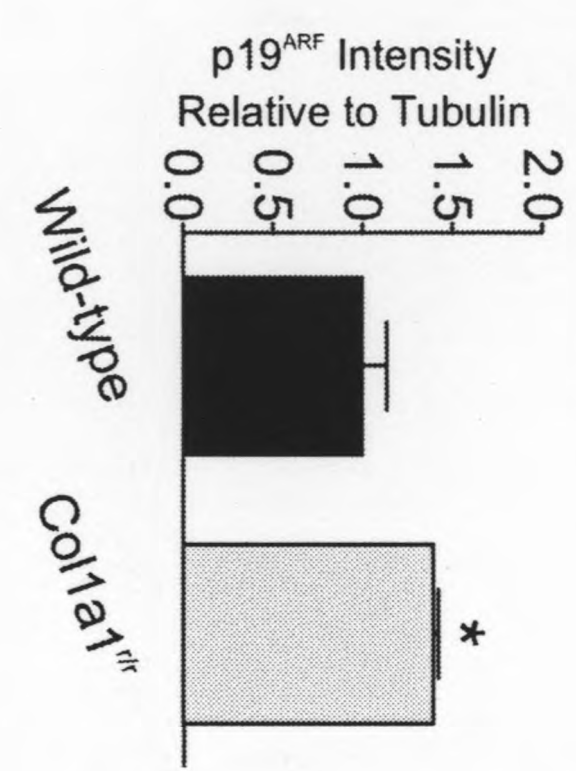
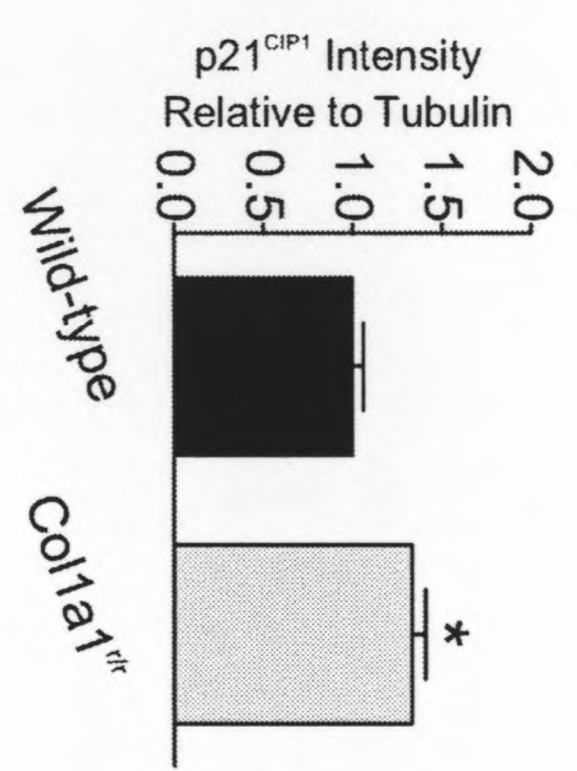
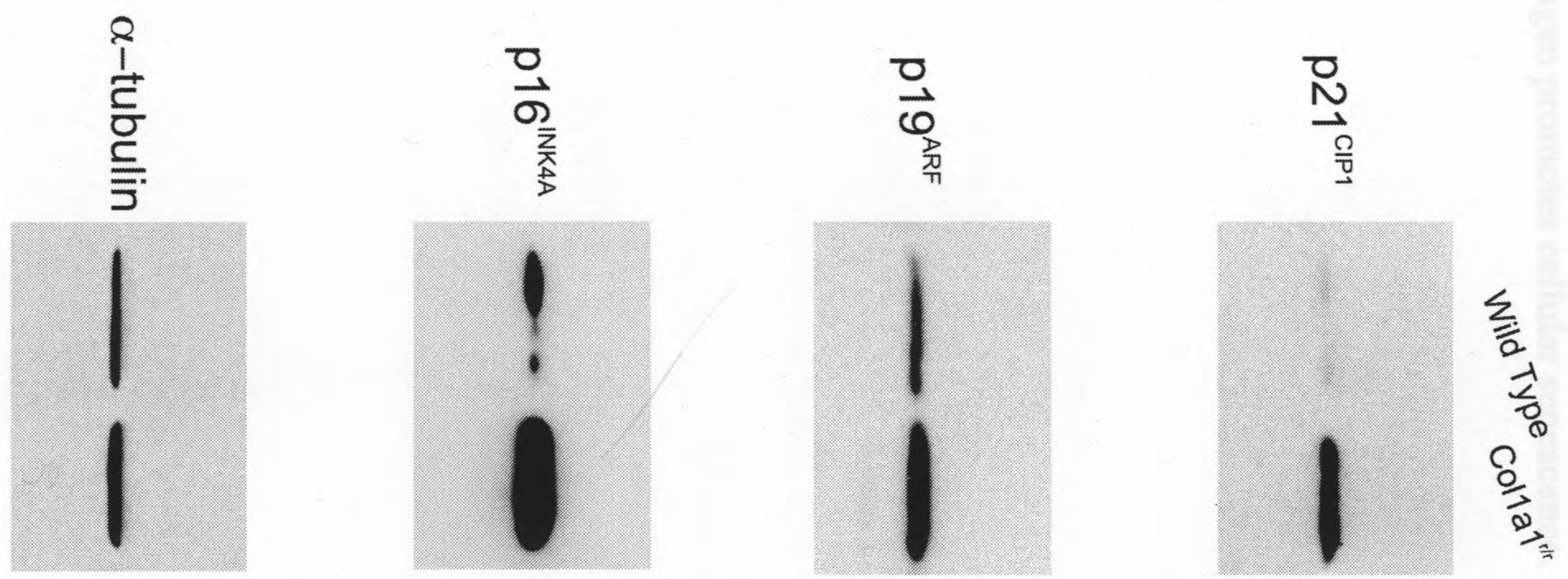
A

B



**Figure 3.15.** Embryonic fibroblasts derived from  $Coll1a1^{tr}$  mice display increased protein expression of the senescence-associated genes  $p21^{CIP1}$ ,  $p19^{ARF}$  and  $p16^{INK4A}$ . Western blots of the senescence-associated genes  $p21^{CIP1}$ ,  $p19^{ARF}$  and  $p16^{INK4A}$  in MEFs derived from  $Coll1a1^{tr}$  and wild-type mice are shown. MEFs were grown *in vitro* to cell passage five or six in the absence of ascorbate and  $\alpha$ -tubulin expression was used as a loading control. There was a significant increase in expression of  $p21^{CIP1}$  (1.3 fold),  $p19^{ARF}$  (1.4 fold) and  $p16^{INK4A}$  (1.3 fold) in  $Coll1a1^{tr}$  MEFs versus wild-type MEFs ( $p < 0.05$ ).

These studies of the impact of endogenous collagen production on the susceptibility of MEFs to premature senescence confirm the hypothesis that collagen-resistant collagen promotes cellular senescence.



These studies of the impact of endogenous collagen production on the susceptibility of MEFs to premature senescence confirm the hypothesis that collagenase-resistant collagen promotes cellular senescence.

## **Chapter 4**

### **Discussion**

Type I collagen, a molecule abundant in the atherosclerotic plaque, undergoes progressive intermolecular cross-linking (Hamlin et al. 1971; Hamlin et al. 1972; Davis et al. 1975; Zwolinski et al. 1976) increasing its resistance to proteolysis by collagenases 1, 2 and 3 (Griffin et al. 2002). Another major component of the atherosclerotic plaque is vascular SMCs. Vascular SMCs must remain viable and highly functional in order to prevent plaque rupture, an event with potentially fatal consequences. SMC senescence has recently been identified as a potential pathway by which SMCs lose their function in atherosclerotic lesions (Matthews et al. 2006). In this thesis, I introduce the novel concept that the ECM is a determinant of cellular lifespan and senescence. I specifically report that aging is functionally linked to the capacity of type I collagen to be cleaved.

Based on my findings, I propose that the inability to cleave type I collagen can promote 1) accelerated aging in mice; 2) premature vascular SMC senescence in culture; 3) premature MEF senescence in culture.

#### **4.1. $Coll1a1^{r/r}$ Type I Collagen Expression Promotes Accelerated Aging in Mice**

The  $Coll1a1^{r/r}$  mouse, generated over 20 years ago, has been previously studied in a number of contexts, but never with respect to features of aging (Liu et al. 1995; Zhao et al. 1999; Zhao et al. 2000; Aihara et al. 2003; Beare et al. 2003; Lindsey et al. 2003; Fukumoto et al. 2004). In our  $Coll1a1^{r/r}$  colonies, I observed a striking reduction in mouse lifespan. This was accompanied by a decrease in body weight, and phenotypic changes that are associated with aging. These changes include increased kyphosis of the spine, decreased body fat composition, decreased bone mineral density, disrupted elastin in the aortic wall and an increased predisposition of aortic SMCs to premature senescence.

One theory of organismal aging is that it is closely linked to an accumulation of senescent cells throughout the body (Chen et al. 2007). This theory is supported by several findings. First, senescent cells are found in sites of age-related disease such as atherosclerotic lesions, ulcers, intervertebral disc degeneration, livers with chronic hepatitis C, kidneys with glomerular disease, and arthritic joints, both *in vivo* and *ex vivo* (Paradis et al. 2001; Krtolica et al. 2002; Campisi 2005; Le Maitre et al. 2007; Sis et al. 2007). Furthermore, senescent cells are found to increase with age in primate skin (Herbig et al. 2006), human vascular tissue (Matthews et al. 2006; Minamino et al. 2007) and human kidneys (Melk et al. 2004). Second, fibroblasts harvested from animals with relatively long lifespans will generally have a greater replicative limit than those derived from animals with short lifespans (Rohme 1981). Also, fibroblasts harvested from human patients with Werner syndrome and Bloom syndrome, disorders related to accelerated aging, undergo premature senescence (Thompson et al. 1983; Davis et al. 2007). A relationship between senescence and aging is also suggested by studies of mice with disrupted p63 expression. Disruption of p63 in mouse keratinocytes in culture resulted in premature senescence as assessed by increased SA- $\beta$ -gal activity. Furthermore, conditional deficiency of p63 in stratified epithelia resulted in features of mouse aging such as hair loss, increased kyphosis, body mass reduction and age-related skin defects, and features of cellular senescence such as increased SA- $\beta$ -gal activity and elevated transcript levels of p16<sup>INK4A</sup> in the skin (Keyes et al. 2005). These findings suggest that cellular senescence and organismal aging are intimately linked.

In addition to studying the endpoints I have reported, there are other indicators of aging that I could potentially study. Previous studies have shown that arterial vessel

stiffening, as the result of a blunted acetylcholine-mediated dilation response, is common in elderly individuals (Taddei et al. 1995). However, vessel stiffening can also be impacted by age-related modifications to the ECM, including the accumulation of type I collagen and an increase in type I collagen cross-linking (Lakatta 2003). Another related endpoint that could be studied is stiffening of the left ventricular myocardium. Left ventricular diastolic filling rate is known to decrease with age, partly due to increased fibrosis as a result of accumulation and cross-linking of collagen (Lakatta et al. 2003) and thus I did not prioritize it for study. I qualitatively observed an increase in fibrosis in the aorta. This could also be assessed in the myocardium, as well as through hemodynamic assessment with intra cardiac catheters (Nguyen et al. 2003).

Another commonly studied endpoint of aging is an increase in oxidative stress. Oxidative stress by ROS is thought to be a major causal factor of premature senescence in aged individuals (Sohal et al. 1996). Studies in aortic endothelial cells of mice have shown that strains known to live longer display an increased resistance to oxidative stress and generate lower levels of cellular ROS (Csiszar et al. 2007). This leads us to speculate that the *Coll1a1<sup>r/r</sup>* mouse might be more susceptible to oxidative damage as a result of both increased levels of ROS and a decreased resistance to oxidative damage. This could be studied by incubating aortic rings with dihydroethidine, which reacts with superoxide in order to generate the fluorescent molecule ethidium bromide. Ethidium bromide fluorescence would then allow us to measure oxidative stress (Pearson et al. 2008).

Another endpoint of aging that is commonly studied is the increased expression of cell-cycle or senescence-associated genes. Previous studies have shown elevated levels of p21<sup>CIP1</sup> (Miao et al. 2008), p16<sup>INK4A</sup> (Keyes et al. 2005) and p19<sup>ARF</sup> (Nishino et al. 2008)

in mice that are old or have premature aging disorders, suggesting that I would find similar results in the vasculature of  $Coll1a1^{r/r}$  mice. Although I attempted to detect elevated levels of  $p16^{INK4A}$  and  $p21^{CIP1}$  in aortas of  $Coll1a1^{r/r}$  mice by immunohistochemistry, I was unable to detect a signal. A more sensitive technique, such as real-time RT-PCR, may be an alternative approach.

Although  $Coll1a1^{r/r}$  mice display specific features of accelerated aging, I am left with the question as to why exactly they die at a younger age than wild-type littermates. Shortened lifespan is not a feature of accelerated aging in and of itself but is caused by some age-related defect. It is thought that the accumulation of senescent cells can cause age-related defects via two pathways: 1) Senescent cells impair the regenerative ability of organs due to the cessation of cellular replication; 2) due to their ECM degradation and inflammatory gene profile, they disrupt tissue structure and perturb the microenvironment of the tissue. Both pathways result in a decline in tissue and ultimately organ function (Chen et al. 2007). I performed serological screening of the mice and concluded that increased mortality was not the result of kidney or liver damage. It was noticed that  $Coll1a1^{r/r}$  mice were experiencing late-stage respiratory distress as indicated by heavy, laboured breathing. Type I collagen accumulation in the lung is associated with acute respiratory distress syndrome and pulmonary fibrosis in humans (Last et al. 1983; Armstrong et al. 1999). Thus, the inability to turnover type I collagen in the lungs of  $Coll1a1^{r/r}$  mice might potentially have similar consequences. Furthermore, forthcoming echocardiography results might indicate the possibility of myocardial wall thickening (left ventricular hypertrophy) due to the accumulation of proteolysis-resistant collagen,

and this can increase the risk for coronary heart disease or other related cardiovascular diseases (Levy et al. 1990).

#### **4.2. Collagenase-resistant Type I Collagen Promotes Cellular Senescence *in vitro***

As noted, in this thesis, I identified the impact of collagenase-resistance on aging of the *Coll1a1<sup>r/r</sup>* mouse as assessed by a panel of age-related endpoints and obtained evidence supporting the notion that collagenase-resistant collagen can promote cellular senescence *in vivo* as indicated by positive SA- $\beta$ -gal activity in vascular SMCs in the aorta. As discussed here, I also determined whether this latter finding might be the result of a direct effect of collagenase-resistant collagen on vascular SMC senescence.

The environment of the atherosclerotic plaque is harsh and can compromise the viability of vascular SMCs that are responsible for maintaining stability in order to prevent plaque rupture. Besides increased susceptibility to apoptosis (Geng et al. 1995; Clarke et al. 2008) and autophagy (Schrijvers et al. 2007), another fate of plaque SMCs is cellular senescence (Matthews et al. 2006). Additionally, type I collagen is a predominant ECM molecule in the fibrous atherosclerotic plaque and is normally degraded and elaborated by SMCs that have migrated from the media into the intima. By making use of recombinant type I collagen that is resistant to proteolytic editing, I specifically examined the phenomenon of collagenase-resistance. Although this specific molecular change is not one associated with aging, the phenomenon of resistance to proteolysis can be considered to phenocopy the natural aging process that is characterized by progressive intermolecular cross-linking.

SMCs derived from the internal thoracic artery of humans replicating on collagenase-resistant collagen displayed decreased lifespan, senescent-like morphological changes, increased SA- $\beta$ -gal activity, and increased transcript levels of the cell-cycle genes p16<sup>INK4A</sup> and p21<sup>CIP1</sup>, suggesting that they are more susceptible to premature senescence. In the presence of stress, specifically serum-deprivation, SMCs plated on collagenase-resistant collagen displayed morphological changes, increased SA- $\beta$ -gal activity, and increased protein expression of the cell-cycle inhibitory genes p16<sup>INK4A</sup>, p21<sup>CIP1</sup> and p14<sup>ARF</sup>. In view of these findings, I propose that resistance to collagen cleavage is a novel promoter of SMC senescence.

The progression of atherosclerotic lesions is the result of many factors such as smoking, cholesterol levels and increasing age (Fabris et al. 1994). Senescent vascular SMCs are one feature of atherosclerosis and one possible contributing factor to the progression of this disease, because senescent cells have an inflammatory and non-proliferative phenotype. Impaired ability to cleave type I collagen and the resulting disproportionate accumulation of fibrillar collagen is a known cause of fibrosis and can consequently impair the atherosclerotic remodelling response.

Type I collagen is soluble in acetic acid and assumes a monomeric form. Although this is convenient for culture studies, as primary cells can be grown on a collagen monolayer and examined, it might not mimic the collagen fibres endogenously assembled and secreted by cells. To specifically examine the effect of endogenous expression of Colla1<sup>r/r</sup> type I collagen, I made use of embryonic fibroblasts derived from mice harbouring this mutation. Serially subcultured MEFs derived from Colla1<sup>r/r</sup> mice displayed a phenotype suggesting premature senescence. This included senescent-like

morphological cell spreading and thinning, multinucleation, increased SA- $\beta$ -gal activity, and elevated expression of cell-cycle inhibitory genes p21<sup>CIP1</sup>, p16<sup>INK4A</sup> and p14<sup>ARF</sup>.

Highly proliferating organs require viable adult stem cells in order to ensure proper regenerative ability (Lee et al. 1998; von Figura et al. 2009). Importantly, this self-renewal ability of stem cells is diminished with age (Edelberg et al. 2008). One proposed mechanism of this is increased expression of p16<sup>INK4A</sup> (Janzen et al. 2006). Therefore, if indeed vascular SMCs on Colla1<sup>r/r</sup> collagen are more susceptible to senescence, one would postulate that this might also hold true in adult stem cells. Evaluating the effect of Colla1<sup>r/r</sup> on variously harvested stem cells, such as mesenchymal stem cells, could thus be performed in a similar manner to what I have presented in this thesis.

### **4.3. Limitations of the Study**

A potential limitation of our assessment for senescence is that senescence-related endpoints are not entirely specific and can be attributed to other factors. For example, serum-deprivation induced cellular quiescence will result in a rapid decline in cumulative population doublings, but this in itself does not mean senescence. However, it is known that SA- $\beta$ -gal activity is not induced in quiescent cells (Dimri et al. 1995). There are nonetheless qualifications in the use of the SA- $\beta$ -gal activity assay. Although SA- $\beta$ -gal activity is associated with senescence, it is not specific (Debacq-Chainiaux et al. 2009). For example, pre-senescent cells in culture at high confluence will exhibit SA- $\beta$ -gal activity that is lost two days after replating to a lower cell density (Dimri et al. 1995). Also, young adult melanocytes and sebaceous and eccrine gland cells express SA- $\beta$ -gal independent of premature senescence while senescent fibroblasts from some mouse

strains do not express SA- $\beta$ -gal at all (Dimri et al. 1995). Thus, in some cases, increased SA- $\beta$ -gal activity as a result of elevated lysosomal activity might be observed independent of senescence.

Similarly, molecular markers such as p21<sup>CIP1</sup>, p14/p19<sup>ARF</sup> and p16<sup>INK4A</sup> are known to be associated with senescence, but in certain cases are not exclusively causative. For example, skin fibroblasts derived from patients with Li-Fraumeni syndrome undergo replicative senescence in the absence of p53 and p21 expression suggesting that p21 is not an absolute requirement for senescence (Medcalf et al. 1996). Moreover, p16<sup>INK4A</sup> and p19<sup>ARF</sup> transcript and protein expression in mouse tissue was found to be considerably lower than primary MEFs grown in culture for less than 14 days (Krishnamurthy et al. 2004). This suggests that the simple act of growing cells in culture can be a form of stress and can subsequently induce the expression of elevated levels of p16<sup>INK4A</sup> and p19<sup>ARF</sup>. Thus, the assessment for cellular senescence cannot rely on a single senescence-related indicator. I chose a panel of endpoints in order to support our interpretation that collagenase-resistant type I collagen is able to promote senescence in human vascular SMCs and MEFs. There are additional protein markers that I could assess to strengthen our hypothesis. For example, in senescent cells, highly condensed regions of chromatin such as SAHFs and telomere dysfunction-induced foci are found to be associated with DNA damage proteins such as p53-binding protein-1 and ATM (Herbig et al. 2004; Zhang et al. 2005). Also, inhibition of cell-cycle progression kinase complexes such as cyclin D/CDK4 results in hypophosphorylated pRb, which in its activated form can inhibit E2F and cyclin E/CDK2 activity (Sherr et al. 2002). Thus,

hypophosphorylation of pRb and decreased levels of cyclin D<sub>1-3</sub>, cyclin E, and E2F-1 can also be used as indicators of senescence (Matthews et al. 2006).

#### 4.4. Potential Future Implications

I made use of a collagenase-resistant type I collagen as a model of the age-related modifications that collagen undergoes. The actual age-related changes in collagen that take place include progressive intermolecular cross-linking resulting in increased resistance to proteolytic editing. One limitation of using Colla1<sup>r/r</sup> collagen as a model of aged collagen is that it may prevent collagenase cleavage to a greater extent than increased cross-linking with age where the formation of intermolecular cross-links leads to a partial increase in resistance to proteolytic editing (Hamlin et al. 1971). Another way that I might examine the effect of increased resistance to proteolytic editing would be to artificially form cross-links in type I collagen.

One method of cross-linking collagen is through the non-enzymatic formation of AGE (Mentink et al. 2002). This cross-linking can be facilitated by incubation of harvested collagen with D-glucose (Chen et al. 2001). Previous studies have shown that young human umbilical vein endothelial cells grown on glycated type I collagen expressed features of premature senescence including increased SA- $\beta$ -gal activity, and increased p53 and p14<sup>ARF</sup> expression (Chen et al. 2002). To date, this effect has not been studied in vascular SMCs.

Another method of artificially cross-linking type I collagen is via the enzymatic action of tissue transglutaminase (tTG), resulting in increased cross-links and increased resistance to proteolytic editing (Chau et al. 2005). In one study, myofibroblastic stellate

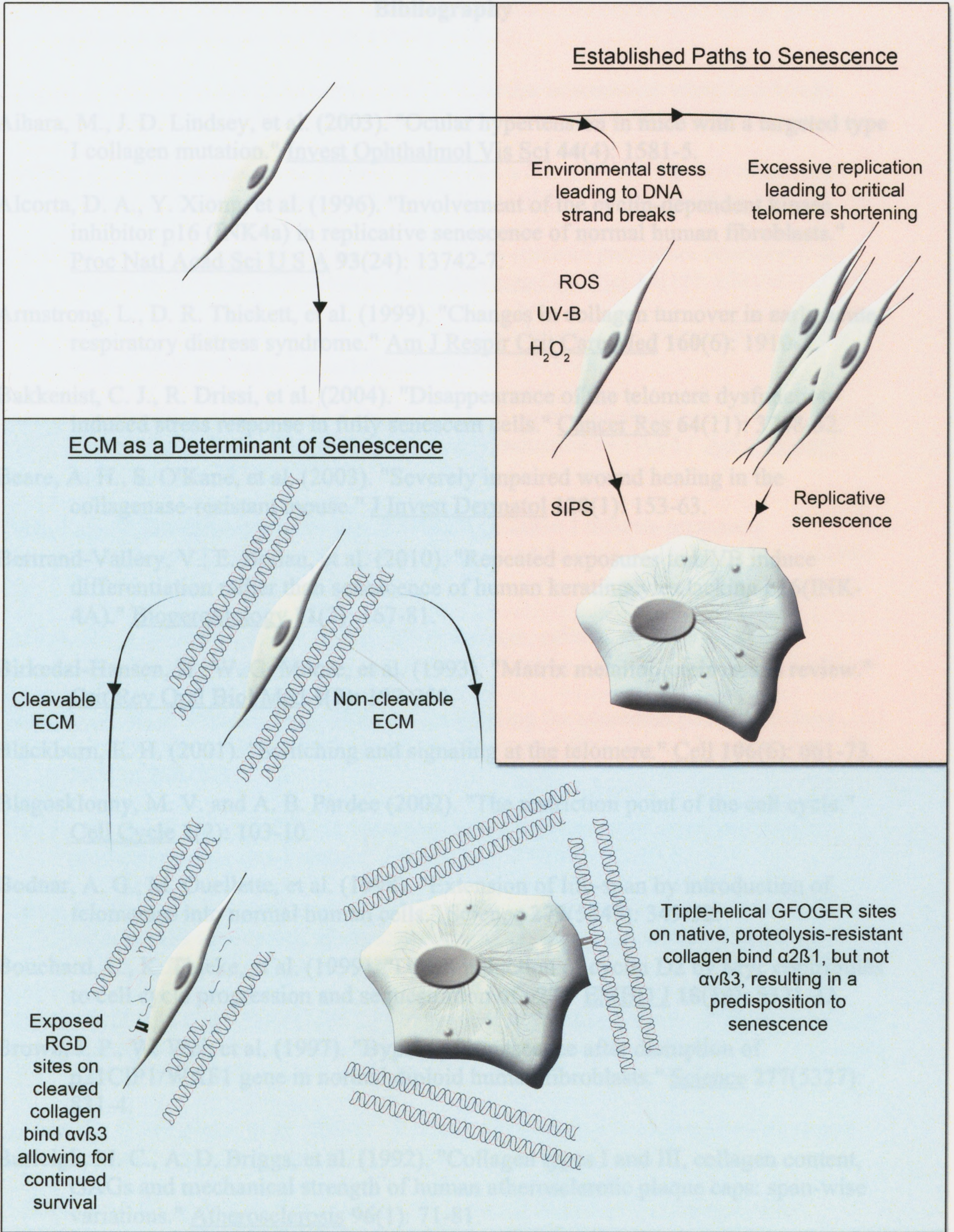
cells plated on tTG-treated type I collagen substrate exhibited similar behaviour to cells plated on  $\text{Coll1a1}^{r/r}$  collagen. In particular, this led to a significant decrease in proliferation rate and an increased expression of p21<sup>CIP1</sup> protein (Zhou et al. 2006). These results suggest that tTG-facilitated cross-linking of type I collagen may also have an effect on proliferation of cultured cells. To ensure that the effect seen in cells grown in the presence of  $\text{Coll1a1}^{r/r}$  collagen is the result of increased resistance to proteolytic editing, these other two models could be studied as well.

Our findings do not address the specific mechanistic pathway by which collagenase-resistance can promote premature senescence. Integrins are cell-surface proteins that transmit signals from neighbouring cells and ECM molecules into the cell. One possible explanation for our findings is an altered engagement of a certain integrin(s) due to the improper proteolysis of type I collagen. Previous studies have shown that human melanoma cells adhere to denatured and native type I collagen via different integrins. Whereas native collagen binds  $\alpha2\beta1$  integrin, native type I collagen also contains cryptic RGD sites that upon denaturation are revealed and are able to engage the  $\alpha\nu\beta3$  integrin (Davis 1992; Messent et al. 1998; Knight et al. 2000).  $\alpha\nu\beta3$  is a known pro-survival integrin and its proper engagement has been associated with SMC migration (Jones et al. 1996), proliferation (Zhou et al. 2004) and IGF-1R signalling (Zheng et al. 1998). This pro-survival signalling is thought to be due to proper engagement of the  $\alpha\nu\beta3$  integrin, presumably by denatured or cleaved type I collagen, and subsequent unimpaired IGF-1R signalling (Maile et al. 2001). This notion is confirmed in an experiment examining the effect of blocking  $\alpha\nu\beta3$  integrin with echistatin in myofibroblastic hepatic stellate cells. In the presence of normal collagen, the blocking of  $\alpha\nu\beta3$  and resulting

absence of bound RGD sites resulted in reduced cellular proliferation and adhesion. On the other hand, this blocking effect was not seen in the presence of Coll1a1<sup>r/r</sup> collagen as these cells already exhibited reduced proliferation and adhesion (Zhou et al. 2006). This implies that Coll1a1<sup>r/r</sup> type I collagen, due to its resistance to proteolytic editing, is not revealing the necessary RGD-ligand binding site for proper engagement of  $\alpha v \beta 3$ . I speculate therefore that the inability to properly cleave type I collagen results in shutting off a switch in signalling mediated by the pro-survival integrin ( $\alpha v \beta 3$ ) ultimately resulting in premature cellular senescence (Figure 4.1).

In summary, the data in this thesis are the first to indicate that the ECM can be a promoter of cellular senescence. I found that proteolysis-resistant type I collagen promotes cellular senescence and accelerates the aging process of mice. My findings thus suggest a novel cross-talk between cells and the insoluble ECM that lead to age-related deterioration in vascular function, and possibly of other tissues as well.

**Figure 4.1** Schematic depicting the ECM as a novel determinant of cellular lifespan and senescence. The two classic ways of categorizing senescence, specifically replicative senescence and SIPS, are shown on the right and highlighted in pink. Another proposed driver of senescence is the ECM and this is shown on the left and highlighted in blue. Normal collagen that is cleaved is a survival signal for the cell and it is able to progress through the cell-cycle unabated. This might be due to RGD sites that are exposed upon collagen cleavage that engage  $\alpha v \beta 3$  integrin, allowing for pro-survival downstream signalling.  $Col1a1^{r/r}$  collagen, or cross-linked collagen, exhibits increased resistance to proteolytic editing. Collagen fibrils remain intact and in their native form and cause a predisposition to premature senescence. This might be due to a switch from  $\alpha v \beta 3$  engagement to  $\alpha 2 \beta 1$  engagement by triple-helical glycine-phenylalanine-hydroxyproline-glycine-glutamic acid-arginine (GFOGER) sites.



## Bibliography

- Aihara, M., J. D. Lindsey, et al. (2003). "Ocular hypertension in mice with a targeted type I collagen mutation." *Invest Ophthalmol Vis Sci* **44**(4): 1581-5.
- Alcorta, D. A., Y. Xiong, et al. (1996). "Involvement of the cyclin-dependent kinase inhibitor p16 (INK4a) in replicative senescence of normal human fibroblasts." *Proc Natl Acad Sci U S A* **93**(24): 13742-7.
- Armstrong, L., D. R. Thickett, et al. (1999). "Changes in collagen turnover in early acute respiratory distress syndrome." *Am J Respir Crit Care Med* **160**(6): 1910-5.
- Bakkenist, C. J., R. Drissi, et al. (2004). "Disappearance of the telomere dysfunction-induced stress response in fully senescent cells." *Cancer Res* **64**(11): 3748-52.
- Beare, A. H., S. O'Kane, et al. (2003). "Severely impaired wound healing in the collagenase-resistant mouse." *J Invest Dermatol* **120**(1): 153-63.
- Bertrand-Vallery, V., E. Boilan, et al. (2010). "Repeated exposures to UVB induce differentiation rather than senescence of human keratinocytes lacking p16(INK-4A)." *Biogerontology* **11**(2): 167-81.
- Birkedal-Hansen, H., W. G. Moore, et al. (1993). "Matrix metalloproteinases: a review." *Crit Rev Oral Biol Med* **4**(2): 197-250.
- Blackburn, E. H. (2001). "Switching and signaling at the telomere." *Cell* **106**(6): 661-73.
- Blagosklonny, M. V. and A. B. Pardee (2002). "The restriction point of the cell cycle." *Cell Cycle* **1**(2): 103-10.
- Bodnar, A. G., M. Ouellette, et al. (1998). "Extension of life-span by introduction of telomerase into normal human cells." *Science* **279**(5349): 349-52.
- Bouchard, C., K. Thieke, et al. (1999). "Direct induction of cyclin D2 by Myc contributes to cell cycle progression and sequestration of p27." *EMBO J* **18**(19): 5321-33.
- Brown, J. P., W. Wei, et al. (1997). "Bypass of senescence after disruption of p21CIP1/WAF1 gene in normal diploid human fibroblasts." *Science* **277**(5327): 831-4.
- Burleigh, M. C., A. D. Briggs, et al. (1992). "Collagen types I and III, collagen content, GAGs and mechanical strength of human atherosclerotic plaque caps: span-wise variations." *Atherosclerosis* **96**(1): 71-81.
- Campisi, J. (1998). "The role of cellular senescence in skin aging." *J Investig Dermatol Symp Proc* **3**(1): 1-5.

- Campisi, J. (2005). "Senescent cells, tumor suppression, and organismal aging: good citizens, bad neighbors." Cell **120**(4): 513-22.
- Campisi, J. and F. d'Adda di Fagagna (2007). "Cellular senescence: when bad things happen to good cells." Nat Rev Mol Cell Biol **8**(9): 729-40.
- Carnero, A., J. D. Hudson, et al. (2000). "p16INK4A and p19ARF act in overlapping pathways in cellular immortalization." Nat Cell Biol **2**(3): 148-55.
- Chainiaux, F., J. P. Magalhaes, et al. (2002). "UVB-induced premature senescence of human diploid skin fibroblasts." Int J Biochem Cell Biol **34**(11): 1331-9.
- Chau, D. Y., R. J. Collighan, et al. (2005). "The cellular response to transglutaminase-cross-linked collagen." Biomaterials **26**(33): 6518-29.
- Chen, J., S. Brodsky, et al. (2001). "Delayed branching of endothelial capillary-like cords in glycated collagen I is mediated by early induction of PAI-1." Am J Physiol Renal Physiol **281**(1): F71-80.
- Chen, J., S. V. Brodsky, et al. (2002). "Glycated collagen I induces premature senescence-like phenotypic changes in endothelial cells." Circ Res **90**(12): 1290-8.
- Chen, J. H., C. N. Hales, et al. (2007). "DNA damage, cellular senescence and organismal ageing: causal or correlative?" Nucleic Acids Res **35**(22): 7417-28.
- Chen, Q. M., K. R. Prowse, et al. (2001). "Uncoupling the senescent phenotype from telomere shortening in hydrogen peroxide-treated fibroblasts." Exp Cell Res **265**(2): 294-303.
- Cho, K. A., S. J. Ryu, et al. (2004). "Morphological adjustment of senescent cells by modulating caveolin-1 status." J Biol Chem **279**(40): 42270-8.
- Clarke, M. C., T. D. Littlewood, et al. (2008). "Chronic apoptosis of vascular smooth muscle cells accelerates atherosclerosis and promotes calcification and medial degeneration." Circ Res **102**(12): 1529-38.
- Conzen, S. D. and C. N. Cole (1995). "The three transforming regions of SV40 T antigen are required for immortalization of primary mouse embryo fibroblasts." Oncogene **11**(11): 2295-302.
- Cooper, C., S. Westlake, et al. (2006). "Review: developmental origins of osteoporotic fracture." Osteoporos Int **17**(3): 337-47.
- Cristofalo, V. J. and J. Kabakjian (1975). "Lysosomal enzymes and aging in vitro: subcellular enzyme distribution and effect of hydrocortisone on cell life-span." Mech Ageing Dev **4**(1): 19-28.

- Cristofalo, V. J., A. Lorenzini, et al. (2004). "Replicative senescence: a critical review." Mech Ageing Dev **125**(10-11): 827-48.
- Csiszar, A., N. Labinskyy, et al. (2007). "Vascular superoxide and hydrogen peroxide production and oxidative stress resistance in two closely related rodent species with disparate longevity." Aging Cell **6**(6): 783-97.
- d'Adda di Fagagna, F., P. M. Reaper, et al. (2003). "A DNA damage checkpoint response in telomere-initiated senescence." Nature **426**(6963): 194-8.
- Davis, G. E. (1992). "Affinity of integrins for damaged extracellular matrix: alpha v beta 3 binds to denatured collagen type I through RGD sites." Biochem Biophys Res Commun **182**(3): 1025-31.
- Davis, N. R., O. M. Risen, et al. (1975). "Stable, nonreducible cross-links of mature collagen." Biochemistry **14**(9): 2031-6.
- Davis, T., F. S. Wyllie, et al. (2007). "The role of cellular senescence in Werner syndrome: toward therapeutic intervention in human premature aging." Ann N Y Acad Sci **1100**: 455-69.
- De Clerck, Y. A., M. I. Darville, et al. (1994). "Characterization of the promoter of the gene encoding human tissue inhibitor of metalloproteinases-2 (TIMP-2)." Gene **139**(2): 185-91.
- Debacq-Chainiaux, F., J. D. Erusalimsky, et al. (2009). "Protocols to detect senescence-associated beta-galactosidase (SA-beta-gal) activity, a biomarker of senescent cells in culture and in vivo." Nat Protoc **4**(12): 1798-806.
- Dimri, G. P., X. Lee, et al. (1995). "A biomarker that identifies senescent human cells in culture and in aging skin in vivo." Proc Natl Acad Sci U S A **92**(20): 9363-7.
- Dumont, P., M. Burton, et al. (2000). "Induction of replicative senescence biomarkers by sublethal oxidative stresses in normal human fibroblast." Free Radic Biol Med **28**(3): 361-73.
- Dyckhuizen, D. (1974). "Evolution of cell senescence, atherosclerosis and benign tumours." Nature **251**(5476): 616-8.
- Edelberg, J. M. and V. L. Ballard (2008). "Stem cell review series: regulating highly potent stem cells in aging: environmental influences on plasticity." Aging Cell **7**(4): 599-604.
- Fabris, F., M. Zanicchi, et al. (1994). "Carotid plaque, aging, and risk factors. A study of 457 subjects." Stroke **25**(6): 1133-40.
- Fang, F., G. Orend, et al. (1996). "Dependence of cyclin E-CDK2 kinase activity on cell anchorage." Science **271**(5248): 499-502.

- Feng, J., W. D. Funk, et al. (1995). "The RNA component of human telomerase." Science **269**(5228): 1236-41.
- Freije, J. M., I. Diez-Itza, et al. (1994). "Molecular cloning and expression of collagenase-3, a novel human matrix metalloproteinase produced by breast carcinomas." J Biol Chem **269**(24): 16766-73.
- Fukumoto, Y., J. O. Deguchi, et al. (2004). "Genetically determined resistance to collagenase action augments interstitial collagen accumulation in atherosclerotic plaques." Circulation **110**(14): 1953-9.
- Geng, Y. J. and P. Libby (1995). "Evidence for apoptosis in advanced human atheroma. Colocalization with interleukin-1 beta-converting enzyme." Am J Pathol **147**(2): 251-66.
- Gille, J. J. and H. Joenje (1992). "Cell culture models for oxidative stress: superoxide and hydrogen peroxide versus normobaric hyperoxia." Mutat Res **275**(3-6): 405-14.
- Gluer, C. C., G. Blake, et al. (1995). "Accurate assessment of precision errors: how to measure the reproducibility of bone densitometry techniques." Osteoporos Int **5**(4): 262-70.
- Goldstein, S. (1990). "Replicative senescence: the human fibroblast comes of age." Science **249**(4973): 1129-33.
- Goncharova, E. I., A. Nadas, et al. (1996). "Serum deprivation, but not inhibition of growth per se, induces a hypermutable state in Chinese hamster G12 cells." Cancer Res **56**(4): 752-6.
- Gorenne, I., M. Kavurma, et al. (2006). "Vascular smooth muscle cell senescence in atherosclerosis." Cardiovasc Res **72**(1): 9-17.
- Granton, P. V., C. J. D. Norley, et al. (2009). Rapid in vivo whole-body composition of rats using cone-beam micro-CT. Unpublished. London, ON, Imaging Research Laboratories, Robarts Research Institute.
- Greenberg, R. A., L. Chin, et al. (1999). "Short dysfunctional telomeres impair tumorigenesis in the INK4a(delta2/3) cancer-prone mouse." Cell **97**(4): 515-25.
- Griffin, M., R. Casadio, et al. (2002). "Transglutaminases: nature's biological glues." Biochem J **368**(Pt 2): 377-96.
- Hamlin, C. R. and R. R. Kohn (1971). "Evidence for progressive, age-related structural changes in post-mature human collagen." Biochim Biophys Acta **236**(2): 458-67.
- Hamlin, C. R. and R. R. Kohn (1972). "Determination of human chronological age by study of a collagen sample." Exp Gerontol **7**(6): 377-9.

- Hansen, L. K., D. J. Mooney, et al. (1994). "Integrin binding and cell spreading on extracellular matrix act at different points in the cell cycle to promote hepatocyte growth." Mol Biol Cell **5**(9): 967-75.
- Harley, C. B., A. B. Futcher, et al. (1990). "Telomeres shorten during ageing of human fibroblasts." Nature **345**(6274): 458-60.
- Hathaway, C. A., D. D. Heistad, et al. (2002). "Regression of atherosclerosis in monkeys reduces vascular superoxide levels." Circ Res **90**(3): 277-83.
- Hathcock, K. S., R. J. Hodes, et al. (2004). "Analysis of telomere length and telomerase activity." Curr Protoc Immunol **Chapter 10**: Unit 10 30.
- Haupt, Y., R. Maya, et al. (1997). "Mdm2 promotes the rapid degradation of p53." Nature **387**(6630): 296-9.
- Hayflick, L. and P. S. Moorhead (1961). "The serial cultivation of human diploid cell strains." Exp Cell Res **25**: 585-621.
- Herbert, K. E., Y. Mistry, et al. (2008). "Angiotensin II-mediated oxidative DNA damage accelerates cellular senescence in cultured human vascular smooth muscle cells via telomere-dependent and independent pathways." Circ Res **102**(2): 201-8.
- Herbig, U., M. Ferreira, et al. (2006). "Cellular senescence in aging primates." Science **311**(5765): 1257.
- Herbig, U., W. A. Jobling, et al. (2004). "Telomere shortening triggers senescence of human cells through a pathway involving ATM, p53, and p21(CIP1), but not p16(INK4a)." Mol Cell **14**(4): 501-13.
- Hogg, N., J. Browning, et al. (1999). "Apoptosis in vascular endothelial cells caused by serum deprivation, oxidative stress and transforming growth factor-beta." Endothelium **7**(1): 35-49.
- Ishizaka, N., H. de Leon, et al. (1997). "Angiotensin II-induced hypertension increases heme oxygenase-1 expression in rat aorta." Circulation **96**(6): 1923-9.
- Janzen, V., R. Forkert, et al. (2006). "Stem-cell ageing modified by the cyclin-dependent kinase inhibitor p16INK4a." Nature **443**(7110): 421-6.
- Jones, J. I., T. Prevette, et al. (1996). "Ligand occupancy of the alpha-V-beta3 integrin is necessary for smooth muscle cells to migrate in response to insulin-like growth factor." Proc Natl Acad Sci U S A **93**(6): 2482-7.
- Kamijo, T., F. Zindy, et al. (1997). "Tumor suppression at the mouse INK4a locus mediated by the alternative reading frame product p19ARF." Cell **91**(5): 649-59.

- Karlseder, J., D. Broccoli, et al. (1999). "p53- and ATM-dependent apoptosis induced by telomeres lacking TRF2." Science **283**(5406): 1321-5.
- Keyes, W. M., Y. Wu, et al. (2005). "p63 deficiency activates a program of cellular senescence and leads to accelerated aging." Genes Dev **19**(17): 1986-99.
- Knight, C. G., L. F. Morton, et al. (2000). "The collagen-binding A-domains of integrins alpha(1)beta(1) and alpha(2)beta(1) recognize the same specific amino acid sequence, GFOGER, in native (triple-helical) collagens." J Biol Chem **275**(1): 35-40.
- Koyama, H., E. W. Raines, et al. (1996). "Fibrillar collagen inhibits arterial smooth muscle proliferation through regulation of Cdk2 inhibitors." Cell **87**(6): 1069-78.
- Krishnamurthy, J., C. Torrice, et al. (2004). "Ink4a/Arf expression is a biomarker of aging." J Clin Invest **114**(9): 1299-307.
- Krtolica, A. and J. Campisi (2002). "Cancer and aging: a model for the cancer promoting effects of the aging stroma." Int J Biochem Cell Biol **34**(11): 1401-14.
- Kunieda, T., T. Minamino, et al. (2006). "Angiotensin II induces premature senescence of vascular smooth muscle cells and accelerates the development of atherosclerosis via a p21-dependent pathway." Circulation **114**(9): 953-60.
- Kuro-o, M., Y. Matsumura, et al. (1997). "Mutation of the mouse klotho gene leads to a syndrome resembling ageing." Nature **390**(6655): 45-51.
- Kurz, D. J., S. Decary, et al. (2000). "Senescence-associated (beta)-galactosidase reflects an increase in lysosomal mass during replicative ageing of human endothelial cells." J Cell Sci **113** ( Pt 20): 3613-22.
- Lakatta, E. G. (2003). "Arterial and cardiac aging: major shareholders in cardiovascular disease enterprises: Part III: cellular and molecular clues to heart and arterial aging." Circulation **107**(3): 490-7.
- Lakatta, E. G. and D. Levy (2003). "Arterial and cardiac aging: major shareholders in cardiovascular disease enterprises: Part II: the aging heart in health: links to heart disease." Circulation **107**(2): 346-54.
- Last, J. A., A. D. Siefkin, et al. (1983). "Type I collagen content is increased in lungs of patients with adult respiratory distress syndrome." Thorax **38**(5): 364-8.
- Laxton, R. C., Y. Hu, et al. (2009). "A role of matrix metalloproteinase-8 in atherosclerosis." Circ Res **105**(9): 921-9.
- Le Maitre, C. L., A. J. Freemont, et al. (2007). "Accelerated cellular senescence in degenerate intervertebral discs: a possible role in the pathogenesis of intervertebral disc degeneration." Arthritis Res Ther **9**(3): R45.

- Lee, H. W., M. A. Blasco, et al. (1998). "Essential role of mouse telomerase in highly proliferative organs." Nature **392**(6676): 569-74.
- Lee, R. T. and P. Libby (1997). "The unstable atheroma." Arterioscler Thromb Vasc Biol **17**(10): 1859-67.
- Levine, A. J. (1997). "p53, the cellular gatekeeper for growth and division." Cell **88**(3): 323-31.
- Levy, D., R. J. Garrison, et al. (1990). "Prognostic implications of echocardiographically determined left ventricular mass in the Framingham Heart Study." N Engl J Med **322**(22): 1561-6.
- Li, S., J. Lao, et al. (2003). "Genomic analysis of smooth muscle cells in 3-dimensional collagen matrix." FASEB J **17**(1): 97-9.
- Lindsey, M. L., J. Yoshioka, et al. (2003). "Effect of a cleavage-resistant collagen mutation on left ventricular remodeling." Circ Res **93**(3): 238-45.
- Linskens, M. H., J. Feng, et al. (1995). "Cataloging altered gene expression in young and senescent cells using enhanced differential display." Nucleic Acids Res **23**(16): 3244-51.
- Lipetz, J. and V. J. Cristofalo (1972). "Ultrastructural changes accompanying the aging of human diploid cells in culture." J Ultrastruct Res **39**(1): 43-56.
- Liu, X., H. Wu, et al. (1995). "A targeted mutation at the known collagenase cleavage site in mouse type I collagen impairs tissue remodeling." J Cell Biol **130**(1): 227-37.
- Lodish, H. F. (2003). Molecular cell biology. New York, W.H. Freeman and Company.
- Lutgens, E., E. D. de Muinck, et al. (1999). "Biphasic pattern of cell turnover characterizes the progression from fatty streaks to ruptured human atherosclerotic plaques." Cardiovasc Res **41**(2): 473-9.
- Mach, F., U. Schonbeck, et al. (1997). "Activation of monocyte/macrophage functions related to acute atheroma complication by ligation of CD40: induction of collagenase, stromelysin, and tissue factor." Circulation **96**(2): 396-9.
- MacSweeney, S. T., J. T. Powell, et al. (1994). "Pathogenesis of abdominal aortic aneurysm." Br J Surg **81**(7): 935-41.
- Maile, L. A., J. Badley-Clarke, et al. (2001). "Structural analysis of the role of the beta 3 subunit of the alpha V beta 3 integrin in IGF-I signaling." J Cell Sci **114**(Pt 7): 1417-25.

- Marcotte, R. and E. Wang (2002). "Replicative senescence revisited." J Gerontol A Biol Sci Med Sci **57**(7): B257-69.
- Matsumura, T. (1980). "Multinucleation and polyploidization of aging human cells in culture." Adv Exp Med Biol **129**: 31-8.
- Matthews, C., I. Gorenne, et al. (2006). "Vascular smooth muscle cells undergo telomere-based senescence in human atherosclerosis: effects of telomerase and oxidative stress." Circ Res **99**(2): 156-64.
- Medcalf, A. S., A. J. Klein-Szanto, et al. (1996). "Expression of p21 is not required for senescence of human fibroblasts." Cancer Res **56**(20): 4582-5.
- Melk, A., B. M. Schmidt, et al. (2004). "Expression of p16INK4a and other cell cycle regulator and senescence associated genes in aging human kidney." Kidney Int **65**(2): 510-20.
- Mentink, C. J., M. Hendriks, et al. (2002). "Glucose-mediated cross-linking of collagen in rat tendon and skin." Clin Chim Acta **321**(1-2): 69-76.
- Meredith, J. E., Jr., B. Fazeli, et al. (1993). "The extracellular matrix as a cell survival factor." Mol Biol Cell **4**(9): 953-61.
- Messent, A. J., D. S. Tuckwell, et al. (1998). "Effects of collagenase-cleavage of type I collagen on alpha2beta1 integrin-mediated cell adhesion." J Cell Sci **111** ( Pt 8): 1127-35.
- Miao, D., H. Su, et al. (2008). "Severe growth retardation and early lethality in mice lacking the nuclear localization sequence and C-terminus of PTH-related protein." Proc Natl Acad Sci U S A **105**(51): 20309-14.
- Michiels, C., O. Toussaint, et al. (1990). "Comparative study of oxygen toxicity in human fibroblasts and endothelial cells." J Cell Physiol **144**(2): 295-302.
- Millis, A. J., H. M. McCue, et al. (1992). "Metalloproteinase and TIMP-1 gene expression during replicative senescence." Exp Gerontol **27**(4): 425-8.
- Minamino, T. and I. Komuro (2007). "Vascular cell senescence: contribution to atherosclerosis." Circ Res **100**(1): 15-26.
- Mott, J. W., J. Wang, et al. (1999). "Relation between body fat and age in 4 ethnic groups." Am J Clin Nutr **69**(5): 1007-13.
- Munro, J., F. J. Stott, et al. (1999). "Role of the alternative INK4A proteins in human keratinocyte senescence: evidence for the specific inactivation of p16INK4A upon immortalization." Cancer Res **59**(11): 2516-21.

- Napoli, C., F. P. D'Armiento, et al. (1997). "Fatty streak formation occurs in human fetal aortas and is greatly enhanced by maternal hypercholesterolemia. Intimal accumulation of low density lipoprotein and its oxidation precede monocyte recruitment into early atherosclerotic lesions." J Clin Invest **100**(11): 2680-90.
- Narita, M., S. Nunez, et al. (2003). "Rb-mediated heterochromatin formation and silencing of E2F target genes during cellular senescence." Cell **113**(6): 703-16.
- Nguyen, Q. T., F. Colombo, et al. (2003). "AT1 receptor antagonist therapy preferentially ameliorated right ventricular function and phenotype during the early phase of remodeling post-MI." Br J Pharmacol **138**(8): 1485-94.
- Nishino, J., I. Kim, et al. (2008). "Hmga2 promotes neural stem cell self-renewal in young but not old mice by reducing p16Ink4a and p19Arf Expression." Cell **135**(2): 227-39.
- Novikoff, P. M., N. F. La Russo, et al. (1983). "Immunocytochemical localization of lysosomal beta-galactosidase in rat liver." J Cell Biol **97**(5 Pt 1): 1559-65.
- Ohtani, K. (1999). "Implication of transcription factor E2F in regulation of DNA replication." Front Biosci **4**: D793-804.
- Pandey, S., C. Lopez, et al. (2003). "Oxidative stress and activation of proteasome protease during serum deprivation-induced apoptosis in rat hepatoma cells; inhibition of cell death by melatonin." Apoptosis **8**(5): 497-508.
- Paradis, V., N. Youssef, et al. (2001). "Replicative senescence in normal liver, chronic hepatitis C, and hepatocellular carcinomas." Hum Pathol **32**(3): 327-32.
- Pearson, K. J., J. A. Baur, et al. (2008). "Resveratrol delays age-related deterioration and mimics transcriptional aspects of dietary restriction without extending life span." Cell Metab **8**(2): 157-68.
- Petersen, S., G. Saretzki, et al. (1998). "Preferential accumulation of single-stranded regions in telomeres of human fibroblasts." Exp Cell Res **239**(1): 152-60.
- Pickering, J. G., L. Weir, et al. (1992). "Smooth muscle cell outgrowth from human atherosclerotic plaque: implications for the assessment of lesion biology." J Am Coll Cardiol **20**(6): 1430-9.
- Pinnell, S. R. and G. R. Martin (1968). "The cross-linking of collagen and elastin: enzymatic conversion of lysine in peptide linkage to alpha-amino adipic-delta-semialdehyde (allysine) by an extract from bone." Proc Natl Acad Sci U S A **61**(2): 708-16.
- Radeva, G., T. Petrocelli, et al. (1997). "Overexpression of the integrin-linked kinase promotes anchorage-independent cell cycle progression." J Biol Chem **272**(21): 13937-44.

- Robbins, E., E. M. Levine, et al. (1970). "Morphologic changes accompanying senescence of cultured human diploid cells." J Exp Med **131**(6): 1211-22.
- Robins, S. P. and A. J. Bailey (1975). "The chemistry of the collagen cross-links. The mechanism of stabilization of the reducible intermediate cross-links." Biochem J **149**(2): 381-5.
- Rohme, D. (1981). "Evidence for a relationship between longevity of mammalian species and life spans of normal fibroblasts in vitro and erythrocytes in vivo." Proc Natl Acad Sci U S A **78**(8): 5009-13.
- Ross, R. (1993). "The pathogenesis of atherosclerosis: a perspective for the 1990s." Nature **362**(6423): 801-9.
- Ross, R. (1999). "Atherosclerosis--an inflammatory disease." N Engl J Med **340**(2): 115-26.
- Ruoslahti, E. (1996). "RGD and other recognition sequences for integrins." Annu Rev Cell Dev Biol **12**: 697-715.
- Saito, H. and J. Papaconstantinou (2001). "Age-associated differences in cardiovascular inflammatory gene induction during endotoxic stress." J Biol Chem **276**(31): 29307-12.
- Schrijvers, D. M., G. R. De Meyer, et al. (2007). "Phagocytosis in atherosclerosis: Molecular mechanisms and implications for plaque progression and stability." Cardiovasc Res **73**(3): 470-80.
- Sedelnikova, O. A., I. Horikawa, et al. (2004). "Senescing human cells and ageing mice accumulate DNA lesions with unrepairable double-strand breaks." Nat Cell Biol **6**(2): 168-70.
- Sell, D. R., K. M. Biemel, et al. (2005). "Glucosepane is a major protein cross-link of the senescent human extracellular matrix. Relationship with diabetes." J Biol Chem **280**(13): 12310-5.
- Serrano, M., G. J. Hannon, et al. (1993). "A new regulatory motif in cell-cycle control causing specific inhibition of cyclin D/CDK4." Nature **366**(6456): 704-7.
- Serrano, M., H. Lee, et al. (1996). "Role of the INK4a locus in tumor suppression and cell mortality." Cell **85**(1): 27-37.
- Serrano, M., A. W. Lin, et al. (1997). "Oncogenic ras provokes premature cell senescence associated with accumulation of p53 and p16INK4a." Cell **88**(5): 593-602.
- Sherr, C. J. (2000). "The Pezcoller lecture: cancer cell cycles revisited." Cancer Res **60**(14): 3689-95.

- Sherr, C. J. and F. McCormick (2002). "The RB and p53 pathways in cancer." Cancer Cell **2**(2): 103-12.
- Siegel, R. C. (1976). "Collagen cross-linking. Synthesis of collagen cross-links in vitro with highly purified lysyl oxidase." J Biol Chem **251**(18): 5786-92.
- Siegel, R. C. and G. R. Martin (1970). "Collagen cross-linking. Enzymatic synthesis of lysine-derived aldehydes and the production of cross-linked components." J Biol Chem **245**(7): 1653-8.
- Singh, R., A. Barden, et al. (2001). "Advanced glycation end-products: a review." Diabetologia **44**(2): 129-46.
- Sis, B., A. Tasanarong, et al. (2007). "Accelerated expression of senescence associated cell cycle inhibitor p16INK4A in kidneys with glomerular disease." Kidney Int **71**(3): 218-26.
- Smogorzewska, A. and T. de Lange (2002). "Different telomere damage signaling pathways in human and mouse cells." EMBO J **21**(16): 4338-48.
- Sohal, R. S. and R. Weindruch (1996). "Oxidative stress, caloric restriction, and aging." Science **273**(5271): 59-63.
- Sary, H. C. (1989). "Evolution and progression of atherosclerotic lesions in coronary arteries of children and young adults." Arteriosclerosis **9**(1 Suppl): I19-32.
- Sary, H. C., D. H. Blankenhorn, et al. (1992). "A definition of the intima of human arteries and of its atherosclerosis-prone regions. A report from the Committee on Vascular Lesions of the Council on Arteriosclerosis, American Heart Association." Circulation **85**(1): 391-405.
- Stott, F. J., S. Bates, et al. (1998). "The alternative product from the human CDKN2A locus, p14(ARF), participates in a regulatory feedback loop with p53 and MDM2." EMBO J **17**(17): 5001-14.
- Sukhova, G. K., U. Schonbeck, et al. (1999). "Evidence for increased collagenolysis by interstitial collagenases-1 and -3 in vulnerable human atheromatous plaques." Circulation **99**(19): 2503-9.
- Taddei, S., A. Virdis, et al. (1995). "Aging and endothelial function in normotensive subjects and patients with essential hypertension." Circulation **91**(7): 1981-7.
- Tanzer, M. L. (1973). "Cross-linking of collagen." Science **180**(86): 561-6.
- Thompson, K. V. and R. Holliday (1983). "Genetic effects on the longevity of cultured human fibroblasts. II. DNA repair deficient syndromes." Gerontology **29**(2): 83-8.

- Toussaint, O., P. Dumont, et al. (2000). "Stress-induced premature senescence. Essence of life, evolution, stress, and aging." Ann N Y Acad Sci **908**: 85-98.
- Toussaint, O., E. E. Medrano, et al. (2000). "Cellular and molecular mechanisms of stress-induced premature senescence (SIPS) of human diploid fibroblasts and melanocytes." Exp Gerontol **35**(8): 927-45.
- Trifunovic, A., A. Wredenberg, et al. (2004). "Premature ageing in mice expressing defective mitochondrial DNA polymerase." Nature **429**(6990): 417-23.
- Trimarchi, J. M. and J. A. Lees (2002). "Sibling rivalry in the E2F family." Nat Rev Mol Cell Biol **3**(1): 11-20.
- Vater, C. A., E. D. Harris, Jr., et al. (1979). "Native cross-links in collagen fibrils induce resistance to human synovial collagenase." Biochem J **181**(3): 639-45.
- Virmani, R., F. D. Kolodgie, et al. (2000). "Lessons from sudden coronary death: a comprehensive morphological classification scheme for atherosclerotic lesions." Arterioscler Thromb Vasc Biol **20**(5): 1262-75.
- Vlassara, H. (1994). "Recent progress on the biologic and clinical significance of advanced glycosylation end products." J Lab Clin Med **124**(1): 19-30.
- von Figura, G., D. Hartmann, et al. (2009). "Role of telomere dysfunction in aging and its detection by biomarkers." J Mol Med **87**(12): 1165-71.
- von Zglinicki, T., R. Pilger, et al. (2000). "Accumulation of single-strand breaks is the major cause of telomere shortening in human fibroblasts." Free Radic Biol Med **28**(1): 64-74.
- von Zglinicki, T., G. Saretzki, et al. (1995). "Mild hyperoxia shortens telomeres and inhibits proliferation of fibroblasts: a model for senescence?" Exp Cell Res **220**(1): 186-93.
- von Zglinicki, T., G. Saretzki, et al. (2005). "Human cell senescence as a DNA damage response." Mech Ageing Dev **126**(1): 111-7.
- Wang, Y., G. Blandino, et al. (1999). "Induced p21<sup>waf</sup> expression in H1299 cell line promotes cell senescence and protects against cytotoxic effect of radiation and doxorubicin." Oncogene **18**(16): 2643-9.
- West, M. D., O. M. Pereira-Smith, et al. (1989). "Replicative senescence of human skin fibroblasts correlates with a loss of regulation and overexpression of collagenase activity." Exp Cell Res **184**(1): 138-47.
- West, M. D., J. W. Shay, et al. (1996). "Altered expression of plasminogen activator and plasminogen activator inhibitor during cellular senescence." Exp Gerontol **31**(1-2): 175-93.

- Wright, W. E. and J. W. Shay (2002). "Historical claims and current interpretations of replicative aging." Nat Biotechnol **20**(7): 682-8.
- Wu, H., M. H. Byrne, et al. (1990). "Generation of collagenase-resistant collagen by site-directed mutagenesis of murine pro alpha 1(I) collagen gene." Proc Natl Acad Sci U S A **87**(15): 5888-92.
- Xu, J. (2005). "Preparation, culture, and immortalization of mouse embryonic fibroblasts." Curr Protoc Mol Biol **Chapter 28**: Unit 28 1.
- Xu, Y., E. M. Yang, et al. (1998). "Involvement of p53 and p21 in cellular defects and tumorigenesis in Atm<sup>-/-</sup> mice." Mol Cell Biol **18**(7): 4385-90.
- Yanagitani, Y., H. Rakugi, et al. (1999). "Angiotensin II type 1 receptor-mediated peroxide production in human macrophages." Hypertension **33**(1 Pt 2): 335-9.
- Yang, X., Z. He, et al. (2000). "LMP1 of Epstein-Barr virus suppresses cellular senescence associated with the inhibition of p16INK4a expression." Oncogene **19**(16): 2002-13.
- Yoshida, K., A. Oshima, et al. (1991). "Human beta-galactosidase gene mutations in GM1-gangliosidosis: a common mutation among Japanese adult/chronic cases." Am J Hum Genet **49**(2): 435-42.
- Zhang, R., M. V. Poustovoitov, et al. (2005). "Formation of MacroH2A-containing senescence-associated heterochromatin foci and senescence driven by ASF1a and HIRA." Dev Cell **8**(1): 19-30.
- Zhao, W., M. H. Byrne, et al. (1999). "Bone resorption induced by parathyroid hormone is strikingly diminished in collagenase-resistant mutant mice." J Clin Invest **103**(4): 517-24.
- Zhao, W., M. H. Byrne, et al. (2000). "Osteocyte and osteoblast apoptosis and excessive bone deposition accompany failure of collagenase cleavage of collagen." J Clin Invest **106**(8): 941-9.
- Zheng, B. and D. R. Clemmons (1998). "Blocking ligand occupancy of the alphaVbeta3 integrin inhibits insulin-like growth factor I signaling in vascular smooth muscle cells." Proc Natl Acad Sci U S A **95**(19): 11217-22.
- Zhou, X., A. Jamil, et al. (2006). "Impaired proteolysis of collagen I inhibits proliferation of hepatic stellate cells: implications for regulation of liver fibrosis." J Biol Chem **281**(52): 39757-65.
- Zhou, X., F. R. Murphy, et al. (2004). "Engagement of alphavbeta3 integrin regulates proliferation and apoptosis of hepatic stellate cells." J Biol Chem **279**(23): 23996-4006.

Zhu, J., D. Woods, et al. (1998). "Senescence of human fibroblasts induced by oncogenic Raf." Genes Dev **12**(19): 2997-3007.

Zwolinski, R. J., C. R. Hamlin, et al. (1976). "Age-related alteration in human heart collagen." Proc Soc Exp Biol Med **152**(3): 362-5.